

NO_x Control and Environmental Regulation: Techniques and Discriminatory Social Outcomes

by

Alan Shihadeh

B. S. Mechanical Engineering
The University of Texas at Austin, 1989

Submitted to the Department of Mechanical Engineering
in Partial Fulfillment of the Requirements for the Degrees of

Master of Science in Mechanical Engineering
and
Master of Science in Technology and Policy

at the
Massachusetts Institute of Technology
February 1994

© 1994 Massachusetts Institute of Technology
All rights reserved

Signature of Author _____
Department of Mechanical Engineering
Technology and Policy Program, February 1994

Certified by _____
Professor Janos M. Beér
Department of Chemical Engineering
Thesis Supervisor

Certified by _____
Professor David Gordon Wilson
Department of Mechanical Engineering
Department Reader

Accepted by _____
Professor Richard de Neufville
Chairman, Technology and Policy Program

Accepted by _____
Professor Ain A. Sonin
Chairman, Department Graduate Committee

MASSACHUSETTS INSTITUTE
OF TECHNOLOGY

MAR 08 1994

ARCHIVES

Acknowledgments

Is this fun or what? Its very early and very dark, and "green eggs and swine" is groovin' in the background. The coffee buzz slowly fades as I dive into yet another section of my thesis. The last. Luckily Norm is screaming curses across the hall, from the room he broke into earlier in the evening to print his final copy. So thanks, Norm, for amusing me over the past couple of years, keeping me awake, and making life at MIT bearable, especially over the past few months of all-nighters. Thanks for the late night beers. What a character!

Thanks to Professor Beér for giving me the chance to work with one of the greats, and the opportunity to come to MIT. It has been an incredible learning experience, and a privilege. Thanks to Majed Toqan who guided much of this work, and with whom I gathered most of the data for this thesis. You're positive outlook, enthusiasm, and infinite energy were always a source of inspiration, and perspiration. By now you're a legend among former CRF grad students. Thanks also to Paul Lewis who reviewed my work, kept us on schedule, and shared his stories about the 60's. Thanks to the rest of the CRF gangsters who always made life interesting, multi-cultural, and loud - Omowoleola, Jose, Kai, Laszlo, Peter, Joel, Scott, Robert, Derek, and Bonnie, who actually runs this place.

Thanks to Don Bash for working miracles with the CRF, but also for the colorful language that provided hours of entertainment for my room mate Eric, whose desk was only one thin wall away from Don's, and who would always call me down to listen to Don on the phone. What a riot! I could always look forward to a good time working with Mark, Rich, and Billy during our many test runs.

Thanks to my family for enduring my endless complaints about the weather, and always providing love and encouragement during the difficult times. Thanks mom and dad for the sacrifices you made to give me all the opportunities I could ever hope for, and thanks leeno for being such an awesome little sister.

My buds Eric (Gangsta D and OG), Serge (the Sarge), Jon (Fox butt 10), Norm (Norma), Steve, Eric, Chris, Mike, and the rest of you: YOU'RE A BUNCH OF IDIOTS! I love you all. This place would have sucked without you. Gus, thanks for the excellent ice cream, java, and stories about Austin that kept me going night after night. Go Tosci!

Jenn Wilinsky you are a doll, a roller-blading fool, and one of the kindest people I've ever known. Thanks for making life sweeter the past 6 months. Before I go home this morning, I'm dropping this page off at your door. Give me a call sometime. That applies forever.

Smartie, thanks for all the incredible weekends we spent together up here. I can't tell you how much better you made my first two years at MIT, not to mention the two years prior to that. Whenever I'm down, I think of one of the million good times we had together, and it always works. You'll always have a special place in my heart, cutie benuti fiorenza di medici.

Steve Smith, you're the funniest man on Earth, even if no one else thinks so. Thanks for the hilarious e-mail week after week. I can't think of anyone else I'd rather drink a cappuccino with at Dolce and Freddo, or a beer at the Gingerman. Can we make 5 New Year's in a row?

Thanks to the people at *The Thistle* for being such role models. I don't know how you do it week after week, but when I grow up, I want to be like you. Thanks to Noam Chomsky for so lucidly pointing out the hypocrisy in this violent nation's political culture, and being patient with my ignorant questions. Thanks to all activists in the world who make sacrifices to benefit this human race. Don't let the man's pimps and whores get you down.

Peace.

Table of Contents

Abstract.....	3
Acknowledgements	5
Table of Contents	7
CHAPTER 1 Introduction	
1.1 Motivation	10
1.2 Thesis Objectives.....	11
1.2.1 Technical	11
1.2.2 Social Dimensions	12
1.3 Thesis Organization	14
CHAPTER 2 Nitrogen Chemistry in Combustion	
2.1 NO _x Formation Mechanisms.....	16
2.1.1 Thermal Mechanism	17
2.1.2 Prompt Mechanism	18
2.1.3 Fuel-N Conversion.....	18
2.2 NO _x Destruction	20
2.3 Implications for NO _x Control by Combustion Modification	21
2.3.2 Two-Stage Combustion	22
2.3.3 Reburn.....	23
2.4 Chemical Kinetic Modeling.....	24
2.4.1 Modeling Parameters.....	25
2.4.2 Methane Modeling Results	26
2.4.3 No. 6 Fuel-Oil Modeling Results	31
2.5 NO _x Chemistry and The RSFC Burner	37
CHAPTER 3 RSFC Burner Aerodynamics	
3.1 Turbulence Damping	39
3.2 Swirl and Flame Structure	42
3.3 Aerodynamics of RSFC burner flames	44
CHAPTER 4 Experimental Method and Apparatus	
4.1 Experimental Objectives	48
4.2 Methodology	49
4.2.1 Parametric Studies.....	49
4.2.2 Detailed Flame Structure Study	50
4.3 Experimental Apparatus	51
4.3.1 Experimental Furnace.....	51
4.3.2 The RSFC Burner	53

CHAPTER 5 Experimental Results

5.1 Primary and Tertiary Air Swirl.....	57
5.2 External Air Staging	63
5.3 Flue Gas Recirculation	67
5.4 Firing Rate.....	69
5.5 Atomization	70
5.6 Flame Structure Study	74
5.7 Pre-combustor	79
5.8 Summary & Future Work.....	83

Chapter 6 Race and Class in Environmental Regulation

6.1 Introduction	85
6.2 Evidence Of Environmental Discrimination.....	86
6.3 Legal Remedy.....	90
6.3.1 Litigation Strategies	93
6.3.2 Legislation	97
6.4 Environmental Politics: Limits To Legal Remedy	99
6.4.1 Hegemony in Environmental Politics	102
6.4.2 Hegemony in the History of Regulation.....	103
6.5 Conclusion	107

Chapter 7 Summary, Conclusions & Recommendations

7.1 Summary	109
7.1.1 Primary and Tertiary Air Swirl	110
7.1.2 External Staging.....	111
7.1.3 Flue Gas Recirculation	111
7.1.4 Firing Rate	112
7.1.5 Atomization.....	112
7.1.6 Pre-Combustor.....	113
7.1.7 Detailed Flame Study.....	113
7.2 Conclusions.....	114
7.3 Recommendations	115

References	117
------------------	-----

APPENDIX

Raw data for detailed flame map	122
Reaction mechanism used in chemical kinetic modeling	133

CHAPTER 1

Introduction

1.1 Motivation

The nitrogen oxides NO and NO_2 , collectively referred to as NO_x , are atmospheric pollutants produced by fossil fuel combustion in automobiles, power plants, and other industrial processes. Initially, concern about NO_x emission stemmed from its role in nitric acid deposition, though more recently the discovery of its role in tropospheric ozone formation has shifted the emphasis of NO_x control to ozone abatement. It is now known that in the presence of sunlight NO_x combines with volatile organic compounds (VOCs) to produce ozone and other photochemical oxidants commonly known as smog. Because ozone poses direct human health risks, this discovery greatly increased the attention given to NO_x emissions, with tighter restrictions being imposed on polluters.

The 1990 Clean Air Act Amendments, for example, brought NO_x emission from power plants under the ozone abatement provisions of Title I of the Act, making NO_x subject for the first time to federal ozone abatement regulations for non-attainment areas. In addition, under the acid rain regulations of Title IV, the Amendments reduced allowable NO_x emission to 0.5 lb/mmBTU for wall-fired boilers, and 0.45 lb/mmBTU for tangentially fired boilers. As a result of the new regulations, private firms and universities have focused more attention on researching methods

for NO_x control, particularly in response to the emergence of lucrative markets for what the business press describes as “environmentally friendly” technologies.

In stationary combustion, NO_x emission can be reduced by post-combustion cleanup, such as Selective Catalytic Reduction (end-of-pipe), and by combustion process modification (prevention). With a few exceptions, only post combustion cleanup systems have been able to meet the most stringent NO_x emission standards. Selective Catalytic Reduction, for example, has been demonstrated to provide 70-90 % NO_x reduction, in comparison to 40-55 % for low-NO_x burner retrofits.¹ Post-combustion cleanup systems, however, typically create undesirable solid wastes, and are associated with higher construction and operating costs for toxic waste disposal and catalyst replacement. Capital cost for SCR ranges from \$70/kW to \$150/kW for retrofit applications, whereas capital costs for combustion process modifications range from \$8/kW to \$25/kW.² As a result, much recent research has focused on improving the performance of combustion process modifications, with the ultimate goal of supplanting post combustion cleanup systems altogether.

1.2 Thesis Objectives

1.2.1 Technical

One widely implemented combustion process modification in industrial and electric utility boilers is air staging, in which the combustion is carried out in two stages: a fuel-rich primary stage, followed by a fuel-lean burnout stage. Typically, staging is achieved by introducing only a portion of the required combustion air through the burner, and injecting the remainder of the air, sometimes referred to as “over-fire air,” at a location downstream of the burner. Drawbacks to this method include difficulty retrofitting existing systems, increased corrosion of the heat

¹Torrens and Platt [1994]

²ibid.

transfer surfaces in the fuel-rich first stage, and higher cost. An alternative to relying on over-fire air is to induce staged conditions aerodynamically, i.e. by altering the fuel-air mixing pattern to produce a fuel-rich and fuel-lean zone internally. This aerodynamic process is referred to as “internal staging.”

The Radially Stratified Flame Core (RSFC) Burner was developed at MIT with this purpose in mind. The burner utilizes a fluid dynamic phenomena known as turbulence damping to create two distinct combustion zones: one characterized by suppressed mixing between the fuel and air, so that the fuel pyrolyzes in a locally fuel-rich atmosphere, and a second zone in which the remaining fuel and air mix vigorously. While this process has been demonstrated to reduce NO_x emission from natural gas flames to very low levels (15 ppm NO_x @ 3% O₂, with 30% FGR and 0.12 lb/lb steam injection), it not clear whether the RSFC burner would be equally effective in reducing NO_x emission from heavy (No. 6) fuel oil flames. No. 6 fuel oil presents special difficulties for low NO_x operation because it contains organically bound nitrogen which can easily convert to NO during combustion. Furthermore, attention must be given to spray atomization, which impacts nitrogen and oxidation chemistry, as well as the combustion aerodynamics.

This thesis presents experimental studies and computer simulations carried out to understand how these additional complexities can be addressed to achieve low NO_x combustion with No. 6 oil. It incorporates a detailed experimental investigation aimed at understanding the overlapping mixing and chemistry processes present in RSFC flames. The ultimate purpose of the technical portion of this thesis is to develop optimal design and operating criteria for minimizing NO_x and CO emissions while burning heavy (No. 6) fuel oil with the RSFC burner.

1.2.2 Social Dimensions

Various groups in the United States, such as the United Church of Christ, the Southwest Network for Environmental and Economic Justice, and the Human Environment Center have complained

that minorities and the poor are disproportionately exposed to environmental hazards; that business, with government assistance, practices “environmental discrimination” by targeting those communities for polluting activities. Many studies in the last 20 years show that this segment of society does in fact experience a higher incidence of environmental hazards, and where data are available, show that minorities and the poor experience elevated levels of bloodstream contaminants, along with deleterious health effects.³

Social advocacy groups have also pointed to inequities in the distribution of institutional response to pollution, i.e. that the enforcement of environmental regulations in these communities is less stringent than in predominantly white or affluent areas. This problem partially explains the previous one; all else being equal, polluting industries are more likely to locate where enforcement is lax. This “incentive,” however, must be considered along with other determinants in the distributional dynamics of environmental quality, such as the availability of cheap land in poor neighborhoods, proximity to industrial infrastructure, zoning laws, and the ability of the affected communities to marshal the political resources needed to countervail siting decisions.

The distributional dynamics are also affected by the EPA, which by promulgating national standards that would seem to equalize environmental protection across class and race boundaries⁴ has had a substantial effect on the location and relocation of pollution and polluting industries,⁵ often redistributing risks toward poor and minority communities.⁶ For example, the previously mentioned Selective Catalytic Reduction method for NO_x reduction results in toxic solid wastes that must be transported to landfills or treatment centers which are often located in a different community than that affected by the original emissions.

³Wood et al [1974]

⁴Gelobter [1992:73]

⁵Gelobter [1992:73]

⁶Lazarus [1992]

The central objective of the thesis is to qualitatively analyze the distributional dynamics of environmental quality, primarily in order to determine where and how institutional intervention can succeed in reducing inequities. The thesis will review evidence for environmental discrimination, identify strategies for legal redress, and finally, discuss why they might fail. An underlying objective is to investigate whether bias arises through formal decision process (written rules and regulations, legal jurisdiction), structural processes (race/class relationships, mobility of pollution sources), or informal processes (definition of pollution “problems,” application of sanctions).⁷

1.3 Thesis Organization

Before continuing, it may be useful to present an overview of the following chapters, and in the process, hopefully illuminate the logic underlying the thesis structure.

Chapter 2 provides an overview of nitrogen chemistry in combustion, including the chemical kinetic pathways to NO_x formation and destruction. A presentation of the chemistry underlying various NO_x control strategies is given, including the chemistry of internal staging. Results of chemical kinetic studies using numerical simulation are presented to identify the most important control parameters in low NO_x combustion. The chapter focuses attention on the potential fate of fuel-bound nitrogen, and illustrates how NO_x control strategies change when nitrogen is present in the fuel.

The purpose of Chapter 3 is to describe the aerodynamic phenomena employed by the R3FC burner to induce internal staging. The phenomena include turbulence damping, radial stratification, and internal recirculation, all of which result from imposing swirl on the combustion air. The possible flame structures created by combining varying degrees of swirl and fuel jet momentum are described qualitatively, as are the attendant implications for NO_x

⁷Gelobter [1993]

emission. Finally, the chapter describes the important aerodynamic features of typical low NO_x RSFC flames.

Chapters 4 and 5 describe the experimental investigations performed at the MIT Combustion Research Facility (CRF) with No. 6 fuel oil flames. Chapter 4 explains the experimental method, including the important parameters and measurements, as well as the experimental setup. A brief description of the prototype RSFC burner and CRF furnace is also included. Chapter 5 presents the experimental result, and identifies the optimal burner configuration for low NO_x, low CO combustion with No. 6 oil. Recommendations for future experimental work and possible burner modifications are also given in this chapter.

Inequity in the demographic distribution of environmental hazards are discussed in Chapter 6. On the surface, this portion of the thesis is separate from the rest, though its implications are fundamentally relevant to emission controls, and the strategies chosen to implement them. This aspect of pollution control has received far less attention from the academic community than the conventional technical and regulatory issues of environmental protection, partly because the people who are most concerned with distributional inequities in the incidence of environmental hazards, i.e. the people who live in affected communities, do not customarily finance university research.

Chapter 7 is a summary of the major conclusions of the study, and presents recommendations for future work with the RSFC burner.

CHAPTER 2

Nitrogen Chemistry In Combustion

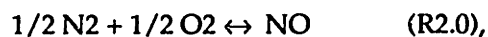
Any effective low NO_x combustion system design must start with an accounting of the underlying nitrogen chemistry. System parameters, such as the time and temperature history, fuel-equivalence ratio, and mixing pattern, are chosen based on the constraints given by NO_x formation and destruction pathways and the associated reaction rates. This chapter reviews NO_x formation and destruction in combustion, and presents the attendant implications for NO_x control methods.

2.1 NO_x Formation Mechanisms

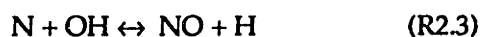
There are essentially two sources of NO_x in combustion: atmospheric nitrogen fixation, and conversion of organically bound nitrogen species found in the fuel. Atmospheric nitrogen fixation occurs either by oxidation at high temperature through the “thermal” mechanism, or by hydrocarbon radical attack in the flame zone, the “prompt” mechanism.

2.1.1 Thermal Mechanism

Thermal NO is the primary source of NO emission from burning fuels such as natural gas that do not contain organically bound nitrogen. It is formed by the fixation of atmospheric nitrogen at high temperature (> 1000 K). The overall highly endothermic reaction can be expressed as



though the direct oxidation of nitrogen is much too slow to be significant in practical systems. Instead, NO formation through the thermal mechanism occurs primarily by O radical attack on molecular nitrogen, initiating the following chain mechanism first postulated by Zeldovich et al. [1947]:



Reaction 2.1 is the rate limiting step (due to the high activation energy associated with breaking the strong N₂ triple bond, 941 KJmol⁻¹), and it is generally slow compared to the fuel oxidation reactions. Therefore when modeling a particular flame, the thermal NO formation reactions can be decoupled from the fuel oxidation process (i.e., by assuming that the O, H, and OH radicals are present in their equilibrium concentrations) when calculating the thermal NO formation rate. Reactions 2.2 and 2.3 are more important in fuel-lean and fuel-rich flames, respectively.

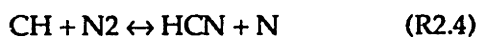
Due to the high activation energy of reaction 2.1, the formation rate of thermal NO is sensitive to temperature, doubling with every 40 K rise, and becomes significant above 1800 K.⁸ Thus to minimize thermal NO formation, off-stoichiometric combustion, where the adiabatic flame temperature is lower, can be employed. Further, minimizing residence time under high-temperature conditions helps to reduce thermal NO formation.

⁸Sarofim and Flagan [1976]

2.1.2 Prompt Mechanism

Another route for NO formation from atmospheric nitrogen is through the “prompt” mechanism, in which hydrocarbon radicals attack molecular nitrogen, leading to formation of amines or cyano compounds that subsequently react to form NO. These reactions have relatively low activation energy and can proceed at a rate comparable to the fuel oxidation rate. NO formed through this mechanism is termed “prompt” because it occurs early (i.e., within the flame) relative to that formed by the Zeldovich mechanism (in the post-combustion gases). Formation of prompt NO increases with the equivalence ratio. Typical levels of prompt NO range from a few ppm to more than 100 ppm.⁹

CH and CH₂ are considered to be the major contributors to prompt NO in hydrocarbon flames¹⁰ through the following reactions:¹¹



Because the prompt NO formation rate is of the order of the fuel oxidation rate, the NO kinetics cannot be decoupled from the hydrocarbon combustion mechanism, although some simplifications have been proposed.¹²

2.1.3 Fuel-N Conversion

When fuels containing chemically bound nitrogen are burned, the principal source of NO_x emissions is the conversion of these nitrogen species. Figure 2.1 indicates the relative contribution of fuel-NO_x to total NO_x from laboratory pulverized coal combustion experiments

⁹Miller and Bowman [1989: 6]

¹⁰Miller and Bowman [1989: 26]

¹¹Miller and Bowman [1989: 6]

¹²Sarofim and Pohl [1973]

by Pershing and Wendt¹³, clearly indicating the importance of fuel nitrogen. The "fuel NO" curve was generated by replacing the combustion air with a mixture of oxygen, argon, and carbon dioxide that was selected to give the same adiabatic flame temperature as combustion at the same equivalence ratio in air.

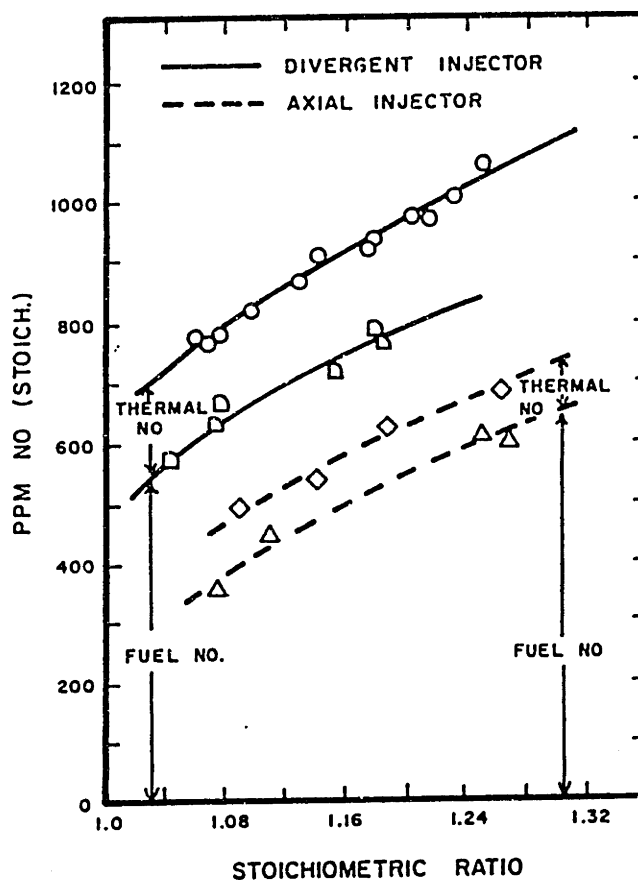


Figure 2.1 Contribution of thermal-NO_x and fuel-NO_x to total NO_x emissions in the laboratory pulverized coal combustion experiments of Pershing and Wendt (1977).

Measurements on laboratory-scale burners with a variety of model fuel nitrogen compounds indicate that the conversion to NO is independent of the identity of the model compound, but strongly depends on the local temperature and stoichiometry, as well as the initial concentration of the nitrogen compound in the fuel.¹⁴ Available data also indicates that the gas-phase fuel nitrogen reaction sequence is initiated by a rapid conversion of the parent fuel nitrogen

¹³Pershing and Wendt [1977]

¹⁴Miller and Bowman [1989: 16]

compounds (predominantly in pyridine and pyrrole groups¹⁵) to HCN and NH₃.¹⁶ The fuel-N chemistry can be described by the following schematic:

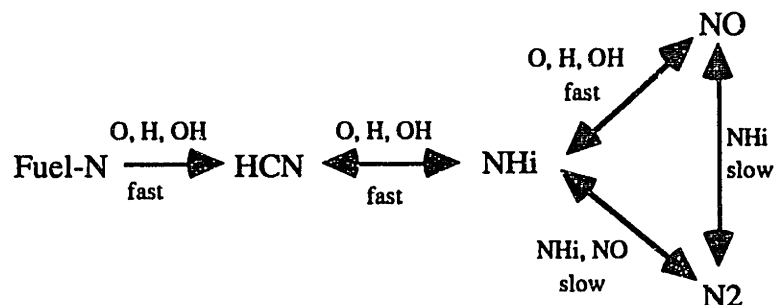


Figure 2.2 Simplified Fuel-N Chemistry in Hydrocarbon Combustion.

Under fuel-lean conditions, where the oxygen atom concentration is high, the NH_i's are likely to form NO. In fuel-rich conditions, NH_i will react with other NH_i or NO molecules to form N₂. However, because N₂ formation requires the reaction of two fixed nitrogen species, one being present only in very small concentrations (due to the rapid consumption of N, NH, and NH₂), N₂ formation proceeds slowly. Therefore, to maximize fuel-N conversion to N₂ rather than to NO_x, a fuel-rich zone with an extended residence time is needed. The residence time required for conversion is inversely correlated with temperature; residence time can be traded for higher temperatures.

2.2 NO_x Destruction

NO formed during combustion can be converted to N₂ through NO "reburn", in which NO reacts with hydrocarbon free radicals, to form HCN:



¹⁵Flagan and Seinfeld [1988: 181]

¹⁶Miller and Bowman [1989: 16]

The HCN that is formed can then follow either of two competing paths, either to N₂ or back to NO, as indicated in the previous simplified nitrogen chemistry diagram. As mentioned, the path to N₂ is favored under fuel-rich conditions, reaching an optimum reduction rate for a fuel equivalence ratio of about 1.15.¹⁷

The reburn mechanism can be exploited to reduce NO_x emissions in practical combustion systems. Conventionally this entails fuel-staging whereby a fuel-lean first stage, where NO_x production is high, is followed by a fuel-rich NO_x reduction stage where a hydrocarbon fuel is injected. A more sophisticated technique for implementing NO reburn is to utilize a recirculation zone that recycles NO through the fuel-rich core of a the flame, where hydrocarbon radicals are found in high concentration.

2.3 Implications for NO_x Control by Combustion Modification

Given the NO formation/destruction chemistry, two implications for NO suppression are readily apparent: 1) to reduce thermal NO_x formation, fuel-lean high temperature conditions should be avoided, and 2) when fuel-N is present, a long residence time in a fuel-rich, high temperature region will reduce NO_x. Combustion modification techniques designed to create these conditions include flue gas recirculation, fuel staging, and air staging. Each of these techniques is described in this section, followed by a presentation of chemical kinetic modeling results that illustrate their efficacy.

2.3.1 Flue Gas Recirculation

Flue gas recirculation (FGR) entails injecting a portion of the cooled combustion gases back into the combustion zone. The recirculated gases act as a heat sink, reducing flame temperature, and therefore thermal NO_x formation. Another function of FGR is to reduce the local concentration of

¹⁷Kolb et al [1988]

O₂, and therefore the nitrogen fixation reaction rates. Because FGR only attenuates thermal NO_x formation, it is not particularly useful in cases where fuel-N is the primary source of NO production.¹⁸ FGR may actually increase NO in these cases, since the resulting lower temperature may slow the fuel-N conversion process.

In conventional systems, FGR requires extensive ductwork since large volumes of gas are transported. For this reason achieving recirculation through the use of aerodynamic means as in the RSFC burner is an attractive option.

2.3.2 Two-Stage Combustion

Staged combustion refers to carrying out the combustion in two steps: a fuel-rich primary stage where only a portion of the combustion air is introduced, followed by a fuel-lean burnout stage in which the remainder of the air is injected (see Figure 2.3). Staging the combustion in this manner has two beneficial effects. First, the reaction zone

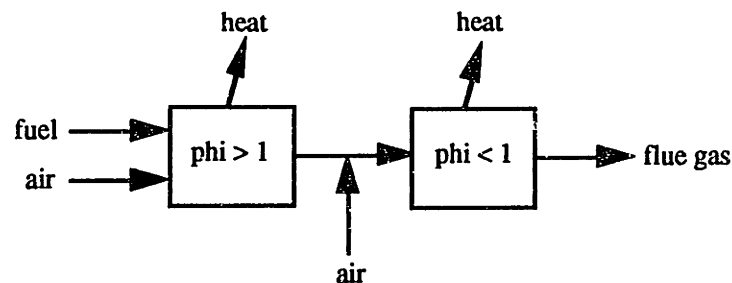


Figure 2.3 Air-Staged Combustion Process Diagram

is effectively lengthened, reducing the volumetric heat release rate, and thereby limiting peak flame temperature; by the time that the gases exit the first stage, heat will have been transferred to the combustion chamber surfaces, so that when the final burnout occurs, the temperature will be much lower than the adiabatic flame temperature and therefore thermal NO_x formation will

¹⁸Wark and Warner [1981: 18]

be kinetically limited. Furthermore, NO_x production is limited in the first stage by the relative scarcity of O_2 .

Secondly, by creating a fuel-rich primary stage, fuel-N conversion to N_2 is favored, as are the NO reduction reactions. With sufficient residence time in the primary zone, much of the fuel-N can be reduced, resulting in lower NO_x emission.

Practical drawbacks to staging include the increased possibility of corrosion in the fuel-rich stage, the need for additional ductwork, and the increased likelihood of polycyclic compound formation. An important design objective, then, is to gain the benefits of staging without resorting to a high degree of staging. One way to minimize the required degree of staging is to optimize the heat removal rate and residence time in the primary stage.

2.3.3 Reburn

Another way to reduce NO_x emissions is to stage both the fuel and the air to create a lean-rich-lean combustion sequence (see Figure 2.4). In this case, the majority of the fuel is burned in the fuel-lean first stage, and a large quantity of NO is generated.

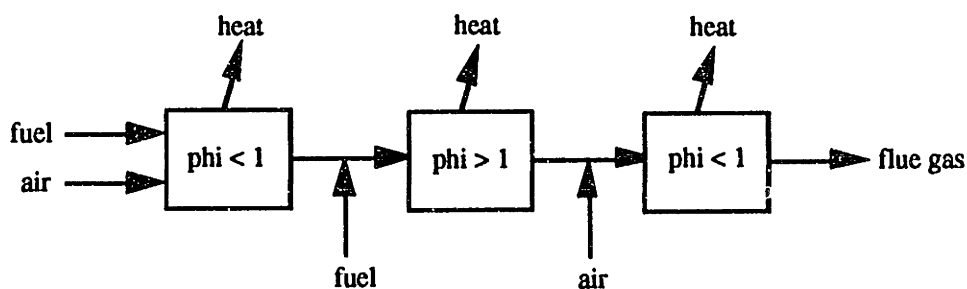


Figure 2.4 Fuel and Air Staging Reburn Process Diagram

In the second stage, additional fuel is injected, creating a fuel-rich environment in which the NO reburn mechanism, discussed above, reduces the NO formed in the first stage back to N_2 .

Finally, after sufficient residence time, additional air is added to create a slightly fuel-lean environment for burnout.

2.4 Chemical Kinetic Modeling

A chemical kinetic model of a plug flow reactor was used to help quantify the relationship of NO_x emission to various combustion parameters such as temperature and stoichiometry. Trends derived from the models provided a theoretical understanding and basis for the ensuing experimental work with combustion modification methods.

The modeling was carried out using *Chemkin*, a Fortran based chemical kinetics package developed by Sandia Laboratories. The package consists of a stiff ordinary differential equation solver subroutine and a thermodynamic database. A user-supplied program provides the governing equations (species, mass, and heat conservation, for example), from which species concentration and temperature are calculated for a specified time interval and given initial conditions. In addition to the governing equations, a reaction mechanism must be specified by the user. The Miller and Bowman (1989) mechanism was used in this study; it is listed in the Appendix.

The models reported here assume homogeneous, gas phase pre-mixed conditions in a plug flow reactor. Clearly, a diffusion flame with a complex recirculating flow pattern, as exists with the RSFC burner, departs radically from these simplifying assumptions, even more so when the fuel is oil. The purpose of the modeling exercise, however, was not to predict emissions from a practical system, but rather to gain an understanding of the underlying chemical processes in order to guide the experimental work, and to help explain the obtained data. To this end, the modeling was quite useful, as will be shown.

2.4.1 Modeling Parameters

The modeling effort focused on determining the relationship between NO_x emission and: combustion stoichiometry; temperature; and percent flue gas recirculated, for methane and fuel-oil flames. One question was whether an optimum degree of staging exists; another was whether flue gas recirculation would inhibit NO_x emissions from nitrogen bearing fuel-oil flames. To answer these questions and others the following parametric studies were performed using the *Chemkin* code.

1. Methane

adiabatic (573 K preheat) or isothermal (1700, 1800, 1900 K)

FGR: 0, 10, 30 %

phi: 0.2 to 2.1

air preheat temperature: 573, 900 K

2. No 6 Fuel-Oil

isothermal (1700, 1800, 1900 K)

phi: 1 to 2.1

fuel-N: 0, 0.2, 0.3 % (vol)

H/C ratio: 3/2

In accordance with Miller and Bowman's research indicating that fuel-N quickly converts to HCN before other significant nitrogen chemistry proceeds, and that the formation of NO from fuel-N is independent of the identity of the parent N compound, the fuel-N in the No. 6 fuel-oil cases was assumed to be in the form of HCN.

Recent modeling studies by Ballester and Barta (1993) indicate that the evolution rate of HCN from coal particles is an important determinant of the calculated final NO_x concentration. Since HCN conversion occurs on the same time scale as volatile formation, the HCN reactions occur in a temporally unsteady stoichiometric environment. Ballester and Barta found that with the unsteadiness accounted for, however, the observed trends (i.e., NO_x versus Phi) remained the same, though with different absolute values. Furthermore, since oil droplets evaporate much

more rapidly than coal particles devolatilize, taking HCN evolution into account in the fuel-oil calculations was deemed unnecessary.

For the adiabatic methane cases with 573 K preheat, the initial temperature of the mixture was too low to initiate the chain branching reactions of the Miller mechanism, leaving the fuel-air mixture unreacted even at long residence times. To solve this problem, the initial temperature of the mixture was increased to 900 K, and a corresponding amount of fuel was assumed to be "burned" so that the initial mixture contained products as well as reactants. The ratio of reactants to products was adjusted until the adiabatic flame temperature of the mixture with a 900 K initial temperature equaled that of the pure reactants mixture with a 573 K initial temperature. The adiabatic flame temperatures were calculated using the *Stanjan* equilibrium code.

2.4.2 Methane Modeling Results

Figures 2.5 and 2.6 indicate the effects of fuel equivalence ratio and FGR on total bound nitrogen (TBN) and adiabatic flame temperature for the 573 K preheat cases. Clearly, increasing FGR or fuel equivalence ratio has a strong attenuating impact on TBN. For a ϕ of 1.05, increasing FGR from 0 to 30% reduced TBN concentration from 5000 ppm to 75 ppm. Similarly for the 0% FGR cases, increasing fuel equivalence ratio from 1.05 to 1.7 reduced TBN from 5000 ppm to 15 ppm.

For the ranges of FGR and fuel equivalence ratio studied, the effect of both parameters on TBN concentration was of the same order, as may be expected since increasing FGR and fuel-equivalence ratio reduced the adiabatic combustion temperature by similar amounts. For a ϕ of 1.05, for example, increasing FGR from 0 to 30% decreased temperature from 2554 K to 2043 K, whereas for the 0 % FGR cases, increasing fuel equivalence ratio from 1.05 to 1.7 decreased the temperature from 2554 K to 1953 K. As discussed above, the primary source of NO_x in methane flames is thermal NO_x; therefore the correlations between TBN and ϕ or FGR are expected. One feature apparent from Figure 2.6 is the possibility in practical systems of trading-off fuel equivalence ratio (i.e., degree of staging) for FGR, giving the designer another dimension of

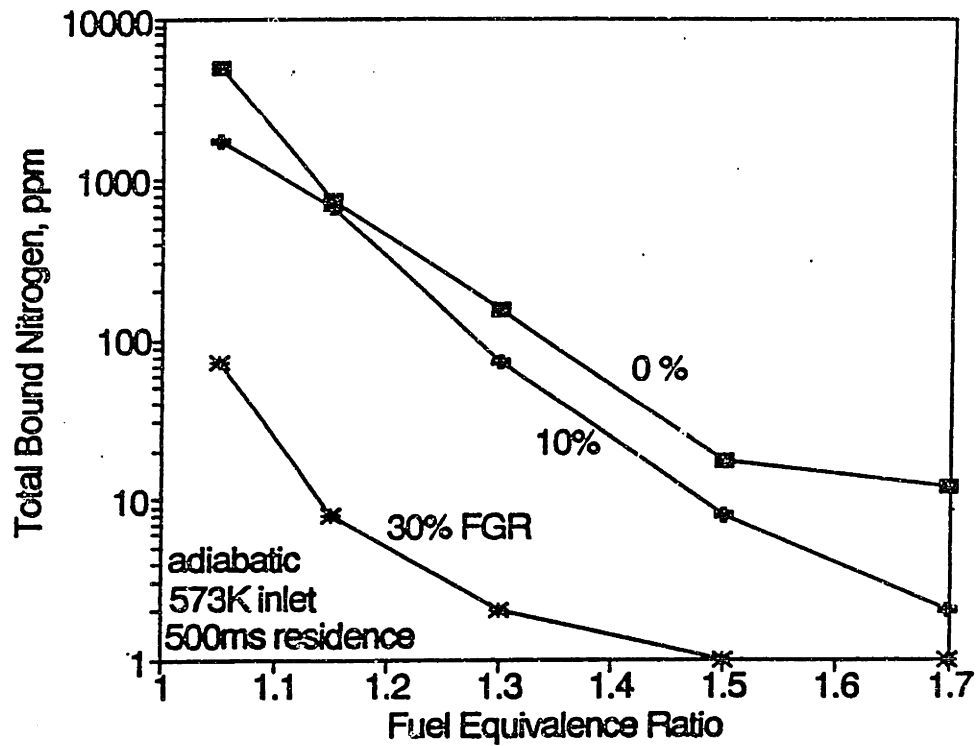


Figure 2.5 TBN is computed after 500 ms in a fuel-rich zone. Combustion air and recirculated flue gas are both delivered at 573 K, and FGR O₂ content is 0.9%. (TBN is reported in actual concentration for all figures in this chapter.)

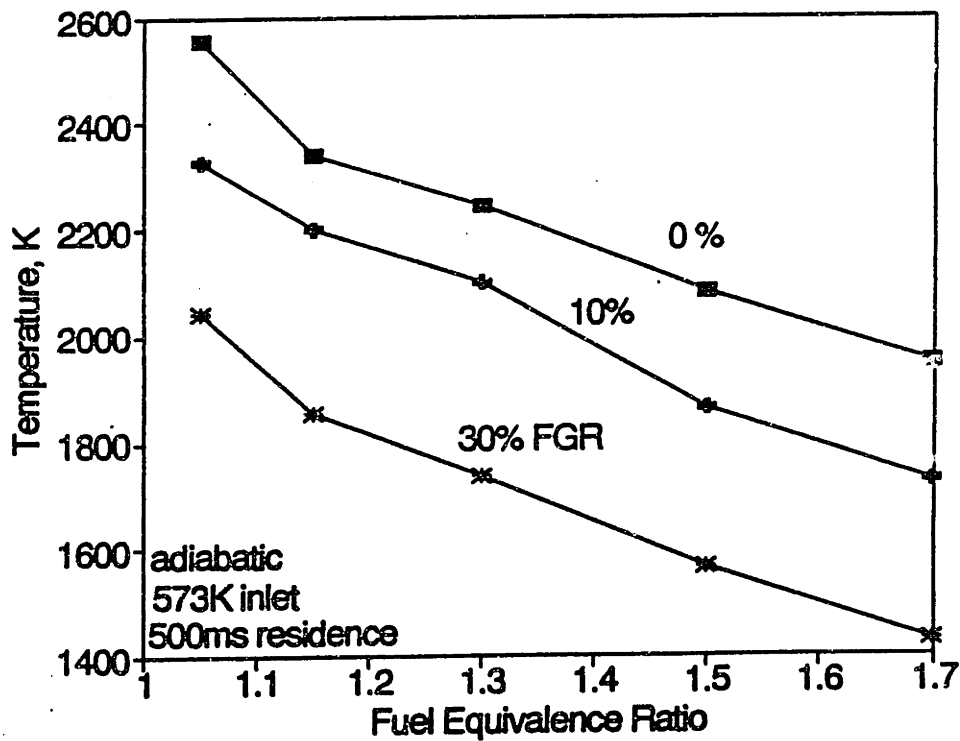


Figure 2.6 Temperatures corresponding to data shown in Figure 2.5.

freedom that can be valuable when either staging or FGR is particularly costly relative to the other.

Figures 2.7, 2.8, and 2.9 illustrate the relationship between FGR, ϕ , and TBN when temperature is set as an independent variable. The results indicate that the benefit from FGR and increasing equivalence ratio is almost solely due to temperature, not gas composition. Figure 2.9, for example, shows that the strong effects of increasing FGR and fuel-equivalence ratio observed in Figure 2.5 are negligible when temperature is controlled for. This shows that the oxygen-diluting effect of FGR is much less important than the heat sink effect.

For completeness, Figure 2.10 shows the effect of fuel equivalence ratio over a wider range (for an air pre-heat temperature of 900 K). The results demonstrate the logic of operating a furnace at off-stoichiometric conditions, either rich or lean. The figure shows that TBN generally follows temperature, with an offset due to the higher oxygen concentration at fuel-equivalence ratios below 1. Thus on the fuel-lean side of the curve, there are two competing effects: higher oxygen concentration versus lower temperature. Clearly, the temperature effect dominates, as shown by the ultra-low TBN concentration for fuel-equivalence ratios below 0.45, where oxygen concentration is high but temperature is low.

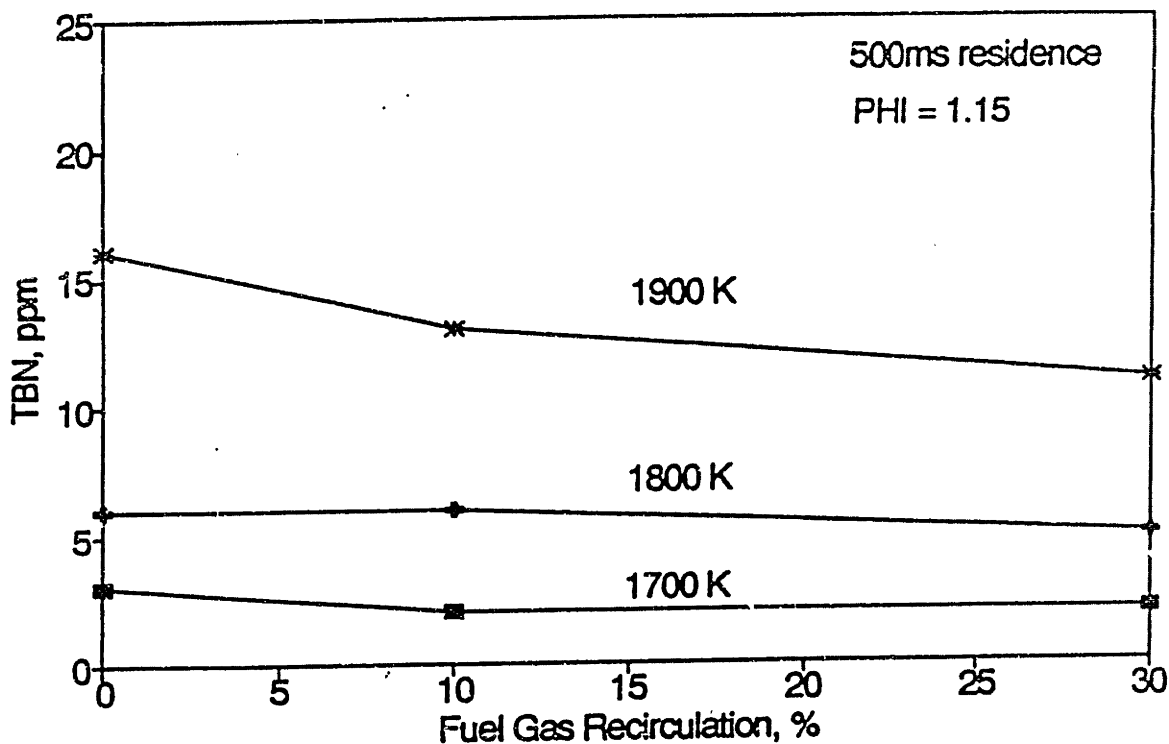


Figure 2.7 Effect of FGR on TBN. TBN is computed after 500 ms in a fuel-rich zone ($\phi = 1.15$) assuming isothermal conditions at 1700 K, 1800 K, 1900 K for various levels of FGR. Combustion air and recirculated flue gas are both delivered at 573 K, and FGR O₂ content is 0.9%.

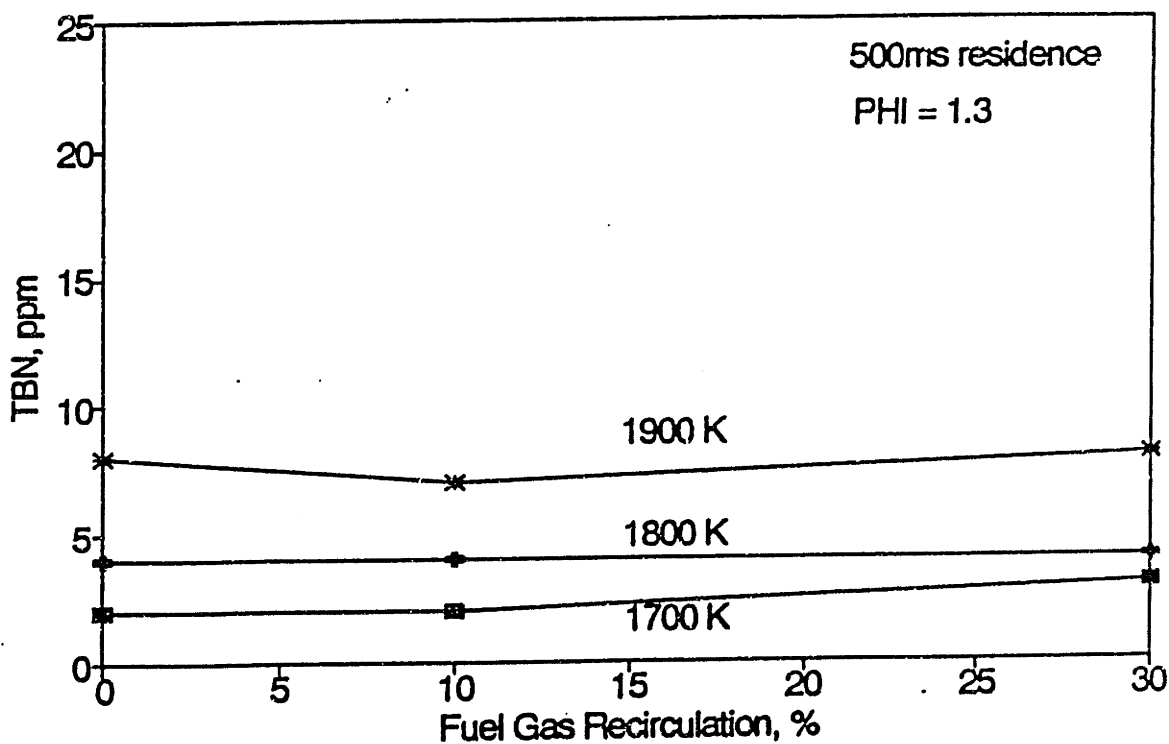


Figure 2.8 Effect of FGR on TBN for $\phi = 1.3$. Conditions listed in previous figure.

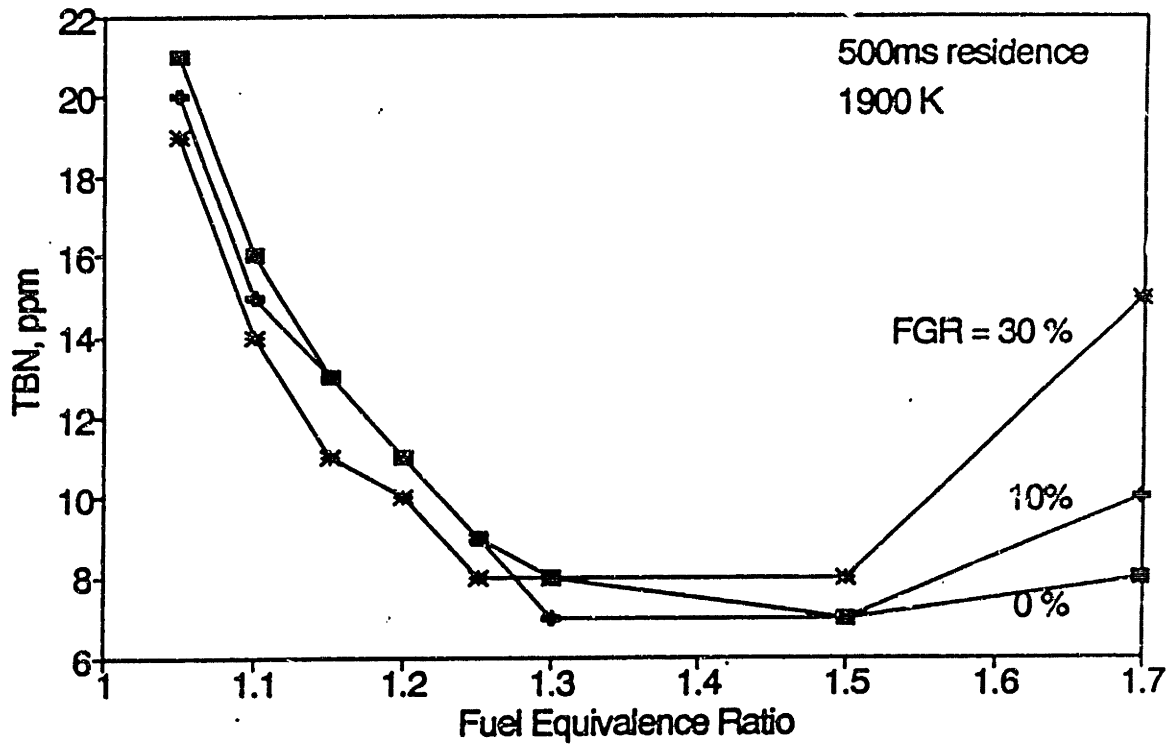


Figure 2.9 TBN versus fuel equivalence ratio as a function of FGR. TBN is computed after 500 ms assuming isothermal conditions at 1900 K.

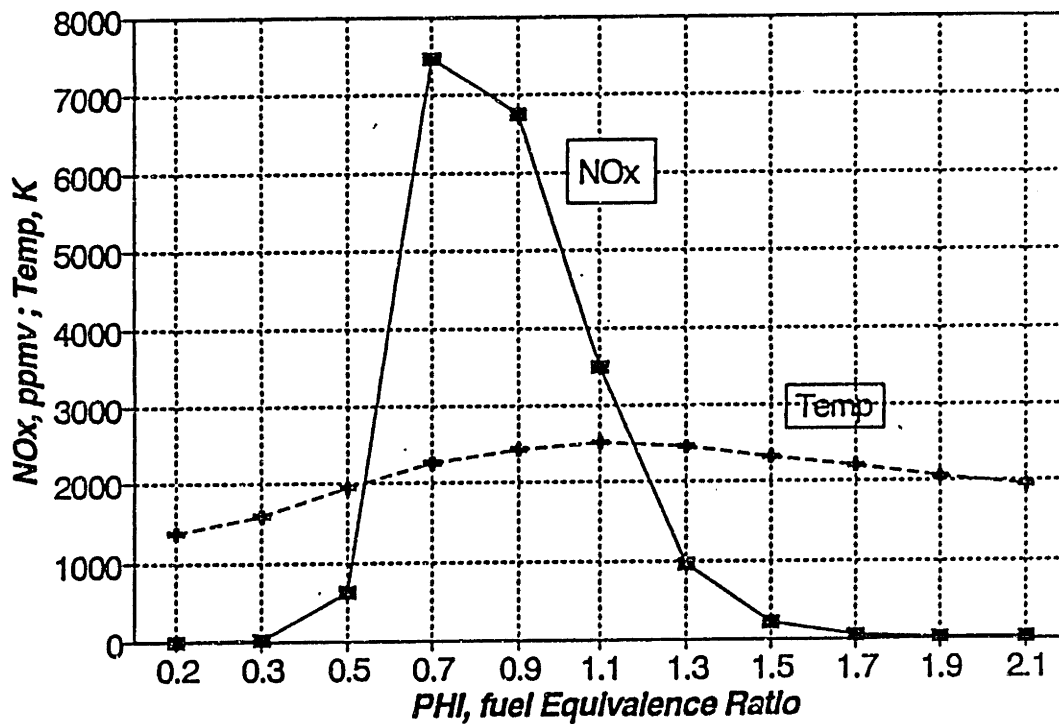


Figure 2.10 Adiabatic flame temperature and TBN versus fuel equivalence ratio for 900 K initial combustion air temperature. 500 ms residence time.

2.4.3 No. 6 Fuel-Oil Modeling Results

Figure 2.11 shows the evolution of TBN and its constituents (NO, HCN, NH₃) for a fuel equivalence ratio of 1.5, a fuel-N content of 0.3% wt., and isothermal conditions at 1900 K. Two important qualitative features can be deduced from the figure: first, that, after the first few milliseconds, NO constitutes the greater part of TBN; and second, that the maximum TBN decay rate occurs when HCN accounts for the majority of TBN. Once the HCN is oxidized to NO, the TBN decays much more slowly, indicating that the NO reburn reactions are much slower than HCN conversion to N₂. A future NO_x control strategy, then, might focus on delaying the HCN oxidation.

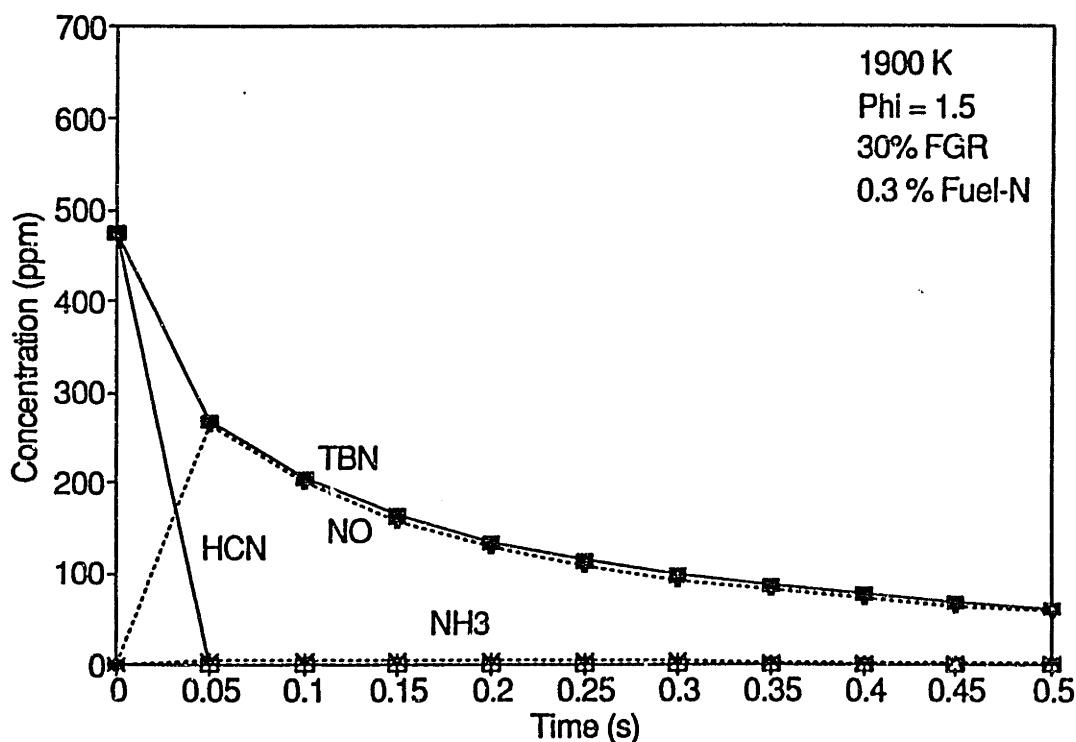


Figure 2.11 Time evolution of bound nitrogen species assuming isothermal conditions at 1900 K for a fuel equivalence ratio of 1.5. 0.3 wt % fuel-N.

Figure 2.12 shows the calculated TBN after removing the original fuel-N, all else being the same. In this case, we see that the calculated TBN is much lower than before, and remains approximately constant. The 10 ppm concentration can be taken as the lower limit of TBN if it

were possible to convert all the fuel-N to N_2 , with prompt NO being the remaining source of TBN (thermal NO production is negligible at this temperature and equivalence ratio.) A direct comparison of the fuel-N containing mixtures to those without fuel-N is made in Figure 2.13 over a wide range of equivalence ratios, showing that in all cases the majority of TBN is formed through fuel-N oxidation, not the prompt or thermal mechanisms, for the 500 ms residence time considered.

The effect of fuel equivalence ratio and combustion temperature on TBN is shown in Figures 2.14 to 2.17 (assuming isothermal conditions). As before, the fuel-N content is 0.3% wt. Each figure represents a "snap shot" at a particular residence time. The figures indicate that for all considered conditions, increasing residence time reduces TBN. Furthermore, an optimum fuel equivalence ratio exists for each combustion temperature, beyond which TBN increases as the mixture becomes deficient in the radicals needed to convert fuel-N and NO. However, as temperature is increased the available radical pool is enlarged, counterbalancing this effect, as shown by the down and rightward shift in NO concentration minima with higher temperature in Figures 2.15, 2.16, and 2.17.

It should be noted that at short residence time, is short the relationship between temperature, equivalence ratio, and TBN is not quite as simple, as shown in Figure 2.14, where the residence time is 20 ms. In this case, the competing thermodynamic and kinetic effects must be taken into account. First, increasing the combustion temperature increases the equilibrium TBN concentration for a given equivalence ratio. Second, increasing equivalence ratio lowers the equilibrium TBN concentration. Thus if a mixture contains a given mole fraction of TBN, and if the equivalence ratio is such that the initial mole fraction of TBN greatly exceeds the equilibrium value, then increasing the combustion temperature will increase the TBN decay rate, despite the attendant increase in equilibrium TBN concentration. Conversely, if the equivalence ratio is such that the equilibrium TBN mole fraction approaches the initial TBN mole fraction, increasing the temperature will only increase the rate at which the mixture approaches a higher TBN value.

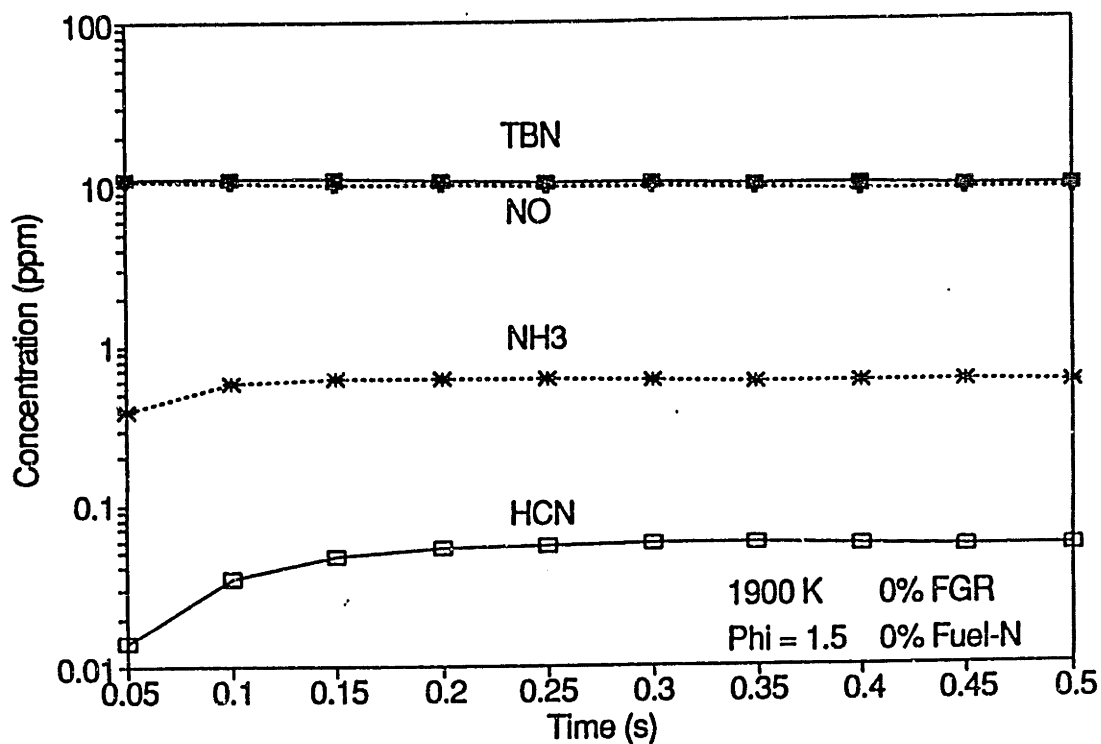


Figure 2.12 Time evolution of bound nitrogen species assuming isothermal conditions at 1900 K for a fuel equivalence ratio of 1.5. Zero fuel-N.

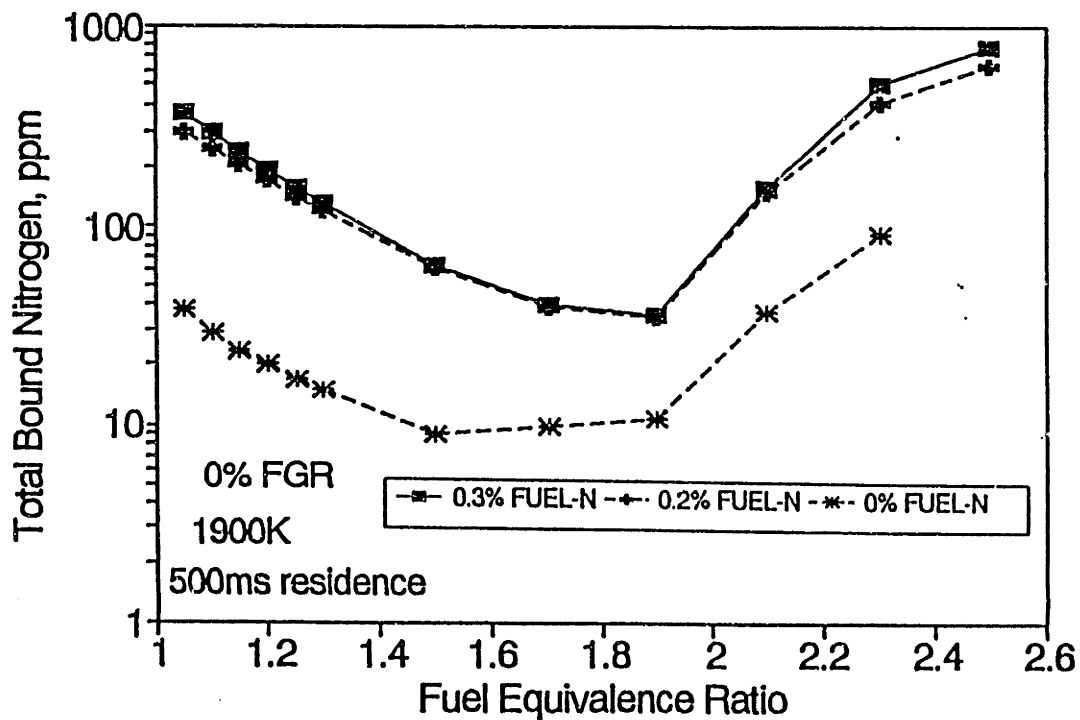


Figure 2.13 TBN versus fuel equivalence ratio for 0, 0.2, and 0.3 wt % fuel-N. TBN computed after 500 ms of isothermal reaction at 1900 K.

These factors explain the trends observed in Figure 2.14. At equivalence ratios below 1.3, the temperature-TBN relation is inverted, with the 1400 K condition leading to lower TBN concentrations than the 1700 K or 1900 K conditions, as shown in Figure 2.14. This is due to the fact that for equivalence ratios below 1.4, the equilibrium TBN concentration rises with temperature to values approaching the initial mixture mole fraction.¹⁹ For an equivalence ratio between 1.3 and 1.5, the 1700 K condition yields the lowest TBN concentration. Finally, at equivalence ratios greater than 1.5, the 1900 K case gives the best results.

When the residence time is increased to 200 ms or greater, then the temperature-TBN relationship is simplified, with higher temperature always yielding lower TBN, as shown in Figures 2.15, 2.16, and 2.17. The implication for a practical system is that to achieve the lowest TBN, greater residence time, temperature, and fuel equivalence ratio are beneficial for converting fuel-N to N₂, provided that they are increased in the proper relation. For instance, as shown in Figure 2.14, increasing fuel equivalence ratio beyond 1.3 could increase or decrease TBN, depending on the temperature.

¹⁹Beér et al [1981]

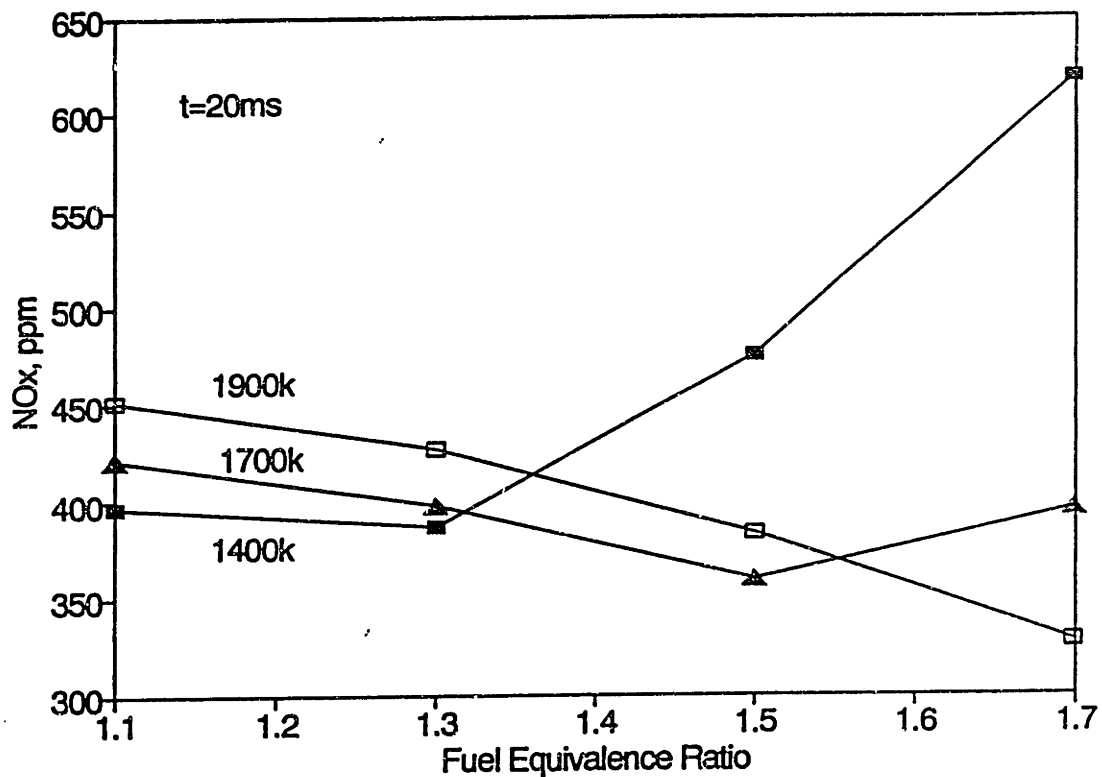


Figure 2.14 TBN versus fuel equivalence ratio after 20 ms residence time for three isothermal cases, 1700 K, 1800 K, and 1900 K 0.3 wt % fuel-N.

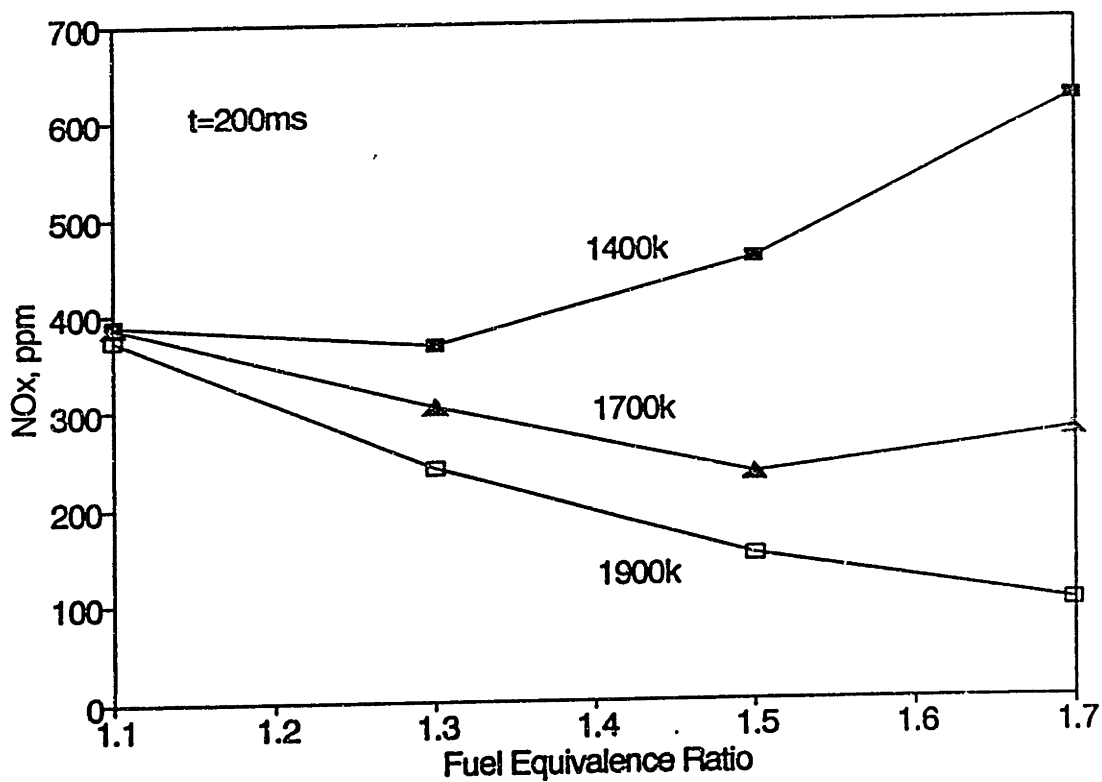


Figure 2.15 200 ms residence time.

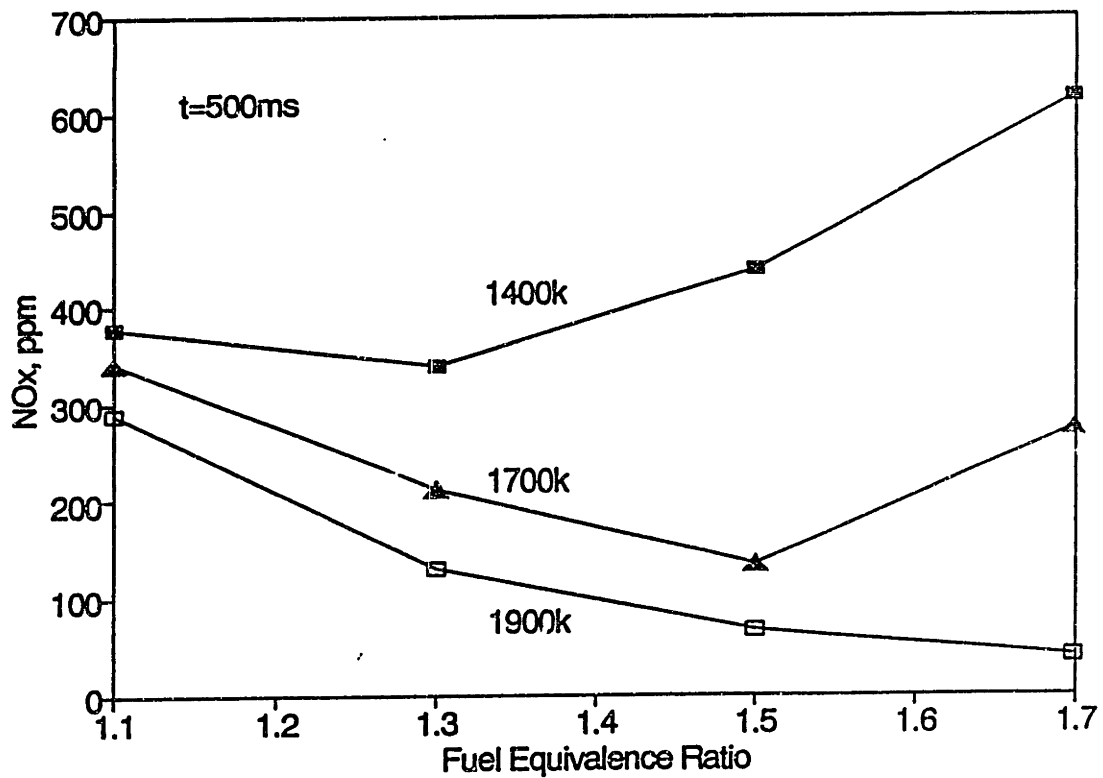


Figure 2.16 500 ms residence time.

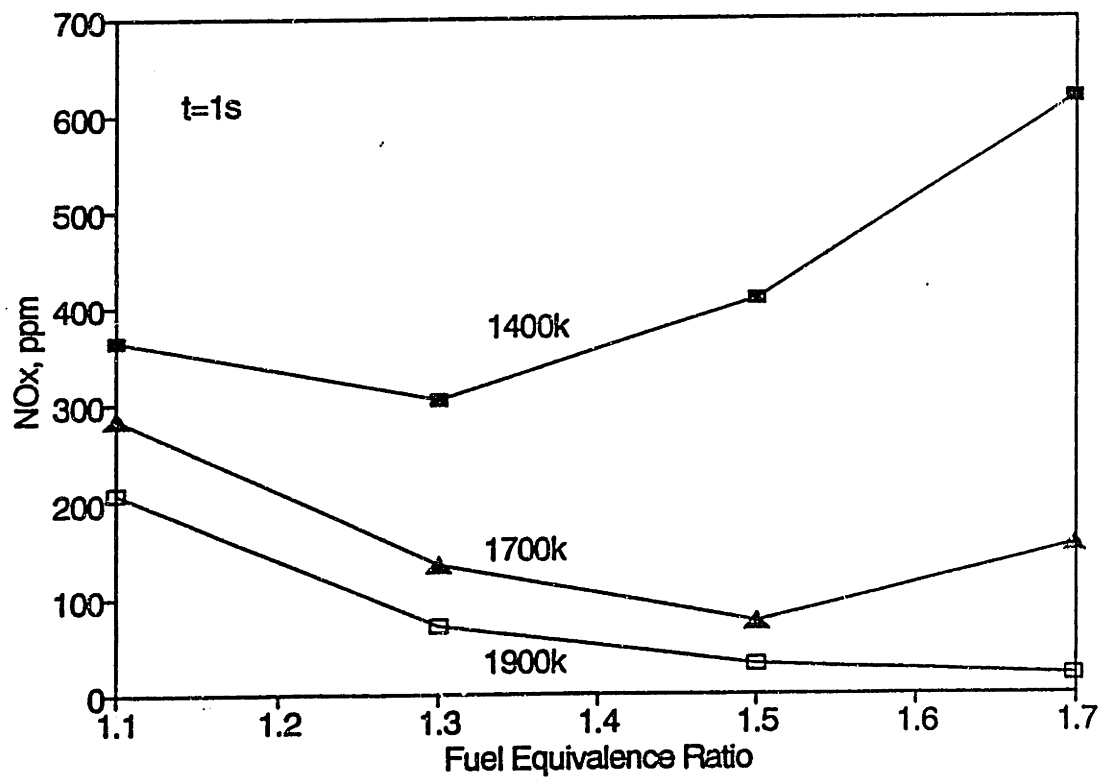


Figure 2.17 1 s residence time.

2.5 NO_x Chemistry and The RSFC Burner

The RSFC burner was designed to utilize the NO_x control techniques described above by creating a flow field that, in effect, induces 'internal' staging and FGR. As discussed above, an optimum combustion process would allow the fuel-air-products mixture a relatively long residence time at high temperature, fuel-rich conditions, followed by a relatively rapid fuel-lean burnout where the temperature is significantly lower than the adiabatic combustion temperature, but high enough to ensure complete burn out.

The primary question that will be addressed in the forthcoming chapters focuses on whether the RSFC burner can create such conditions, and particularly how the 'internal' staging process compares to the traditional 'external' method which utilizes over-fire air. What follows, then, is a discussion of the RSFC burner aerodynamics, and how it performs in experiments.

CHAPTER 3

RSFC Burner Aerodynamics

Combustion air staging has proven to be highly effective for reducing NO_x emission in a number of practical systems. Typically, these systems rely on physically separate fuel-rich and fuel-lean combustion zones, between which “overfire” air is injected. Drawbacks to this method include higher operating costs, corrosion of the heat transfer surfaces in the fuel-rich first stage, and difficulty in retrofitting existing systems due to a lack of space or other limiting factors.

As an alternative to relying on physically separate combustion zones, the Radially Stratified Flame Core (RSFC) burner was designed to implement staging by aerodynamic means, so that all of the combustion air is introduced at one location. This process is referred to here as ‘internal staging.’ In principle, it can be implemented in retrofit applications relatively easily, and is unlikely to cause additional corrosion because the fuel-rich mixture never contacts the heat transfer surfaces.

Analogous to the conventional overfire air systems, the RSFC burner aerodynamically creates two combustion zones, one characterized by a high degree of radial stratification, and the other characterized by mixedness. In the stratified region, a hot, central fuel-rich flame core, which is created by injecting a small portion of the combustion air near the central fuel jet, is surrounded

by relatively cool combustion air, which, under the proper fluid dynamic conditions, admixes gradually. As a result, the fuel, which is contained within the core, pyrolyzes in a locally fuel-rich 'first-stage.' Further downstream, the stratification breaks down, and the surrounding combustion air mixes with the fuel-rich core, creating a fuel-lean burnout stage. The process is illustrated in Figure 3.1.

These two 'stages' are produced by imposing swirl on the combustion air. In the first stage, stratification is maintained by reducing turbulent mixing at the fuel-air interface by swirl-induced turbulence damping, as explained below. The second stage results from vortex breakdown in the swirling flow, leading to vigorous mixing between the peripheral combustion air and the fuel-rich pyrolysis products.

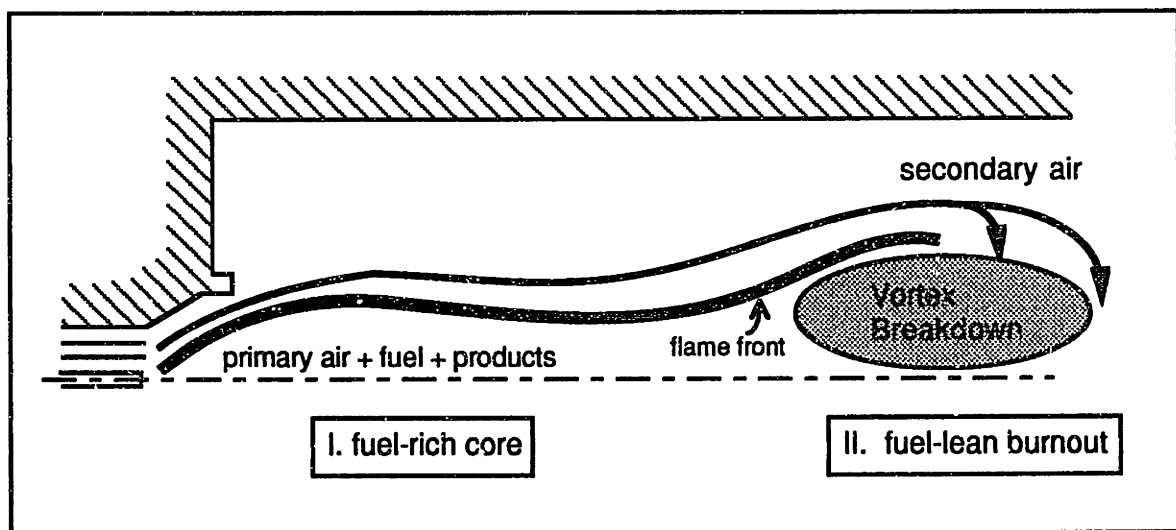


Figure 3.1 Internal staging schematic.

3.1 Turbulence Damping

A key fluid dynamic phenomena on which stratification depends is turbulence (and turbulent mixing) damping at the flame core - secondary air interface. With RSFC flames, turbulence

damping results from a swirl-induced centrifugal force field acting on a radial density gradient which is set up by the density difference between the hot burning core and the surrounding air. Turbulence damping reduces radial fluid interchange between the fuel jet and surrounding air, resulting in a radially stratified flow in which relatively cool, dense combustion air remains at the periphery of a hot, less dense, core for an extended mixing length. The concept originated in the work of Rayleigh (1916), which showed that a rotating fluid is stable with regard to radial interchanges if ρWr , the product of density, tangential velocity, and radial position, increases with radial distance from the axis of rotation.

Chigier and Beér (1971) demonstrated this principle with the famous rotating-screen experiments, in which a turbulent diffusion flame was laminarized by rotating a perforated screen around a central burning fuel jet, imparting swirl on the surrounding air. Schlieren photographs showed the presence of large-scale turbulent eddies when the screen was stationary; when it was rotated, the eddies disappeared, resulting in an elongated laminar flame with a greatly reduced in-flame oxygen concentration. This experiment ultimately led to the RSFC burner concept.

The turbulence damping mechanism in RSFC burner flames can be explained by considering an axial fuel jet burning in a coaxial swirling air flow. When an individual eddy displaces colder (denser) air toward the flame axis, or hotter material outward, work is expended in the centrifugal force field, dissipating turbulent energy. Following Prandtl's mixing length theory, the radial fluctuating velocity for a flow in cylindrical coordinates (r, z), with local mean tangential and axial velocity components W and U , respectively, can be expressed in the form

$$v' \propto \ell \frac{dU}{dr}$$

where ℓ is the mixing length and $\frac{dU}{dr}$ is the radial gradient of the time mean axial velocity of the jet. The kinetic energy of radial motion for a fluid element of volume V and density ρ can then be expressed as

$$\frac{1}{2}\rho V(v')^2 \propto \frac{1}{2}\rho V\ell^2\left(\frac{dU}{dr}\right)^2$$

The work done by moving a fluid element which is in equilibrium with its surroundings in an annular layer of radius r in the rotating flow by a distance ℓ is given by

$$\int_0^\ell F d\ell = -\frac{1}{2} \frac{d\rho}{dr} \frac{W^2}{r} V\ell^2$$

where the radial displacement is taken as equal to the mixing length, and where F is the force $\frac{W^2}{r} \frac{d\rho}{dr} \ell V$. Equating kinetic energy of turbulent motion with the work done by radial displacement of the fluid yields

$$\frac{1}{2}\rho V\ell^2\left(\frac{dU}{dr}\right)^2 = \frac{1}{2} \frac{d\rho}{dr} \frac{W^2}{r} V\ell^2.$$

When this equation is satisfied, turbulence is completely damped. Beér et al. (1971) recommended a non-dimensional criterion, based on this equation, for the quantitative characterization of turbulence damping, which they called the modified Richardson number,

$$Ri^* = \frac{\left(\frac{1}{\rho}\right)\left(\frac{\partial\rho}{\partial r}\right)\left(\frac{W^2}{r}\right)}{\left(\frac{\partial U}{\partial r}\right)^2}$$

While $Ri^* = 1$ corresponds to complete damping, Beer et al. found that turbulence damping is initiated at values of Ri^* as low as 0.04. In recent work with natural gas RSFC flames²⁰, velocity and temperature measurements were used to plot values of Ri^* in the near burner field. The maximum values of Ri^* were located near the fuel-air interface, demonstrating the value of turbulence damping in containing the fuel near the flame axis.

²⁰Toqan et al [1992]

3.2 Swirl and Flame Structure

Apart from its role in turbulence damping, combustion air swirl can affect the flow field by inducing an internal recirculation zone (IRZ), which by recirculating downstream combustion products has a significant impact on flame chemistry; conventionally, swirl is used to stabilize flames by bringing back high temperature products that are rich in H, O, and OH radicals.

The size, strength, and position of the IRZ are functions of swirl number, a non-dimensional ratio of axial and angular momenta:

$$S \equiv \frac{G_z}{G_x R}$$

where R corresponds to the equivalent burner radius. Past experimental studies on swirl indicated that for $S > 0.6$, the adverse pressure gradient along the jet axis cannot be further overcome by the axial momentum, and a recirculating flow is set up in the central portion of the jet between two stagnation points.²¹

The International Flame Research Foundation (IFRF) established a classification scheme that differentiates 4 possible flame types that result from the interaction between air swirl and fuel jet momentum.²² Type I flames are comparatively long and are distinguished by two ignition zones: a short bulbous zone near or in the burner quarl, followed by a long tail. A necessary condition for Type I flames is that the fuel jet momentum be great enough to allow the jet to penetrate through the IRZ. As shown in Figure 3.2.1, the internal reverse flow zone set up by the swirling combustion air occurs in a closed annular zone around the fuel jet. Hot combustion products and some fuel “peel off” the fuel jet during its passage through the reverse flow zone, and are carried back into the quarl. The remainder of the fuel is burned in a long second zone

²¹Chigier and Beér [1983]

²²Fricker and Leuckel [1970]

where the gas jet slowly mixes with the surrounding air. Typically, low NO_x RSFC flames fall within the Type I category.

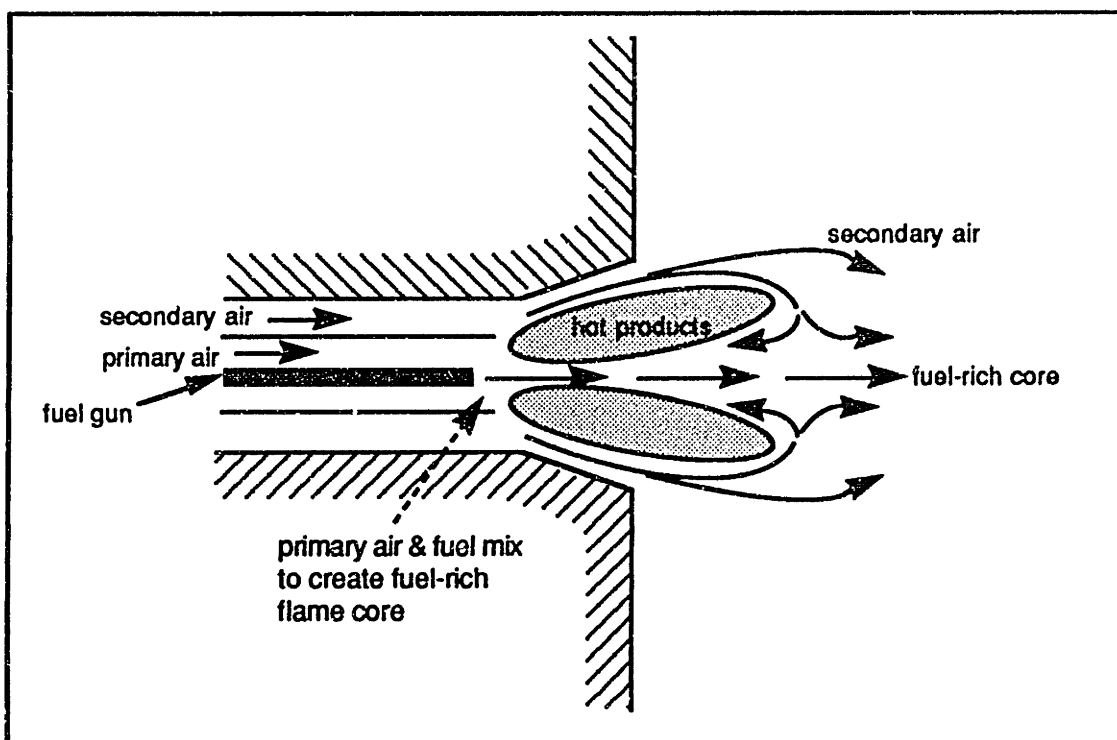


Figure 3.2.1 Near burner flow field for a Type I RSFC burner flame. Fuel jet pierces reverse flow zone set up by swirling annular air jet. Typical for low NO_x RSFC flames.

Type II flames are short and intense and, like the Type I flames, are stabilized by an IRZ which extends into the burner quarl. The difference between the two flame types is that the fuel-jet momentum of the Type II flame is insufficient to allow the fuel to penetrate through the IRZ; instead, the fuel jet is spread radially outwards by the reverse flowing combustion products, as shown in Figure 3.2.2. As a result, the combustion zone is dominated by the IRZ, which effectively acts as a well stirred reactor, precluding radial stratification. Type II flames can be created by imposing very high swirl on the combustion air, or by introducing the fuel at a low velocity. These flames typically emit high levels of NO_x.

Type III and IV flames occur under conditions of very low swirl, where a long, low intensity flame is formed. No internal reverse flow zone is set up, and the flame does not fill the burner quarl, in contrast to the Type I and II flames. Type IV flames are different from Type III flames in that the fuel jet velocity is greater, resulting in lift-off from the burner throat. Type III and IV flames are not inherently stable.

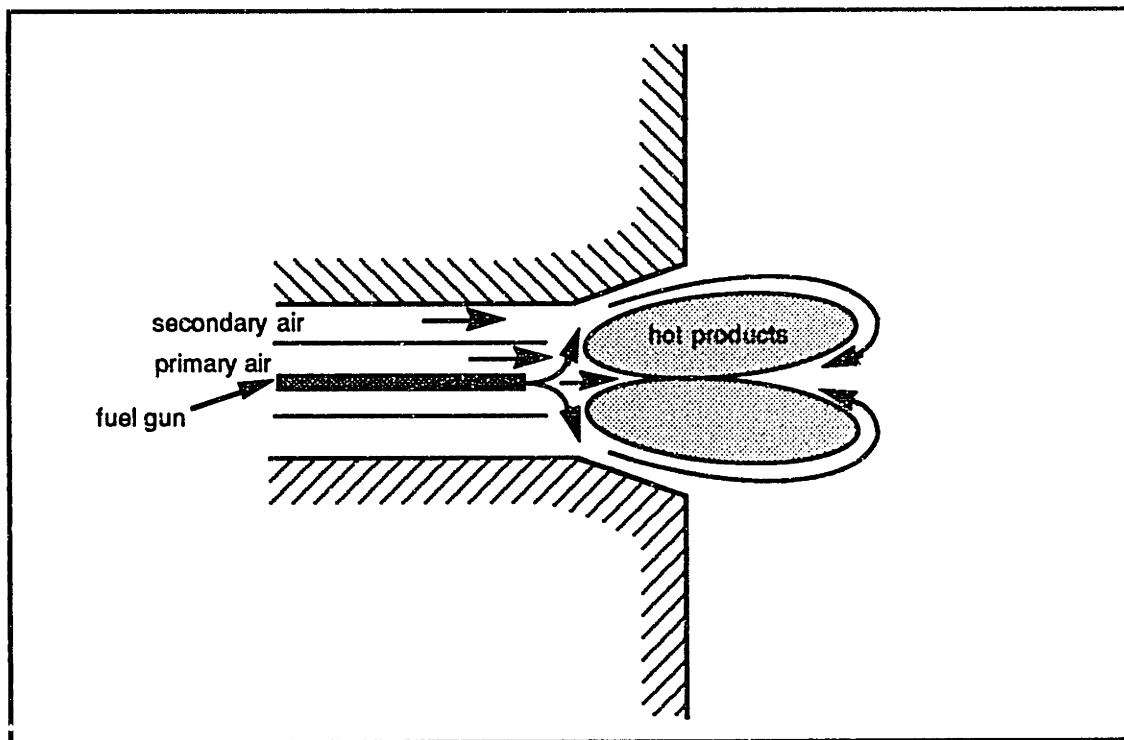


Figure 3.2.2 Near burner flow field for a Type II RSFC burner flame. Fuel jet spreads radially outward around reverse flow zone and mixes rapidly with the annular air jet.

3.3 Aerodynamics of RSFC burner flames

Figure 3.3.1 illustrates the important aerodynamic features of a 'typical' low NO_x RSFC burner flame; it is based on qualitative and quantitative data compiled during the many test runs carried out over the past 2 years. An initial fuel-rich flame core is created by mixing initiated within the

burner between the central fuel jet and the primary air. The secondary air, typically constituting 85% of the total burner air, is introduced through a radially displaced annulus. Therefore the flow is radially stratified from the outset, though turbulence damping is needed to maintain stratification over an extended length.

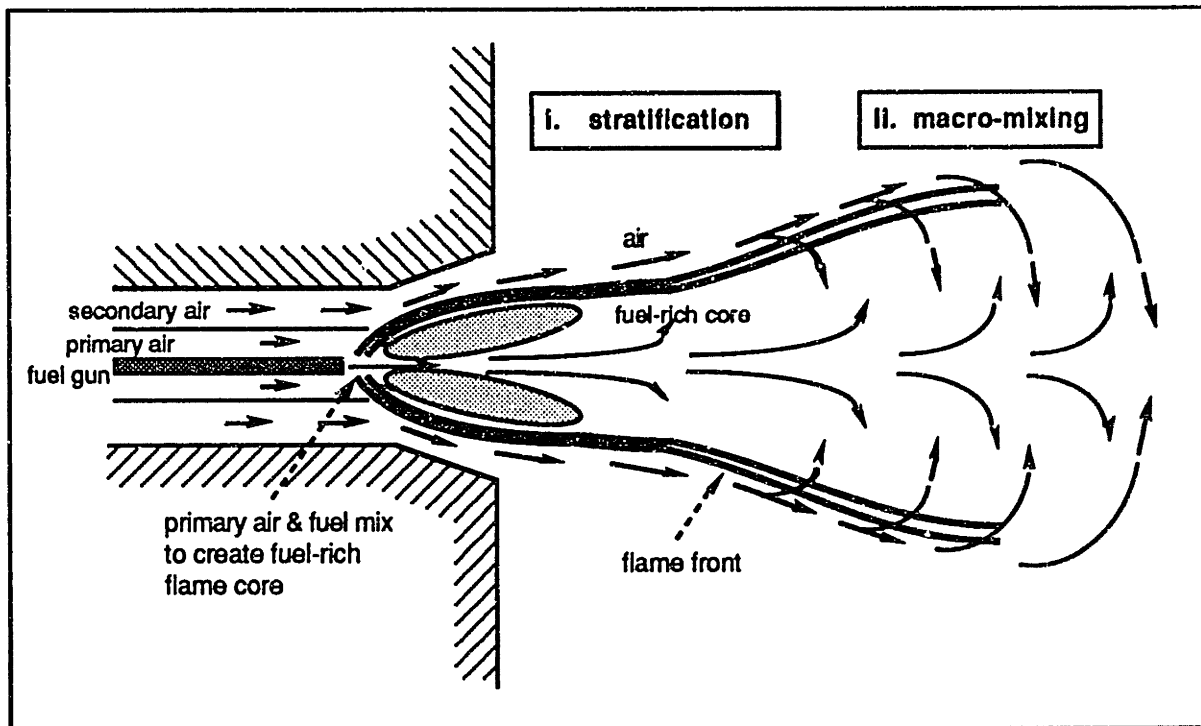


Figure 3.3.1 Typical low NO_x RSFC flow field.

In previous research with low NO_x natural gas RSFC flames, axial velocity measurements indicated the presence of an annular internal recirculation zone which extended into the burner quarl, as shown in Figure 3.3.2. The central methane jet, shown in Figure 3.3.3, penetrated through the IRZ, leading to a Type I flame structure. This structure was duplicated in the experiments described in Chapters 4 and 5.

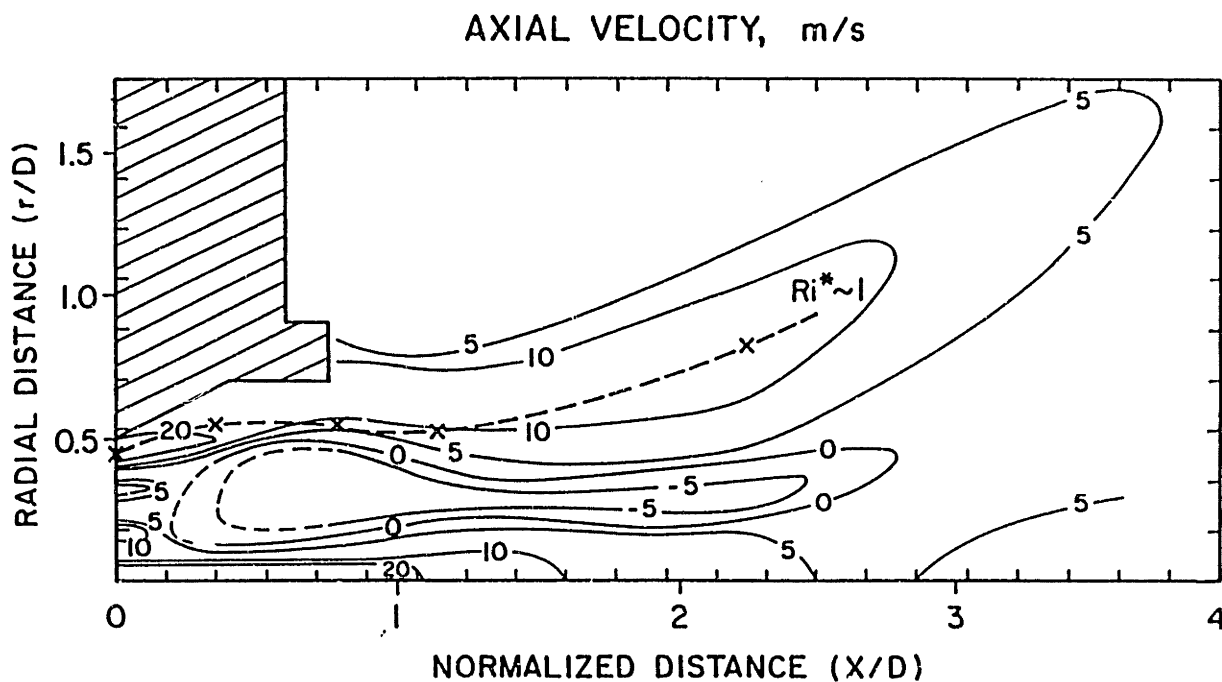


Figure 3.3.2 Measured axial velocity in a low NO_x natural gas RSFC burner flame. (Toqan et al 1992)

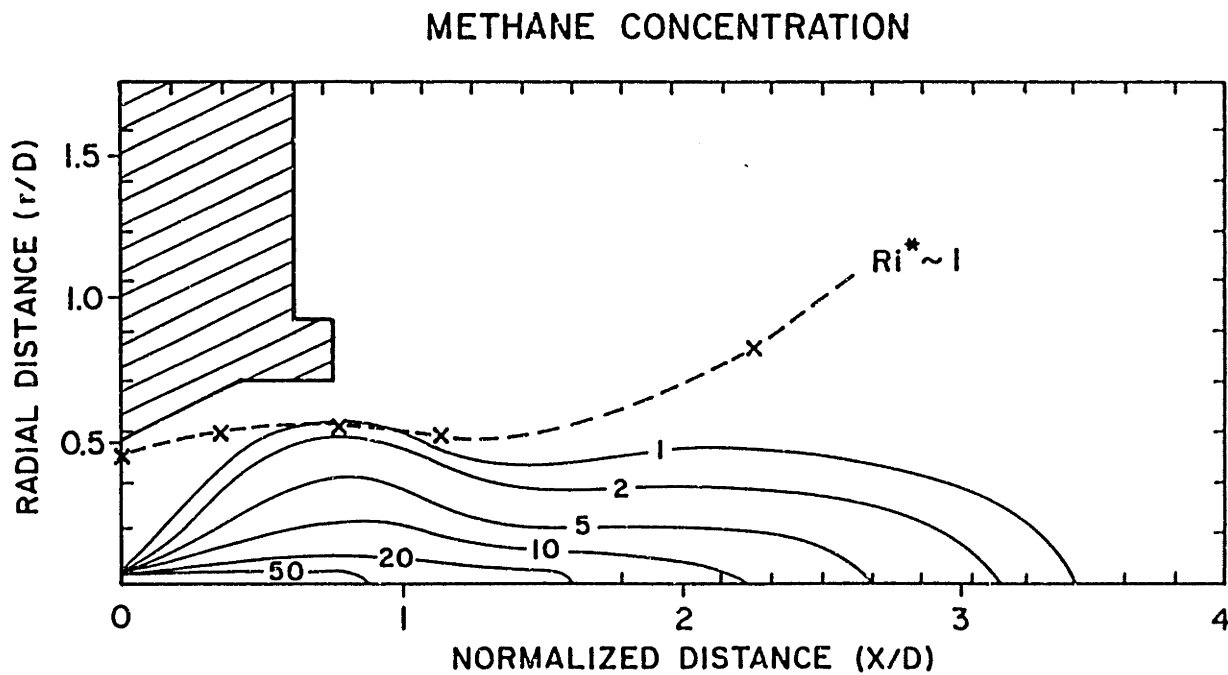


Figure 3.3.3 Measured methane concentration.

Further downstream of the burner (~ 5 burner diameters), stratification ends, largely due to the decay in tangential velocity, and the remaining secondary air mixes rapidly with the fuel-rich core, completing the combustion. With sufficiently high swirl on the secondary air supply, a second IRZ forms due to vortex breakdown and assists in mixing the fuel-rich and fuel-lean streams. The swirl number is not always sufficiently large to induce the second IRZ, though it is typically high enough to cause a reduction in axial velocity several diameters downstream of the burner near the flame axis, resulting in the classical “double-hump” radial velocity profile, as can be seen in Figure 3.3.2 at $X/D = 3$. The resulting shear allows sufficient mixing between the products of the fuel-rich core and the remaining combustion air to ensure complete burnout.

The key low NO_x design criteria for RSFC flames is the length of the stratified region, particularly for nitrogen containing fuels, for which an extended residence time is required to convert fuel-N to N₂ within the stratified zone. Experiments with swirl, reported in Chapter 5, were designed to determine whether the length of the fuel-rich core is sufficient for low NO_x combustion with No. 6 fuel oil.

CHAPTER 4

Experimental Method and Apparatus

4.1 Experimental Objectives

Prior to the beginning of this project, experiments with the RSFC burner focused on empirically validating the concepts described in the previous chapter. These experiments successfully used natural gas to demonstrate the viability of the RSFC burner in a real system, resulting in 15 ppm NO_x emission. Detailed velocity and gas composition measurements with natural gas flames showed that radial stratification via swirl-induced turbulence damping was responsible for the observed low NO_x emission.²³

Having demonstrated the basic principles, and shown the viability of the RSFC with natural gas, the focus of the experimental work shifted to investigate the use of heavy fuel-oil in the RSFC burner, the focus of this thesis. Four questions were posed at the outset:

- Is the residence time and temperature in the fuel-rich core sufficient to allow fuel- N conversion to N₂? What can be done to improve this process?
- What is the optimal burner configuration (air distribution, velocity, atomizers swirl) for oil combustion?

²³Sun [1994]

- Can NO_x emission be further reduced by combining external staging with the RSFC? If so, what does that imply about the effectiveness of the RSFC's internal staging process?
- What is the effect of flue gas recirculation on NO_x emission, particularly in relation to fuel-N reduction chemistry?

The experiments described in the following sections were designed and implemented to answer these questions, with the ultimate purpose of generating a design and operating protocol for low-NO_x oil combustion with the RSFC burner.

4.2 Methodology

The experimental work can be divided into two categories: parametric, and detailed flame structure studies. The parametric studies were used to examine the functional relationships between NO_x emission and: swirl, combustion air velocity and radial distribution, external air staging, firing rate, and fuel-jet angle. The detailed flame structure study consisted of taking measurements of temperature and gas composition at many locations within a parametrically optimized flame in order to elucidate the overlapping mixing and chemistry processes, and to explain the observed parametric relationships.

4.2.1 Parametric Studies

The test matrix shown in Table 4.2.1.1 summarizes the parametric studies that were performed with the RSFC burner. In each case, the parameter of interest was varied and the exit NO_x recorded. In addition, when primary and tertiary air swirl were varied, axial profiles of centerline species concentration and temperature were taken as a check on the relation between mixing suppression and swirl, and as an indication of the length of the fuel rich core; a high oxygen concentration measurement at the centerline, for example, indicates that the fuel-rich core has ended upstream of that particular axial location.

Table 4.2.1.1 Experimental matrix for parametric study.

Experiment	Parameters Varied	Experimental Ranges
I. Swirl	Swirl number, primary tertiary	0.1 - 0.3 0.0 - 0.6
II. External staging	First stage equivalence ratio Position of over-fire air injection Burner inserts (p,s,t)	0.95 - 1.5 1.8 or 3.4 m from burner (3.5, 6.8, 10.5) or (3.5, 7.25, 11) inches
III. FGR	Amount recirculated	0 - 20 %
IV. Firing rate	Thermal input Atomizer type/ medium	0.3 0-1.3 MW 0° Y-jet/air Sonicore/steam
V. Atomization	Atomizer type Fuel jet angle Atomizing medium Atomization pressure	Y-jet or Sonicore 0°, 5° air (Y-jet only) or steam 60 - 100 psig (air) 20 - 160 psig (steam)

4.2.2 Detailed Flame Structure Study

The detailed study consisted of measuring gas composition and temperature at many axial and radial locations in an optimized flame. Measurements were taken over a half-cross section at each axial location, under the assumption that the flow is axi-symmetric. The purpose here was to study the overlapping mixing and chemistry processes, particularly to address the question of fuel-N conversion. These measurements would indicate whether the fuel was confined to a fuel-rich core, and whether the temperature in the fuel rich region was high enough to allow fuel-N conversion within the available residence time.

From the detailed measurements, contour plots of iso-concentration and iso-temperature lines were generated, allowing an identification of various NO_x producing and reducing zones within the flame. This information, when combined with information from the chemical kinetic studies

(Chapter 2) could then be applied to uncover the important mechanisms of NO_x control with the RSFC burner, and how they can be improved.

4.3 Experimental Apparatus

4.3.1 Experimental Furnace

The MIT Combustion Research Facility (CRF) was used for all of the experiments. The CRF is an approximately 10 m long tunnel furnace that consists of several interchangeable water cooled sections, each with either a bare metal or refractory brick lined surface, and a square (1.2 x 1.2 m) or cylindrical (ϕ 0.5 m) cross-section. The thermal capacity of the CRF is 3 MW, though typically it is operated at 1 MW. Because the furnace has a sectional design, the heat extraction along the flame can be varied to simulate the temperature history of large scale practical flames.

An access door in each of the furnace sections allows measurement of gas temperature and composition with intrusive traversing probes, including a suction pyrometer for temperature, a water cooled suction probe for major species, and a steam jacketed suction probe for hot cell fourier transform infrared (FTIR) spectrometry for various trace species. The sampling methods and furnace have been described in detail elsewhere.²⁴

A schematic of the CRF as used in the experiments is shown in Figure 4.3.1.1. For external staging, the over-fire air injection port was positioned at either 1.8 or 3.4 m downstream of the burner. Another change in furnace configuration can be made by inserting a refractory-lined cylindrical section between the burner and the furnace as a "pre-combustor."

²⁴Farmayan [1980]

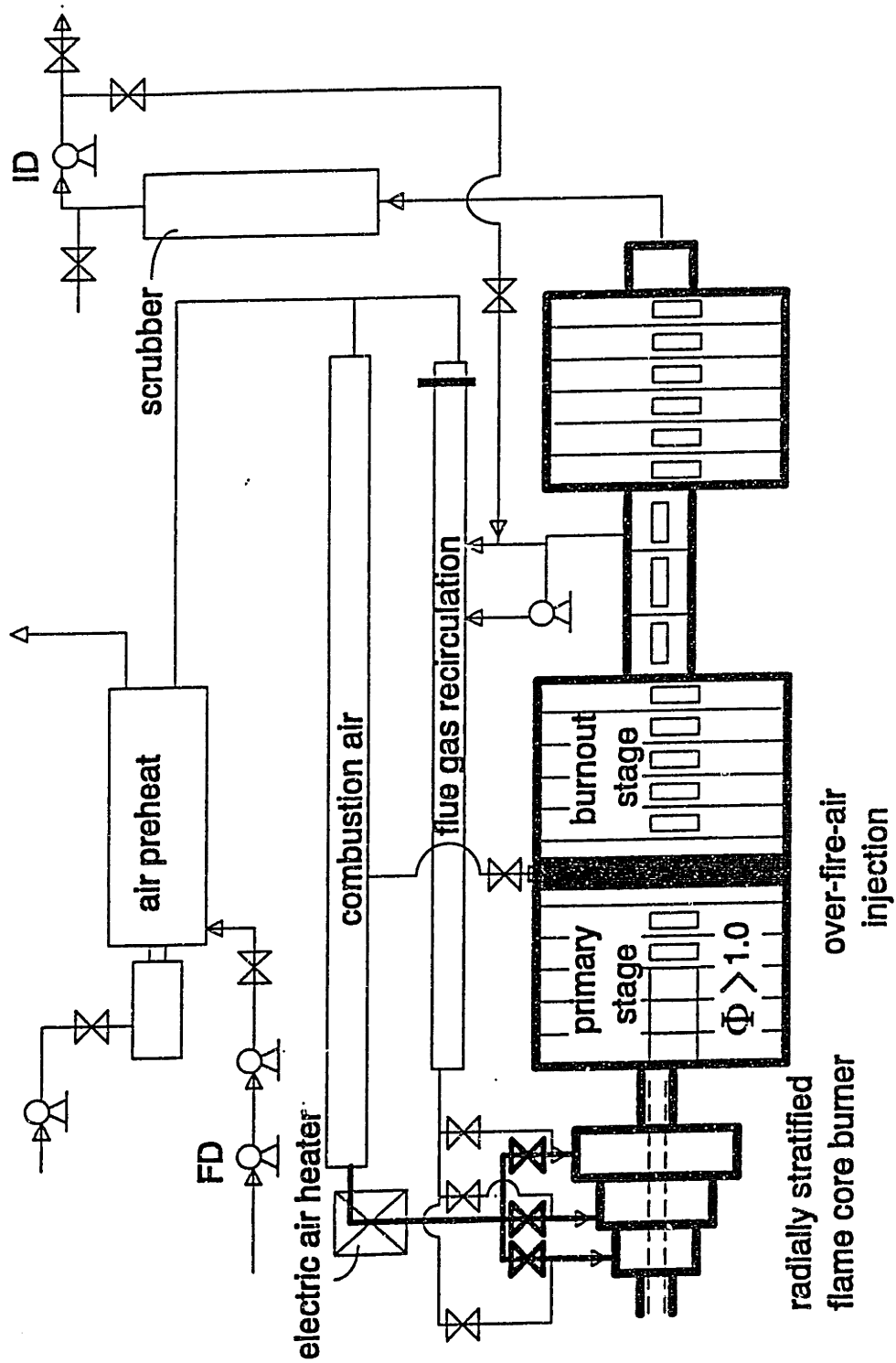


Figure 4.3.1.1 Schematic of the MIT Combustion Research Facility

4.3.2 The RSFC Burner

A schematic of the burner is given in Figure 4.3.2.1. The combustion air is introduced through three concentric annular nozzles, of which the positions of the primary and secondary (as well as the fuel gun) can be adjusted to produce a particular flow field. Each nozzle is equipped with moveable block type swirlers capable of infinitely variable swirl control. The theoretical swirl number of the flow issuing from any nozzle is strictly a function of the burner geometry, and can be calculated for any particular swirl setting. Table 4.3.2.1 indicates swirl number as a function of the swirl setting for the baseline RSFC burner geometry, listed in Table 4.3.2.2. The calculation is based on formulas given in Beér and Chigier (1983).

Table 4.3.2.1 Theoretical swirl numbers for baseline burner geometry.

Swirl Setting	Primary	Secondary	Tertiary
0	0.00	0.00	0.00
1	0.02	0.01	0.04
2	0.04	0.03	0.08
3	0.07	0.04	0.13
4	0.10	0.06	0.18
5	0.13	0.08	0.23
6	0.16	0.09	0.29
7	0.20	0.11	0.35
8	0.23	0.14	0.42
9	0.27	0.16	0.49
10	0.31	0.19	0.57

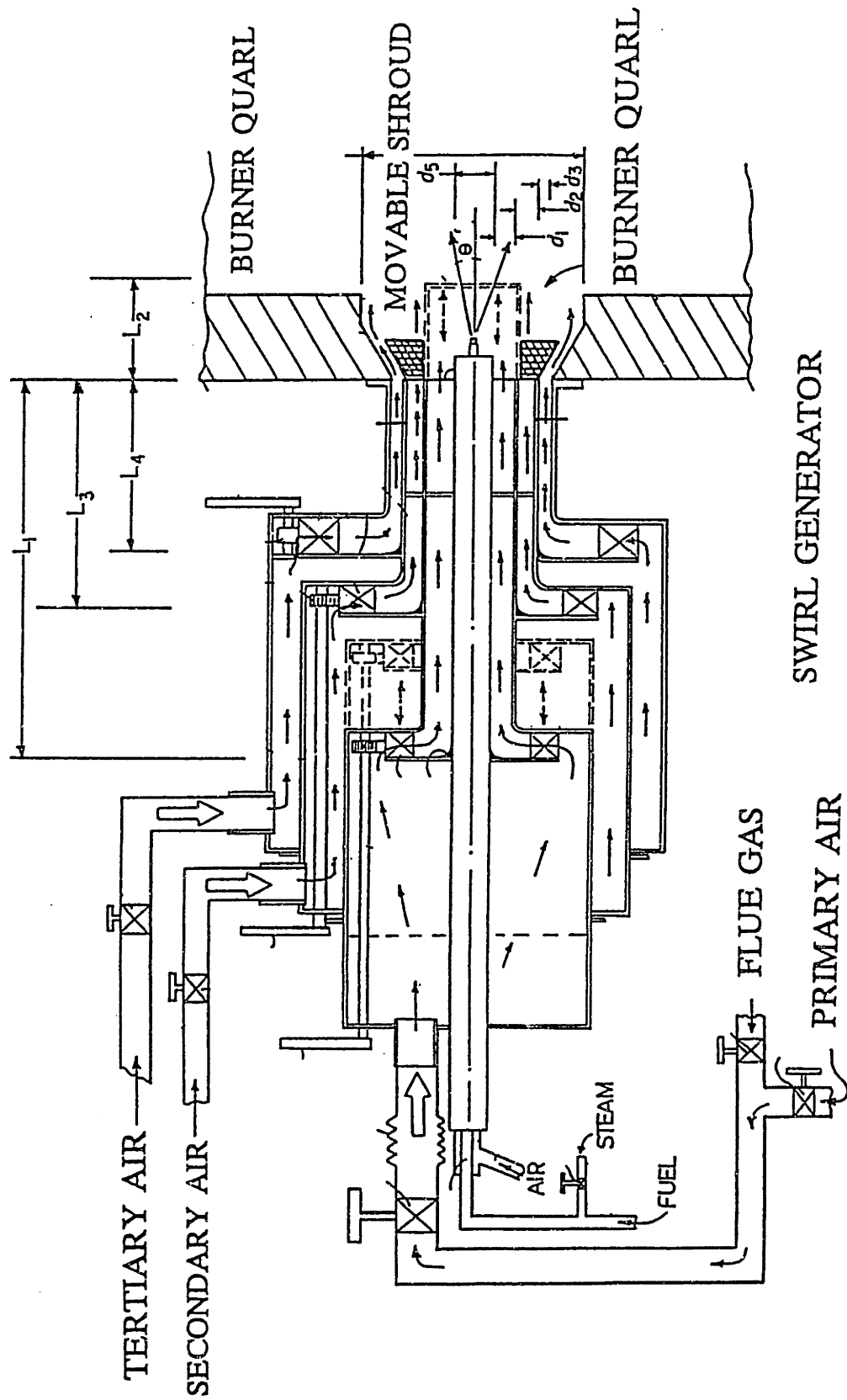


Figure 4.3.1.2 Schematic of the Prototype RSFC Burner

Previous research has shown that to minimize NO_x emission, the majority of the combustion air should be introduced through the tertiary air nozzle, with just enough primary air to ensure stable ignition.²⁵ Accordingly a flow split of 15/85 primary/tertiary air was used during the experiments. The secondary air nozzle was not used; typically it is used to inject recirculated flue gas when burning natural gas.

Table 4.3.2 specifies the burner configuration that was used in all experiments, unless otherwise indicated. Except for the turn-down experiments, the thermal input was maintained at 0.9 MW and the fuel was No. 6 fuel-oil with a 1.5 C/H ratio and a 0.3 wt% N content.

Two twin fluid atomizers, the Y-jet and Sonicore, were used in the experiments, with either air or steam as the atomizing fluid. The Y-jet atomizer, shown in Figure 4.3.2.2, incorporates multi-jet internal mixing, while with the Sonicore atomizer the oil and atomizing fluid mix externally, as illustrated in Figure 4.3.2.3. Because the Sonicore relies on external atomization, it requires a relatively large atomizing fluid flow rate.

Table 4.3.2 Baseline burner geometry.

Barrel	Inner Diameter [in]	Outer Diameter [in]	Swirl Setting	Flow, % of Total Air	Position [in] (flush = 0)
Primary	2.75	3.5	6	15	- 2.6
Secondary	7	7.25	10	0	0
Tertiary	10	11	10	85	0
Fuel gun	x	x	x	x	- 2

²⁵Berg [1991]

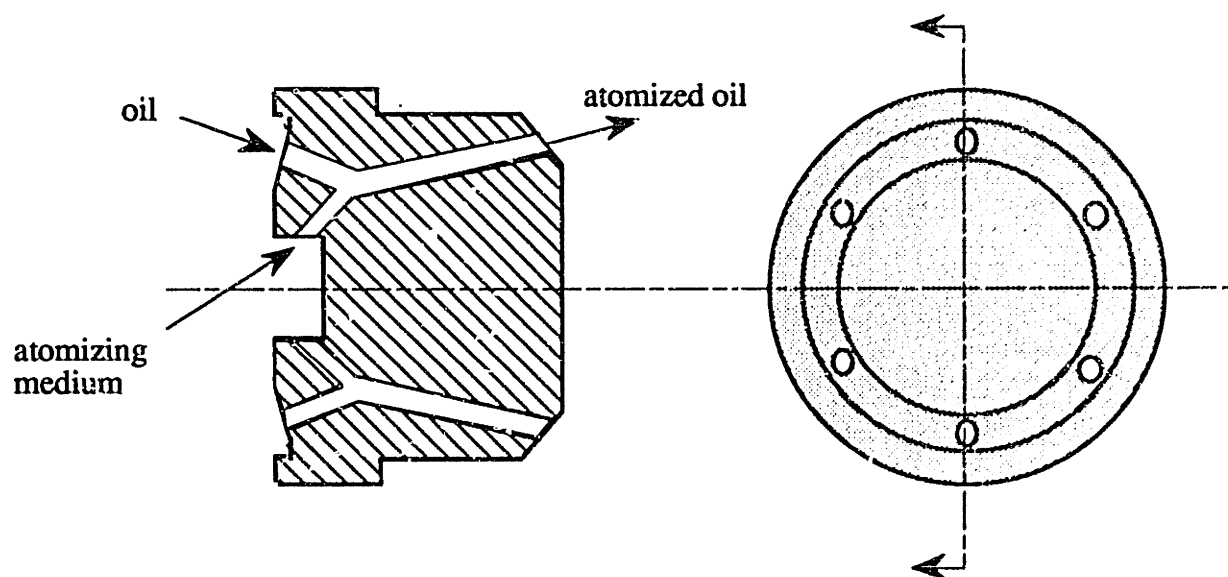


Figure 4.3.2.2 Schematic of a Y-jet atomizer.

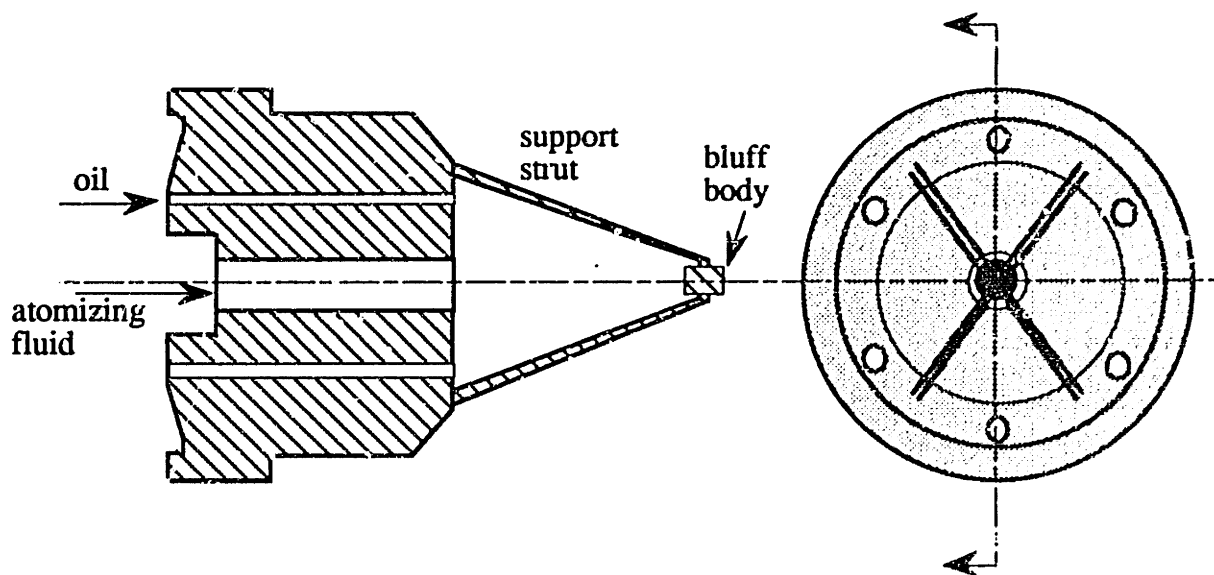


Figure 4.3.2.3 Schematic of a Sonicore atomizer..

CHAPTER 5

Experimental Results

5.1 Primary and Tertiary Air Swirl

Figure 5.1.1 below illustrates the effect of tertiary air swirl on NO_x emission, demonstrating a reduction from 300 ppm at zero swirl, to 120 ppm at the maximum setting, which corresponds to a swirl number of 0.6. The non-zero slope at the maximum setting suggests that further reductions in NO_x might be achieved by modifying the burner to produce a higher tertiary air tangential velocity.

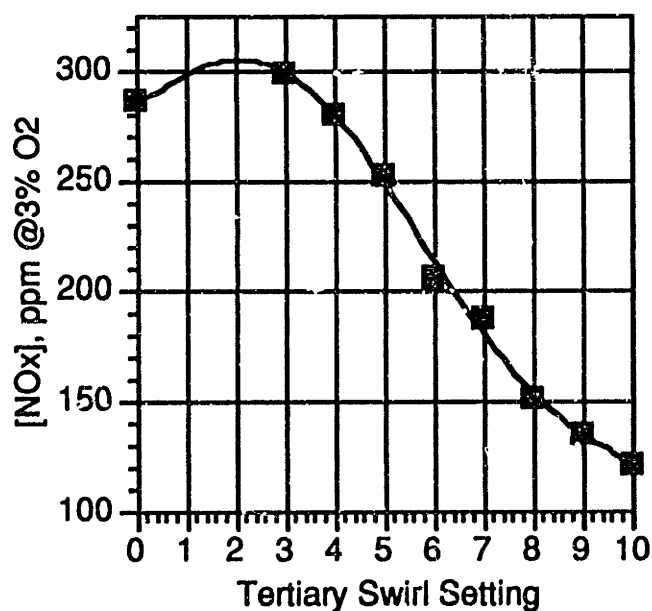


Figure 5.1.1 NO_x emission as a function of tertiary air swirl setting. Data obtained with baseline burner configuration and 5° Y-jet air atomizer (68 psig).

These results are consistent with previous studies on the RSFC burning natural gas, which demonstrated the role of swirl in inducing turbulence damping and thereby producing the desired radial stratification.²⁶ As a simple test that the same process was at work in the oil flames, centerline measurements of gas composition and temperature were taken along the flame axis for maximum and zero tertiary swirl cases. The results, shown in Figures 5.1.2 through 5.1.6 indicate that in the high swirl case, fuel-air mixing is suppressed as would be expected in a Type I stratified flame. Figure 5.1.2 shows that a significant amount of oxygen reaches the flame axis in the no-swirl case, whereas practically none is found at the axis when swirl is applied. Similarly, the CO and CO₂ profiles shown in Figures 5.1.3 and 5.1.4 indicate that with swirl, fuel consumption proceeds more slowly, partly accounting for the lower temperatures shown in Figure 5.1.6.

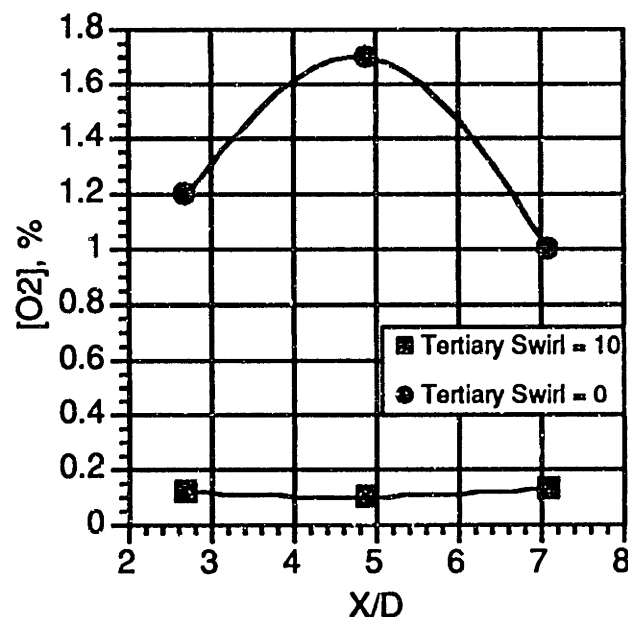


Figure 5.1.2 Axial profile of Oxygen concentration measured at flame centerline for zero and maximum tertiary swirl; axial distance is indicated as burner diameters from burner face. Data obtained with baseline burner configuration and 5° Y-jet air atomizer (68 psig).

²⁶Toqan et al [1992]

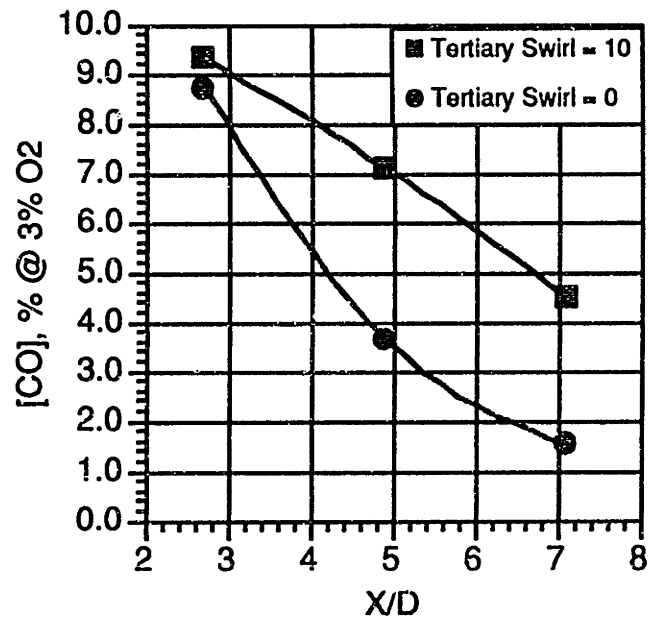


Figure 5.13 Axial profile of CO concentration.

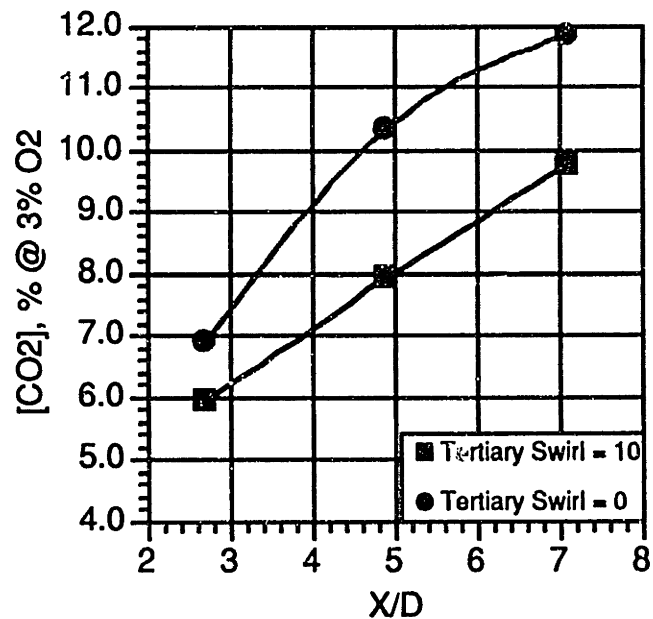


Figure 5.14 Axial profile of CO2 concentration.

These differences account for the striking contrast in NO evolution shown in Figure 5.15. In the no-swirl case, NO concentration increases drastically along the axis, as should be expected given the presence of oxygen, whereas in the maximum swirl case, NO continues to decrease along the axis, since both conditions for NO reduction are met (see Chapter 2): high temperature, and a

fuel rich environment. It is interesting to note that at $X/D = 2.7$, the NO concentration is considerably greater for the high swirl case, possibly due to the fact that the mixture is so rich there that the needed H and OH radicals are present in insufficient concentrations to decompose the NO precursors, such as cyanogen and ammonia species, to N_2 .

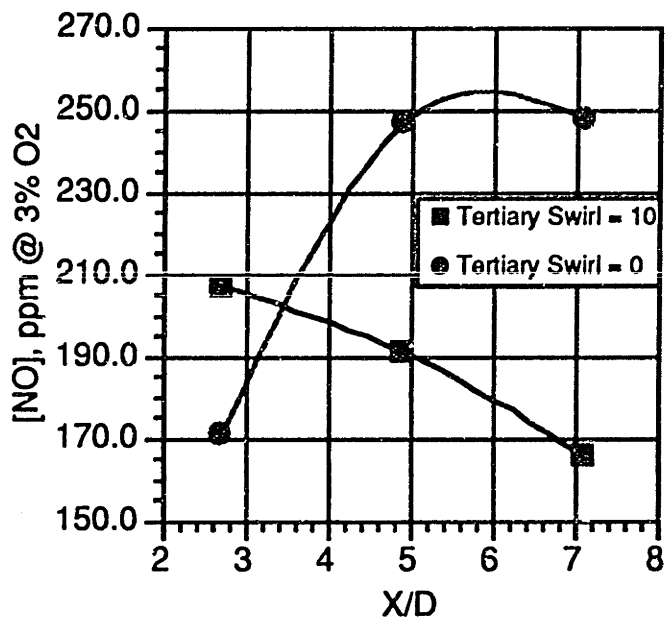


Figure 5.1.5 Axial profile of NO concentration.

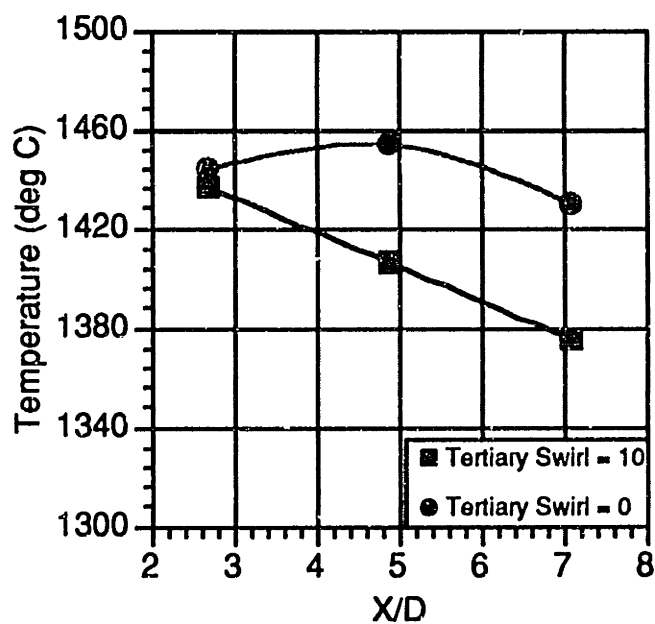


Figure 5.1.6 Axial temperature profile.

Compared to tertiary swirl setting, primary air swirl had the opposite, but quantitatively less significant, effect on NO_x emissions. As shown in Figure 5.1.7, increasing swirl setting from 4 to 10 increased NO_x emission from 92 to 120 ppm. The reason for the opposite trend is that increasing the primary air tangential velocity creates a turbulence-generating shear layer at the fuel-primary air interface, since the fuel jet is introduced with zero tangential velocity. This increasing tangential velocity gradient at the fuel-primary air boundary enhances mixing between the two streams, and tends to reduce stratification very near the burner, resulting in somewhat higher exit NO_x. This increase in mixing rate, however, has the desirable effect of stabilizing the flame; when primary air swirl setting was reduced to below 5, ignition instability became apparent by the soot puffs observed in the TV monitor (fed by a remote camera located at the end of the flame tunnel, oriented facing the burner.)

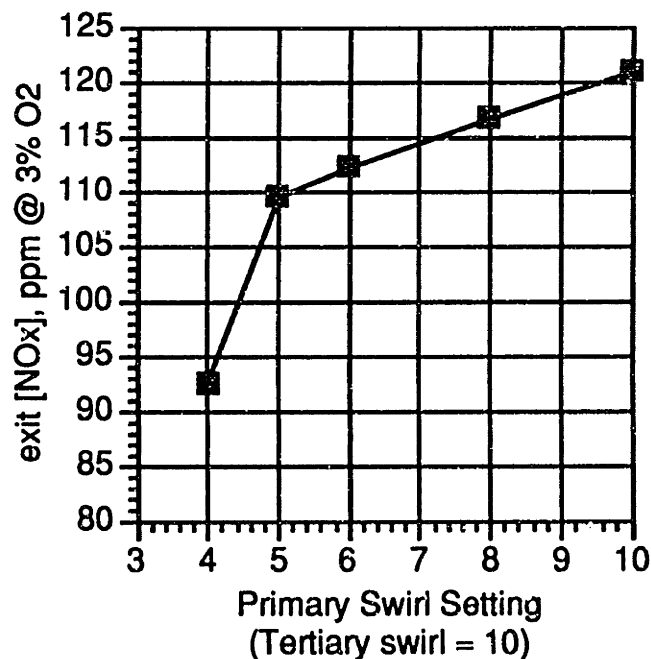


Figure 5.1.7 NO_x emission as a function of primary air swirl setting. Data obtained with baseline burner configuration and 5° Y-jet air atomizer (68 psig).

It should be noted that reducing the primary swirl setting reduces the pressure drop through the primary barrel, resulting in an increased throughput. Relative to the changes caused by increased

swirl, however, this effect is secondary. For example, if the increased throughput were a dominant effect, observed soot would decrease, not increase, with decreasing swirl setting.

Table 5.4.1 indicates the relationship between visually observed soot and primary air swirl. Increasing the air atomization pressure was found to reduce soot production at low swirl, possibly by increasing the availability of oxygen at the centerline enough to stabilize the flame, though for the same reason this also raised NO_x emission.

Table 5.4.1 Effect of primary swirl and air atomization pressure on visually observed soot. Baseline configuration with 5 degree Y-jet air atomizer.

Primary Air Swirl Setting	Visible Soot [puffs/second]	Air Atomization Pressure [psig]	Exit [NO _x] ppm @ 3 % O ₂
6	0.0	68	109
5	0.2	68	109
4	0.9	68	92
4	0.4	74	103
4	0.0	78	111
4	0.0	82	119

A primary air swirl setting of 6 was chosen for the other experiments to ensure that soot production remained low, even though lower NO_x emission could be attained by further reducing the swirl. In optimizing a final RSFC burner design, it may be beneficial to more carefully explore the lower bounds of primary air swirl, and possibly apply swirl to the fuel jet to reduce the tangential velocity gradient at the fuel-primary air interface.

5.2 External Air Staging

Conventional external staging provides an indication of how well the internal staging produced by the RSFC burner reduces NO_x emission. In particular, if NO_x emission decreases further by imposing external staging on an internally staged RSFC flame, then the internal staging process can theoretically be improved, by increasing the length of the stratified zone, by enhancing the stratification itself, or both. As shown in Figure 5.2.1, external staging indeed reduced NO_x emission from 91 ppm to 53 ppm in the best case. Burnout was complete by the furnace exit, and CO emissions were below 50 ppm in all cases.

Figure 5.2.1 illustrates the relationships between NO_x emission and three other parameters: degree of staging (primary stage fuel equivalence ratio), primary stage pathlength, and tertiary air axial momentum (varied by changing annulus area), with pathlength and momentum being varied simultaneously. As shown, increasing the degree of staging, up to $\phi = 1.2$ is quite effective in reducing NO_x emission when the first stage pathlength is 3.4 m; staging is somewhat less effective in the 1.8 m case. This suggests that the internal staging process has an "equivalent" first stage pathlength between 1.8 and 3.4 m, though the comparison is imprecise since the tertiary air momentum was changed for the two cases. As explained in Chapter 2, staging beyond $\phi = 1.2$ is ineffective because the mixture becomes deficient in oxygen containing radicals and loses its ability to decompose the NO_x precursors to N₂.

Increasing the tertiary air axial momentum (by decreasing the annulus area) decreases the swirl number of the flow, adversely affecting the radial stratification. Therefore, the effect of increasing the first stage pathlength is actually underestimated in Figure 5.2.1. A measure of the magnitude of the effect of increasing tertiary momentum on NO_x can be deduced by comparing the low and high axial momentum cases (with steam atomization) in the unstaged condition ($\phi = 0.95$). The corresponding NO_x emissions are 135 and 170 ppm respectively.

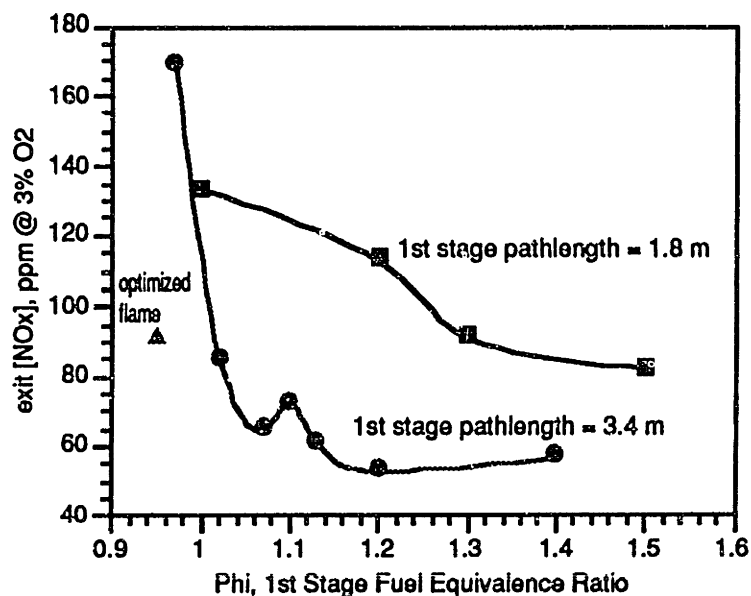


Figure 5.2.1 NO_x emission versus primary stage fuel equivalence ratio. The 1.8 m pathlength curve was obtained with fuel gun positioned flush with burner face, primary swirl = 10, and 0° Y-jet steam atomizer; all other parameters correspond to baseline values. The 3.4 m curve represents data obtained with 10.5, 6.8, and 3.5 inch inserts, fuel gun flush, primary swirl = 10, 0° Y-jet steam atomizer; all else baseline values. The “optimized flame” data point corresponds to baseline configuration with 0° Y-jet air atomizer.

To complete this analysis, future experiments could vary first stage pathlength and fuel equivalence ratio for the low tertiary momentum case. An important point here is that the 53 ppm “best case” may not really be the best case possible, since the tertiary momentum was relatively high. Most likely, by reducing the tertiary momentum, the 53 ppm minimum won’t be greatly reduced, but will shift left on the curve, meaning that less staging will be needed to achieve it.

This conclusion flows from the fact that if stratification is reduced or ends pre-maturely, it will still do so under an overall fuel-rich condition where NO_x continues to be reduced. Relatively less staging will be required to achieve the same result because better stratification will likely improve fuel-N conversion before vortex breakdown occurs. This fact also points to a criterion for future design: if vortex breakdown occurs after all or most fuel-N has been converted to N₂, then external staging will be unnecessary, except perhaps to destroy prompt NO; at present, its

function is only to maintain fuel-rich conditions after vortex breakdown has occurred. This criterion may be difficult to meet, however, if a 3.4 m (11.3 burner diameters) stratification zone is required.

These principles are demonstrated in Figure 5.2.2, where two scenarios are illustrated, one in which the fuel rich core ends before the fuel-N conversion is complete, and another in which the fuel-rich core extends beyond this critical length (L_c). In the first scenario, external staging can be used to reduce NO_x emission if the over-fire air (OFA) is injected downstream of the internal recirculation zone (IRZ) so that the IRZ remains fuel-rich. Otherwise, if the over-fire air is injected upstream of the IRZ, staging will have little or no effect, since the fuel-rich core is already supplying the necessary conditions for NO reduction, and the IRZ will be fuel lean before all fuel-N has been converted.

Thus, as the OFA is positioned further and further downstream of the IRZ, NO_x emission will be reduced, until $L_{OFA} = L_c$, beyond which only small improvements will result. In the second scenario, the fuel-rich core extends beyond L_c , in which case staging becomes essentially redundant since by the onset of the IRZ, all of the fuel-N will have been converted. This latter scenario represents the ideal situation.

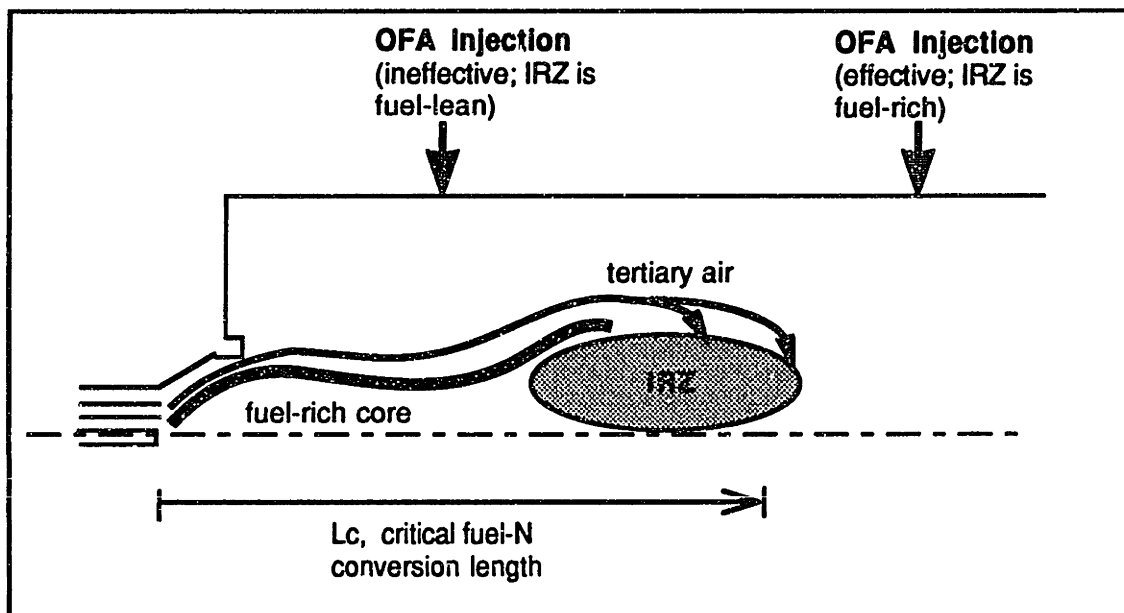


Figure 5.2.2a Onset of IRZ precedes completion of fuel-N reduction reactions.

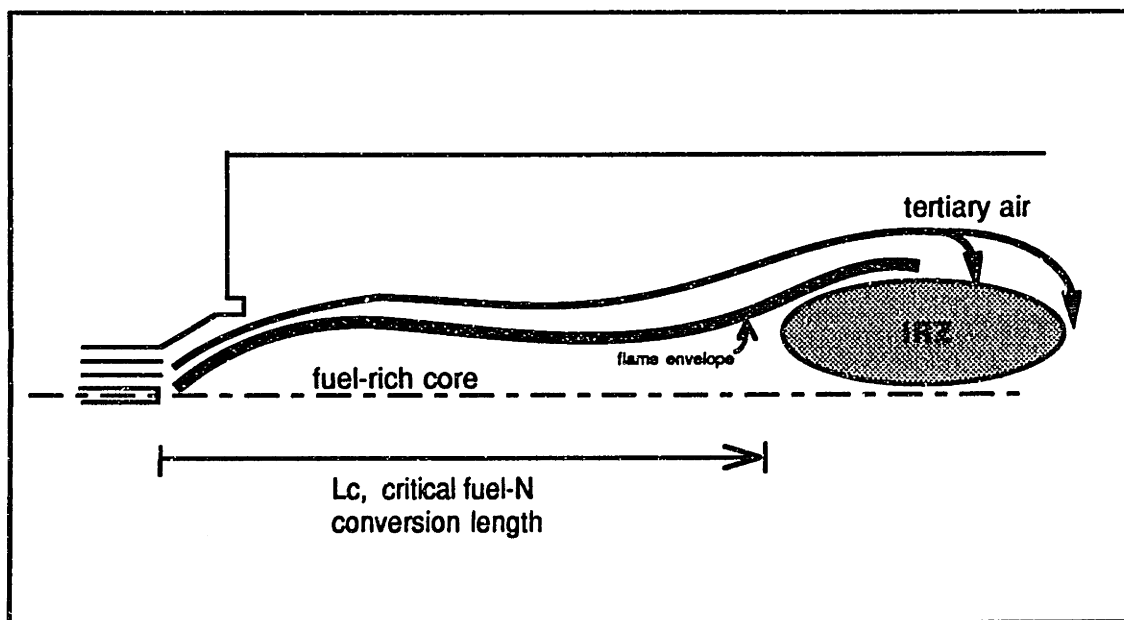


Figure 5.2.2b IRZ occurs after fuel-N conversion reactions equilibrate.

5.3 Flue Gas Recirculation

With natural gas operation, the secondary port of the RSFC burner is used to deliver recirculated flue gas to the combustion zone. This technique was adopted as an alternative to the traditional method of mixing FGR with the combustion air because it concentrates the FGR where it is most needed, i.e. at the fuel-air boundary, and thereby reduces the required percentage of flue gas recirculated.

With the No. 6 oil flames, however, adding FGR through the secondary port rendered the flame unstable with lift-off occurring. Mixing the FGR into the tertiary air solved the stability problem, but the effect on NO_x emission, shown in Figure 5.3.1, was not noticeable beyond the experimental error (which was caused by combustion air fluctuation that resulted from a faulty controller.) This is not to say that the results are inconclusive; the data simply indicate that the effect of FGR is not great, at most responsible for a 20 or 30 ppm drop (out of 120 ppm), when the burner is operated in its optimum low-NO_x configuration. This result should be expected since the major source of NO_x in the low NO_x oil flame is fuel-N, not thermal fixation, as discussed in Chapter 2.

With the high NO_x flame, where thermal fixation is a major source of NO_x, FGR plays a larger role in NO_x inhibition, as shown in Figure 5.3.2, where 11% of the flue gas was recirculated and mixed with the tertiary air, while the tertiary swirl setting was varied. In the highest NO_x flames (tertiary swirl = 3), the effect of FGR was quite clear, as it reduced NO_x emission from 300 ppm to 210 ppm. As the swirl was increased, the difference between the 11 % and 0 % FGR cases diminished, since the role of thermal NO_x also diminished. The conclusion, then, is that FGR can be an effective NO_x control technique for oil combustion in relatively high NO_x flames, but is less useful in the low-NO_x RSFC flames. It is, however, always useful as a soot suppressant.

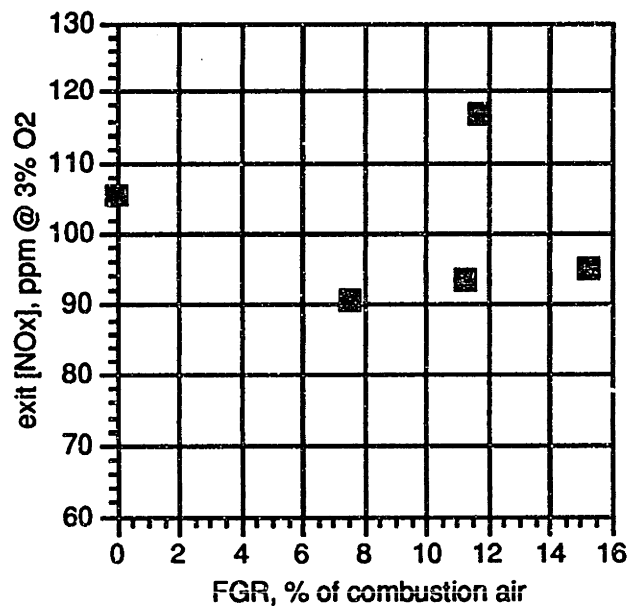


Figure 5.3.1 NOx emission versus FGR. Baseline burner configuration with 5° Y-jet air atomization (68 psig).

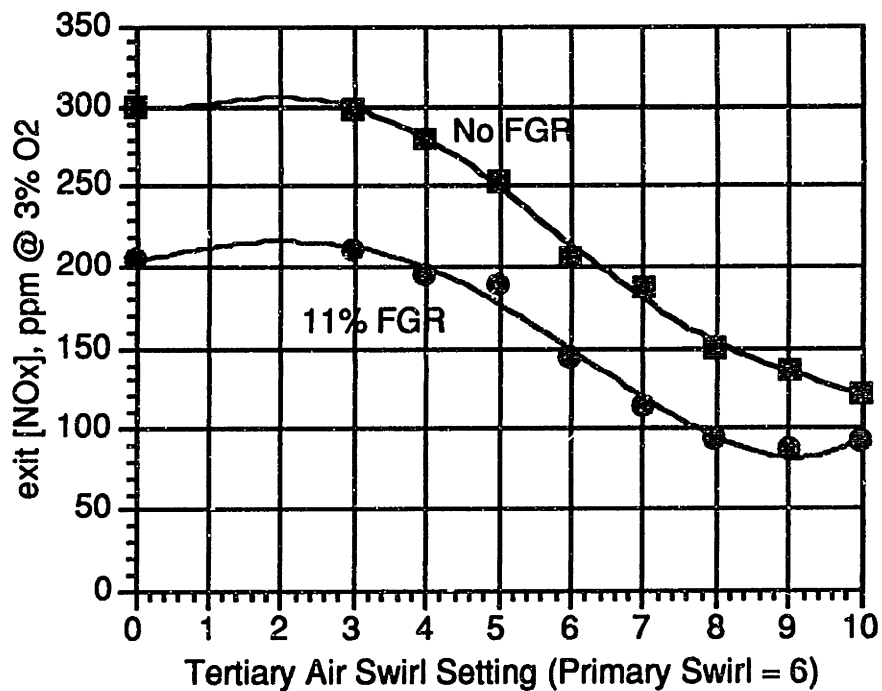


Figure 5.3.2 NOx emission versus tertiary air swirl setting for 0 and 11% FGR cases. Baseline burner configuration with 5° Y-jet air atomizer (68 psig).

5.4 Firing Rate

A series of preliminary tests were conducted to determine the effect of firing rate (varied from 0.3 to 1.3 MW) on NO_x and CO emissions, and on flame stability. Figure 5.4.1 shows the relationship between NO_x emission, firing rate, and furnace exit temperature, indicating that NO_x correlates with both. This makes it difficult to assess the degree to which the change in flow field (caused by changing the combustion air and fuel flows) is responsible for the observed changes in NO_x emission, since the increases in temperature also increase thermal NO_x formation. (CO remained below 40 ppm for all firing rates.)

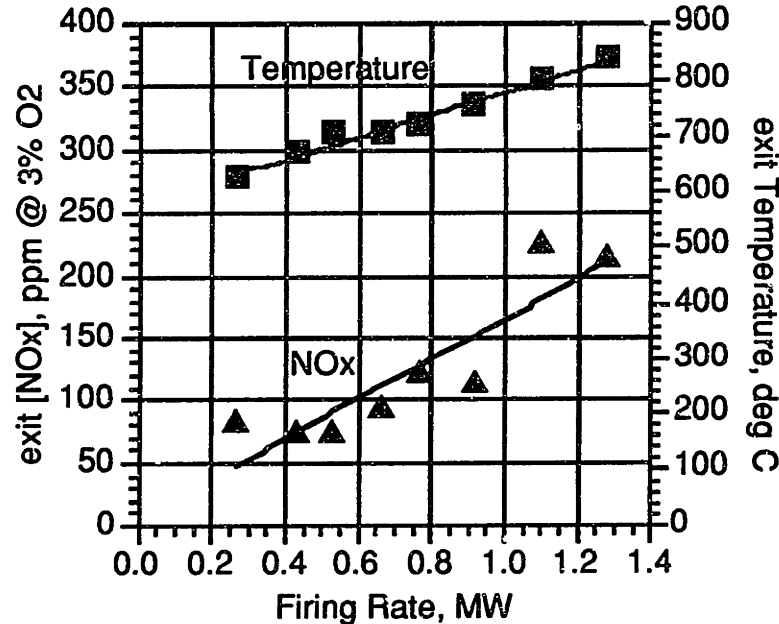


Figure 5.4.1 NO_x emission and furnace exit temperature versus firing rate. Baseline burner configuration with Sonicore atomizer (steam supplied at 50 psig).

As shown in Figure 5.4.1, the temperature at the end of the furnace was not maintained constant by actively controlling the cooling water flow in the walls. As a result, the independent effect of firing rate on NO_x can't be completely deduced from the data for the general case, but can be taken as a rough guide. In a real system, it is unlikely that furnace exit temperature will remain constant while varying the firing rate; the effect of turn-down on NO_x emission is therefore

somewhat site specific. The utility of the experiment then, was to demonstrate that the RSFC as currently designed can be operated over a relatively wide range of firing rates (a 4 to 1 turn-down ratio) without compromising flame stability or burnout efficiency.

5.5 Atomization

In previous studies²⁷ the effect of fuel-jet angle on NO_x emission was studied, and it was found that by increasing the angle from 0° to 25°, NO_x emission jumped from 97 ppm to 170 ppm in the cases studied. The researchers concluded that this increase was caused by greater fuel droplet penetration into the tertiary air jet, thus reducing stratification. As an extension of this work, and in an effort to develop the optimum operating protocol for the RSFC burner, a series of experiments were performed to determine the best atomizer type (Sonicore or Y-Jet), atomizing medium (steam or air), and operating pressure (60 to 100 psig for air, 20 to 160 psig for steam). In addition, since previous experiments with fuel-jet angle utilized only 0°, 10°, and 25°, atomizers, it was possible that an intermediate angle of 5° could reduce coalescing while also avoiding droplet penetration into the tertiary air; an experiment was also performed to test this possibility.

The effect of atomization pressure and jet angle with the Y-Jet atomizer using air as the atomizing medium is shown in Figure 5.5.1. The data indicate that lowering atomization pressure decreased NO_x emission, though it should be noted that when pressure was lowered below 68 psig, soot could be observed in the camera monitor, though CO emission remained below 30 ppm for all conditions. Consistent with what was found in the previously cited research, increasing the jet angle to 5° increased NO_x emission significantly, as shown in Figure 5.5.1.

²⁷Berg [1991], Becker et al [1993]

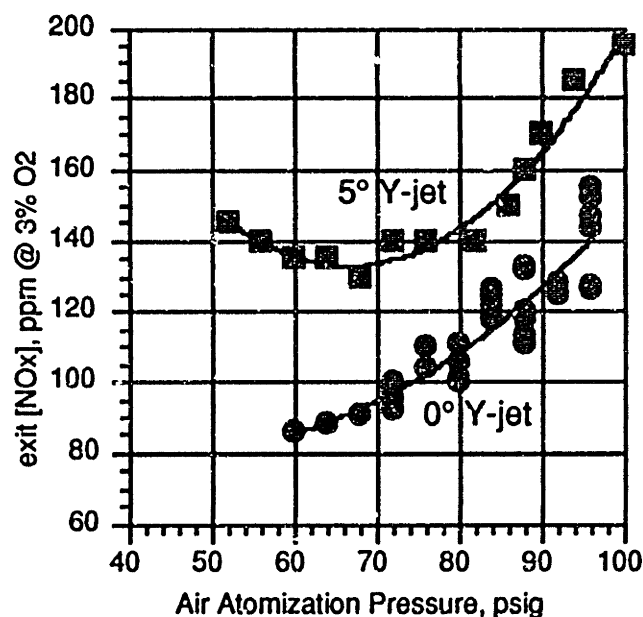


Figure 5.5.1 NO_x emission versus air atomization pressure for 0° and 5° Y-jet atomizers. Burner in baseline configuration.

Figure 5.5.2 shows the results obtained with the same atomizer using steam instead of air as the atomizing medium. The trend is similar to what was obtained before, the main difference being that the curve is shifted upwards, indicating that air atomization is the better option. The minimum NO_x emission level obtained with steam atomization was 110 ppm @ 61 psig, whereas for air the minimum was 91 ppm @ 68 psig. Unlike atomization with air, soot was not observed over the range of pressures tested, even at the lowest atomization pressure. The lack of soot is perhaps due to the fact that water vapor may play a role in the chemistry of soot suppression. Also unlike the air atomized cases, CO emission began to rise as steam atomization pressure was decreased, approaching 110 ppm @ 45 psig.

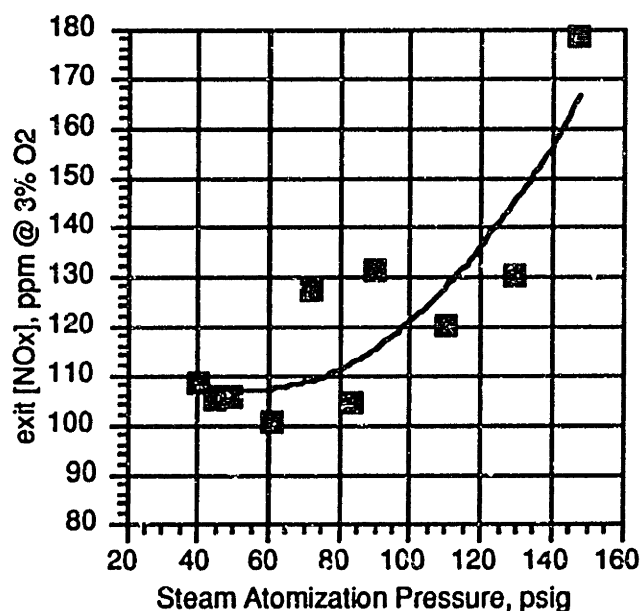


Figure 5.5.2 NO_x emission versus steam atomization pressure for 0° Y-jet atomizer. Burner in baseline configuration.

Atomization pressure affects fluid droplet size, momentum, dispersion, coalescence and atomizing medium flow rate. All of these factors can contribute to the observed trend, though some are more likely than others to be important in this context. Mullholand (1973) has shown that droplet size varies inversely with atomization pressure. Since reducing droplet size decreases fuel vaporization time, a higher atomization pressure allows earlier ignition, which accounts for the increased soot production observed at low atomization pressures. This factor is important because faster ignition translates to better flame stratification, since the needed radial density gradient created by the heat release occurs earlier in the flow field, and therefore reduces the opportunity for pre-flame fuel/air mixing. Furthermore, as atomization pressure is increased, the increase in vaporization rate will allow more gas-phase residence time for fuel-N decomposition.

Competing with both of these effects, however, is the accompanying increase in droplet velocity, which could increase the radial gradient of axial velocity at the fuel-air boundary, and thereby enhance turbulent mixing; similarly, higher fuel-jet momentum could result in greater

entrainment of the surrounding air. Another possible detrimental effect of increasing atomization pressure is that the higher vaporization rate will allow more fuel to diffuse outward from the centerline; one advantage of burning No. 2 fuel-oil over natural gas is considered to be the fact that it is easier to contain a liquid fuel near the axis.

Results obtained with the Sonicore atomizer are shown in Figure 5.5.3. Again, as atomization pressure was increased, NO_x emission rose. The minimum NO_x obtained with this atomizer was 126 ppm @ 60 psig, which was higher than with either of the Y-Jet cases. One difference observed between the Sonicore and the Y-Jet atomizers was that the Sonicore could be operated at very low atomization pressure (~ 20 psig) with no increase in CO emission; CO emission remained at 30 ppm over the test range. This could be due to the fact that the Sonicore atomizer flows more steam than the Y-Jet for the same pressure drop, and thereby increases the fuel-jet momentum, possibly affecting the near-burner flow field.

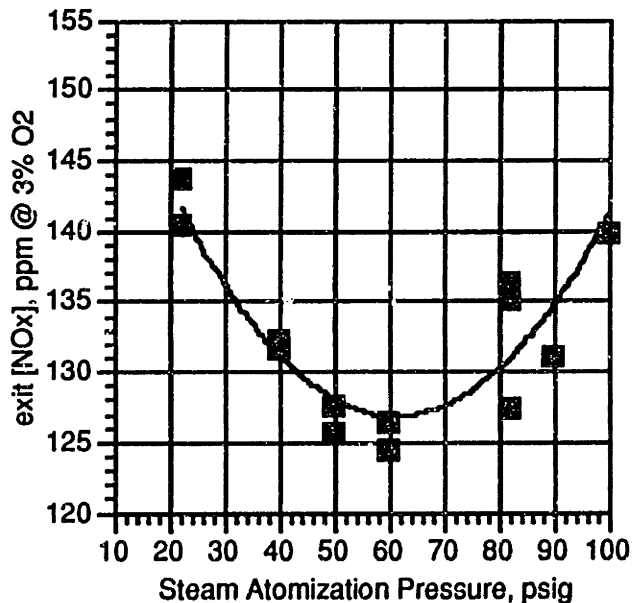


Figure 5.5.3 NO_x emission versus steam atomization pressure for Sonicore atomizer. Burner in baseline configuration.

5.6 Flame Structure Study

Detailed in-flame measurements of gas composition and temperature were taken for a mildly staged, parametrically optimized flame. The burner settings and operating parameters used to generate this flame are listed in the following table.

Table 5.6.1 Burner conditions for detailed flame study.

Barrel	Flow [acfm]	Temperature [deg F]	Insert Size [in]	Position [in]	Swirl Setting
Primary	28	280	3.5	-2.6	10
Secondary	42	374	6.8	flush	10
Tertiary	438	490	10.5	n/a	10

A 0° Y-jet atomizer was used with steam as the atomizing medium. The fuel gun was positioned flush with the burner face. The first stage was operated at a fuel equivalence ratio of 1.13, with the over-fire air injection port positioned at 3.4 m (11 burner diameters) from the burner. These conditions resulted in the following exit emissions:

NO _x	58 ppm
O ₂	2 %
CO ₂	13 %
CO	< 30 ppm

Figures 5.6.1 to 5.6.6 below show measured concentration and temperature distributions in the near-burner field. They illustrate quite well the ways in which the high-swirl RSFC flame yields low NO_x emissions. In Figure 5.6.1 contours of NO concentration are plotted as a function of axial and radial distance (expressed as burner diameters) from the burner. In the figure, the NO formation and destruction chemistry regimes are apparent in two distinct zones, delineated by the 140 ppm iso-concentration line. In the formation zone, fuel-N is oxidized in an oxygen-rich environment, as evidenced by the O₂ contours in Figure 5.6.2, and the absence of CO in the same

region, shown in Figure 5.6.3. As explained in Chapter 2, in a fuel-lean environment fuel-N will be converted to NO_x, and thermal NO_x formation becomes important, explaining the observed increase in NO concentration in this zone.

Within the NO reduction zone, there is a particularly intense region of NO destruction near the burner axis, indicated in Figures 5.6.1 to 5.6.6 by a shaded area. In this region, it can be seen that the O₂ concentration is low, while CO (Figure 5.6.3) and CH₄ (Figure 5.6.4) concentrations are relatively high, indicating a fuel-rich local atmosphere. In this context CH₄ is important as an indicator of the presence of hydrocarbon fragments, such as CH and CH₂. These hydrocarbon fragments play a major role in NO_x reduction via the “reburn” mechanism reviewed in Chapter 2, and are likely responsible for the particularly intense NO destruction seen here. It should also be noted that within this region, the rate of destruction increases along the axis, reaching a maximum at a distance between 2.5 and 3.2 burner diameters. This rate increase can be partly explained by the peaking of gas temperature in the same location, as shown in Figure 5.6.6; in Chapter 2, increasing temperature was shown to accelerate the fuel-N and NO decomposition reactions.

The remainder of the NO reduction zone can be explained by the high temperature, oxygen deficient conditions where “reburn” also occurs, though at a slower pace because of the lower concentration of CH_i fragments there. Returning to the issue of OFA injection port position in the flame tunnel, it can be seen in the NO contour plot that if the OFA had been positioned anywhere within the plotted axial domain, higher NO_x emission would have resulted since the NO reduction reactions had not yet been completed (i.e., taken the mixture to the equilibrium NO_x concentration). For example, if the OFA were positioned at $X/D = 3.9$, it is likely that the exit NO_x emission would have been closer to 120 ppm, rather than the achieved 58 ppm.

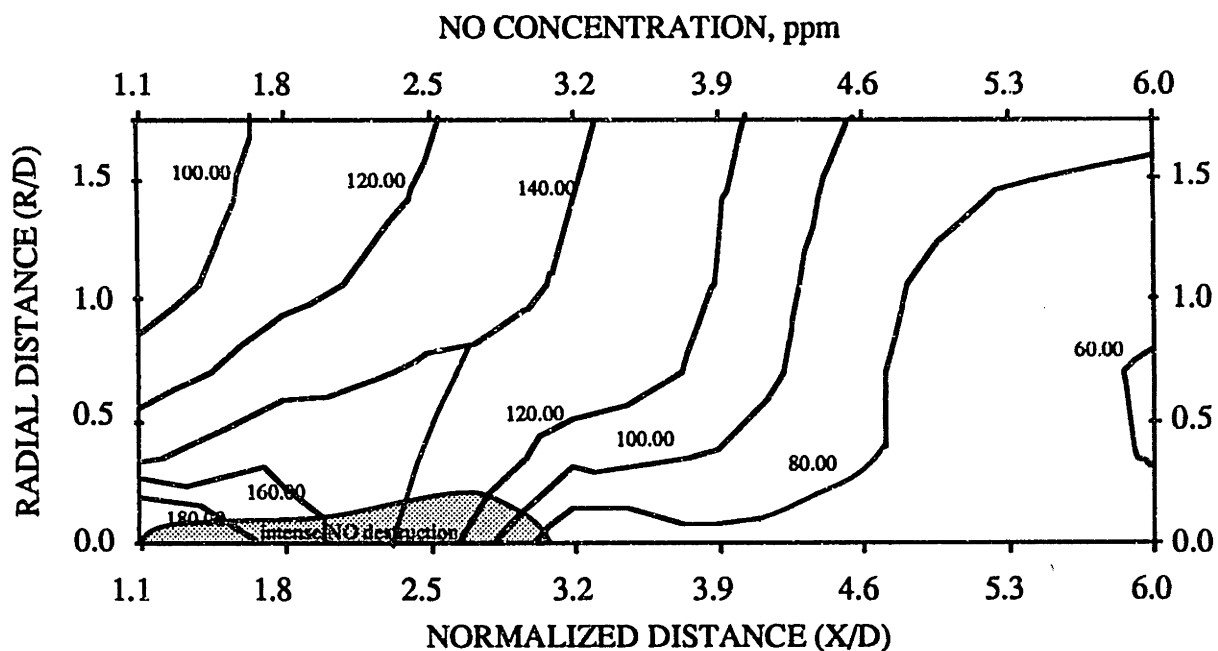


Figure 5.6.1 Measured NO concentration. The NO formation and destruction zones are delineated by the 140 ppm iso-concentration line. The approximate boundary of a highly intense NO destruction region is indicated by the shaded region on this and the following plots.

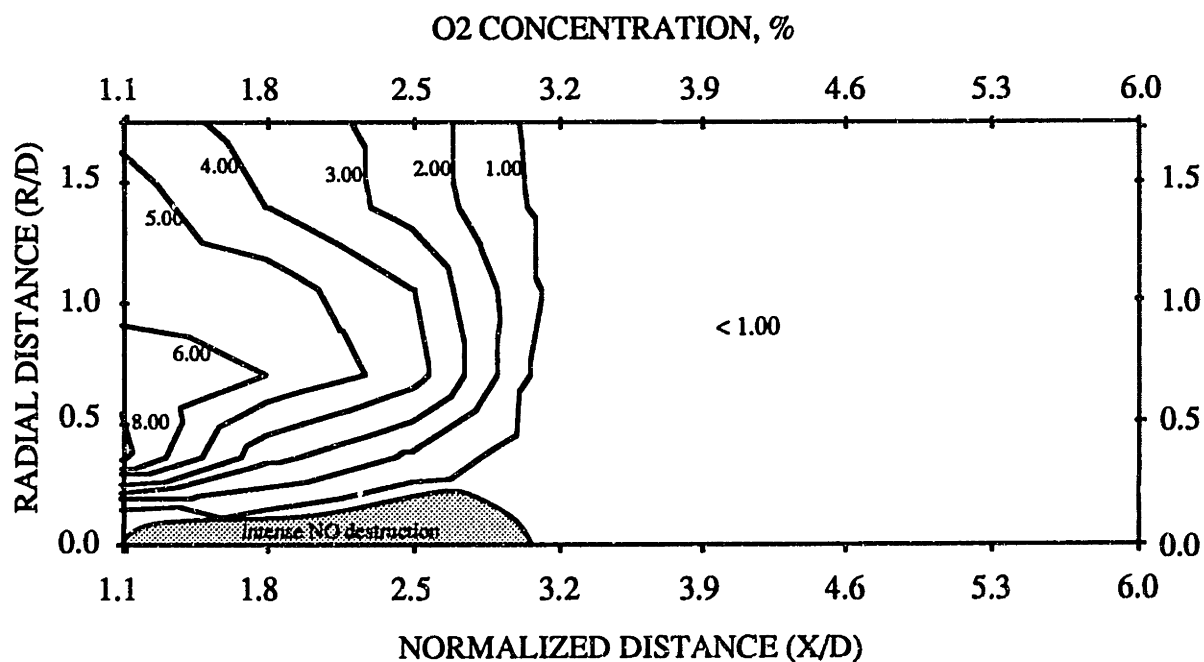


Figure 5.6.2 Measured O₂ concentration. The tertiary air jet trajectory can be traced by the local O₂ maximum at each axial location, and is symbolically indicated by the arrow in the figure. The low O₂ concentration everywhere downstream of $X/D = 3.2$ is explained by the fact that the flame was staged, with the over-fire air injection port positioned at $X/D = 11$, not shown in the plot. (At the exit, the O₂ concentration was 2 %.)

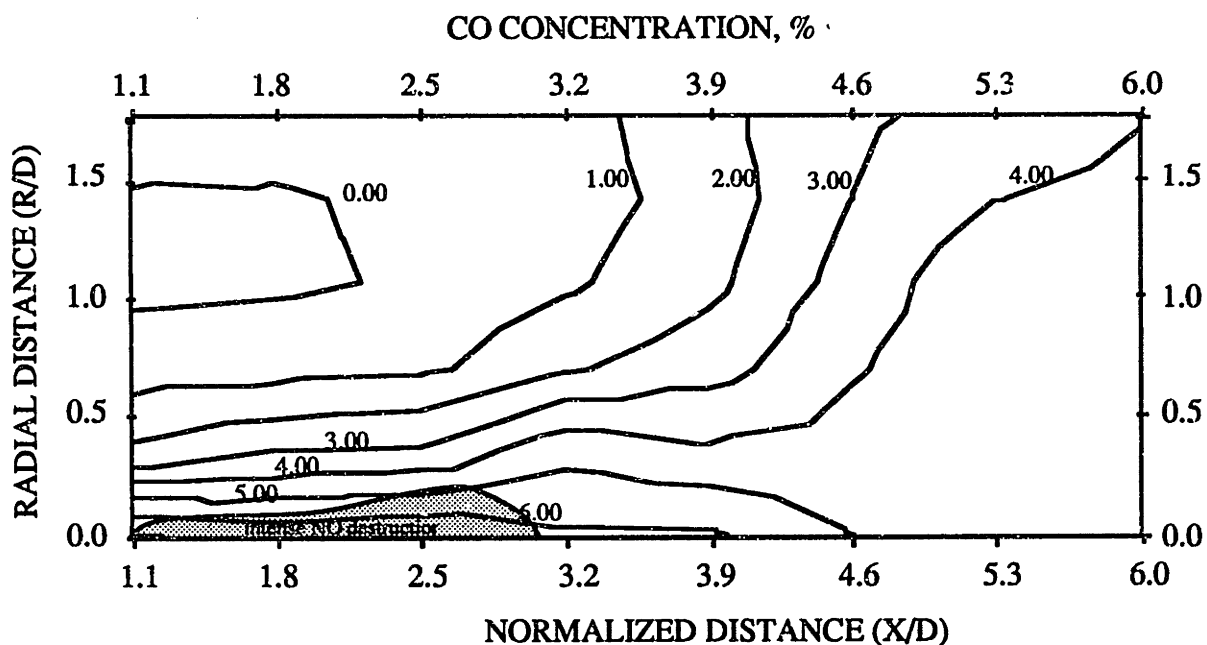


Figure 5.6.3 Measured CO concentration. Up to a normalized axial distance of 3.2, the fuel remains near the burner axis and begins to diffuse outward only downstream of that point.

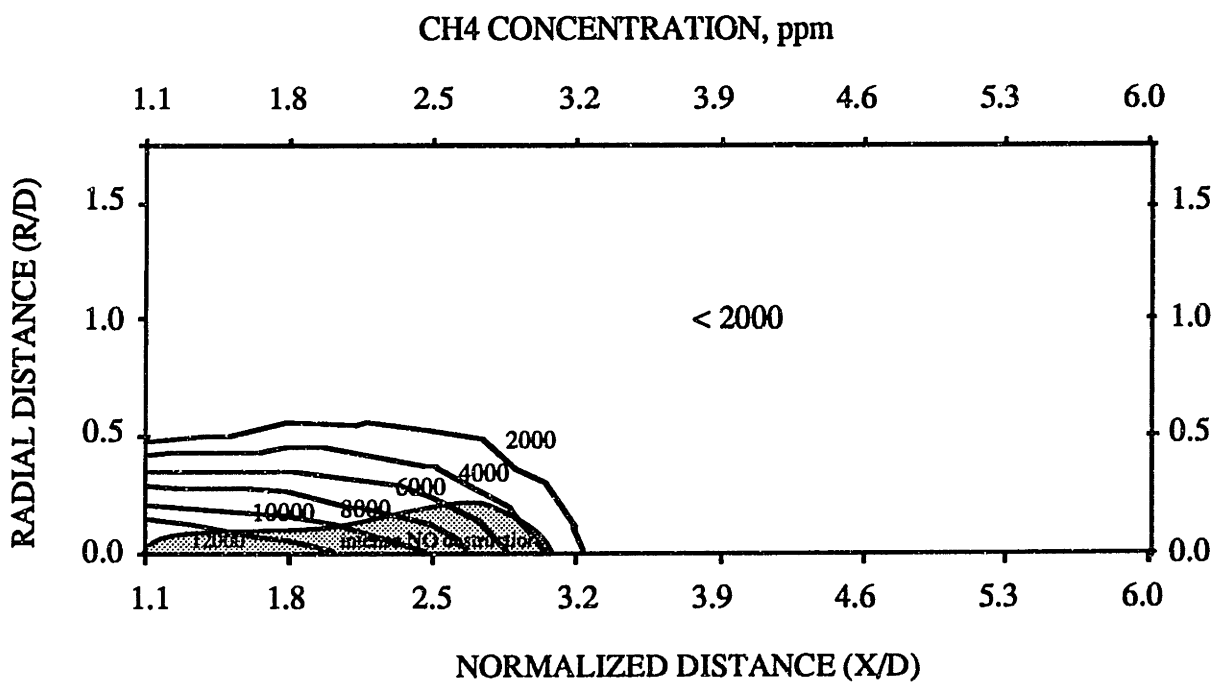


Figure 5.6.4 Measured CH₄ concentration (FTIR measurement). Methane remains near the centerline, and is consumed rapidly along the axis. The presence of methane is important because it can be taken as an indication that hydrocarbon fragments, such as CH and CH₂, are also present.

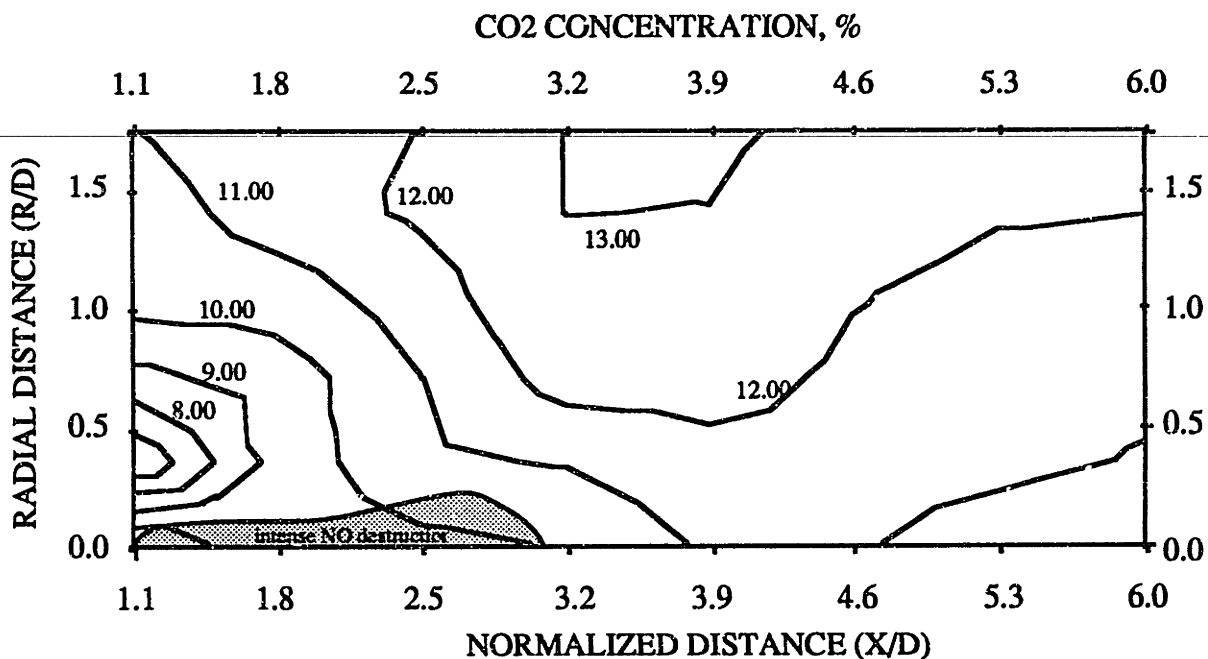


Figure 5.6.5 Measured CO₂ concentration. CO₂ builds relatively slowly along the burner axis (R/D = 0), and its formation generally tends to follow the tertiary air trajectory.

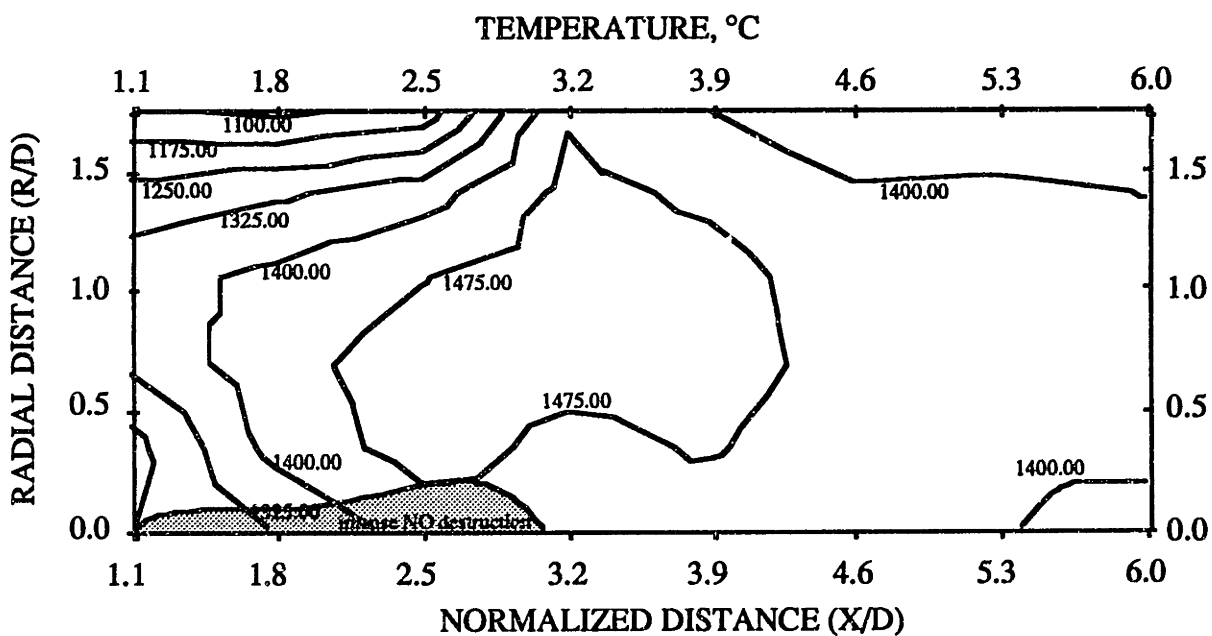


Figure 5.6.6 Measured gas temperature.

5.7 Pre-combustor

In light of these results, it became clear that increasing the temperature earlier in the fuel-rich core could accelerate the NO reduction reactions, leading to lower NO_x emissions. To increase temperature earlier in the flame, the CRF was modified by adding a short cylindrical section (whose diameter is slightly larger than the burner) between the burner and the main combustion chamber, as a “pre-combustor.” It was expected that within the pre-combustor, flame temperature would increase due to: a) the decrease in heat transfer surface area, and b) an increase in volumetric heat release rate, since within the pre-combustor there is no large external recirculation zone bringing back flue gas, as exists in the main combustion chamber.

As shown in Figure 5.7.1, NO_x emission with the pre-combustor was higher for the unstaged condition (116 ppm vs 91 ppm), and when staged, did not meet the 55 ppm minimum obtained with the unmodified configuration. As before, burnout was complete by the furnace exit, with CO emission below 50 ppm in all cases.

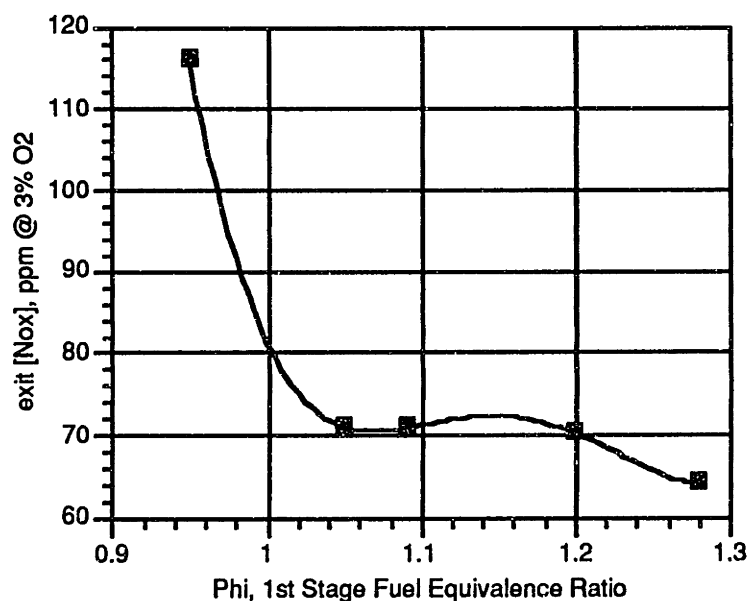


Figure 5.7.1 Effect of external staging on NO_x emission, with pre-combustor. Baseline burner configuration with 0° Y-jet air atomization.

Figures 5.7.2 through 5.7.6 show axial profiles of centerline gas composition and temperature for the unstaged cases with and without the pre-combustor. The temperature profile, shown in Figure 5.7.3, is the key to understanding why the pre-combustor was unsuccessful at reducing NO_x. In it we see that the temperature is lower with the pre-combustor, opposite to what was planned. Apparently, this is not a mixing effect, as seems to be indicated by the gas composition measurements; the CO, O₂, and CO₂ concentration profiles are approximately the same for the two cases. The likely possibility is that the water-cooled pre-combustor wall removes too much heat in the near-burner field.

Regardless of the cause, the lower temperature early in the flame reduces fuel-N conversion efficiency, resulting in higher NO_x emission. With better materials of construction it may be possible to reduce the cooling rate at the wall, and thereby allow higher flame temperatures. This could be implemented in a future study. Various data gathered during the pre-combustor studies are presented in the Appendix for future reference. For the present purposes, they do not add crucial information on oil combustion with the RSFC burner.

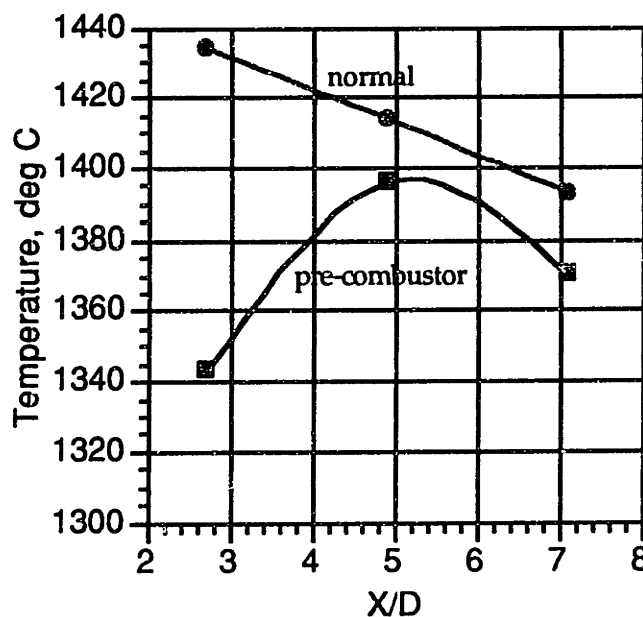


Figure 5.7.2 Measured centerline gas temperature versus normalized axial distance from burner for pre-combustor and normal configurations. Data obtained using baseline burner geometry and 0° Y-jet air atomizer (68 psig).

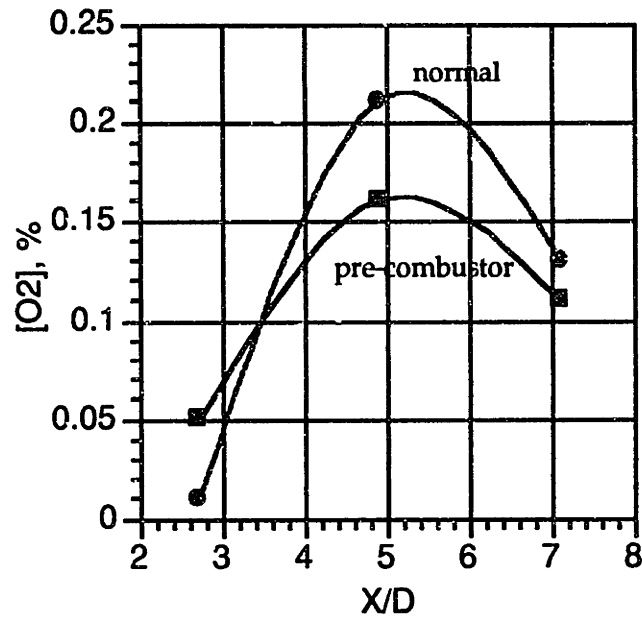


Figure 5.7.3 Measured centerline O₂ concentration versus normalized axial distance from burner, for pre-combustor and normal configurations. Data obtained using baseline burner geometry and 0° Y-jet air atomizer (68 psig).

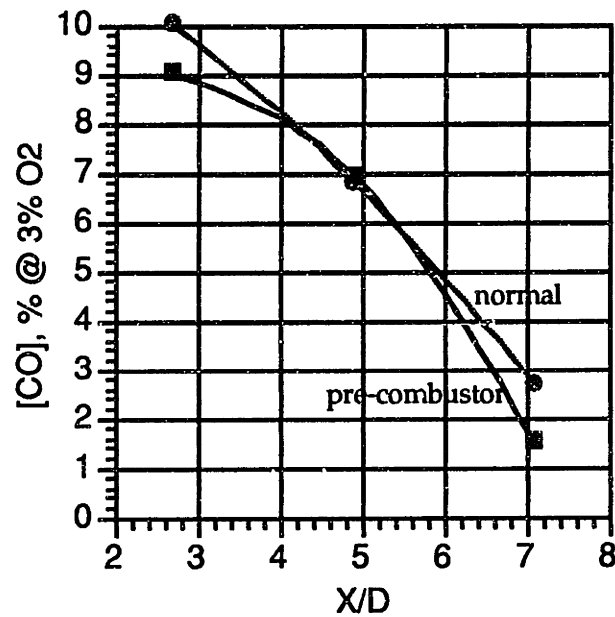


Figure 5.7.4 Measured centerline CO concentration versus normalized axial distance from burner, for pre-combustor and normal configurations. Data obtained using baseline burner geometry and 0° Y-jet air atomizer (68 psig).

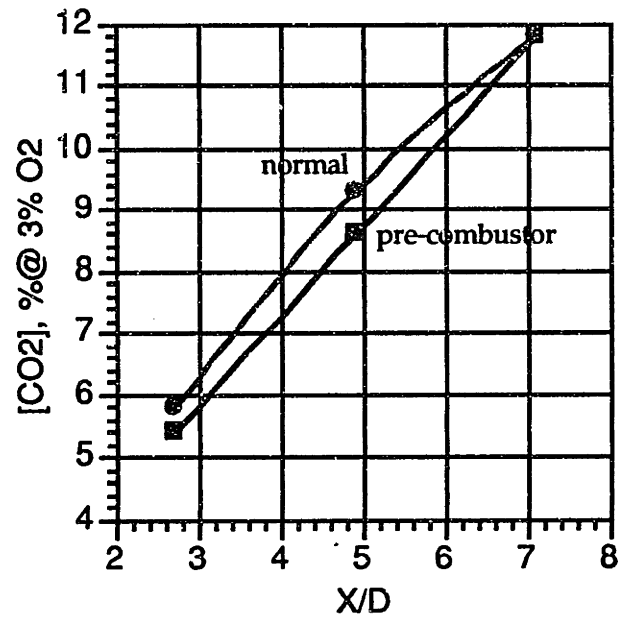


Figure 5.7.5 Measured centerline O₂ concentration versus normalized axial distance from burner, for pre-combustor and normal configurations. Data obtained using baseline burner geometry and 0° Y-jet air atomizer (68 psig).

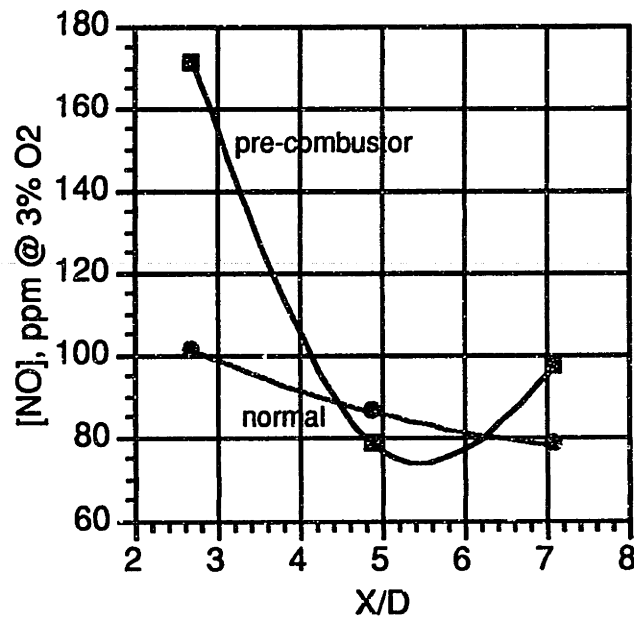


Figure 5.7.6 Measured centerline NO concentration versus normalized axial distance from burner, for pre-combustor and normal configurations. Data obtained using baseline burner geometry and 0° Y-jet air atomizer (68 psig).

5.8 Summary & Future Work

Table 5.8.1 reproduces the experimental matrix shown in Table 4.2.1.1 and indicates the value of each parameter that minimized NO_x emission while maintaining CO emission below 50 ppm. It can be used as a operating guide for future RSFC applications with No. 6 fuel-oil.

Experiment	Parameters Varied	Experimental Ranges	"Optimal" Value
I. Swirl	Swirl number, primary tertiary	0.1 - 0.3 0.0 - 0.6	0.16 0.57
II. External staging	First stage equivalence ratio Position of OFA injection Burner inserts (p,s,t)	0.95 - 1.5 1.8 or 3.4 m from burner {3.5, 6.8, 10.5} or {3.5, 7.25, 11} inches	1.2 3.4 m {3.5, 7.25, 11} inch
III. FGR	Amount recirculated	0 - 20 %	inconclusive
IV. Firing rate	Thermal input Atomizer type/ medium	0.3 0-1.3 MW 0° Y-jet/air Sonicore/steam	n/a
V. Atomization	Atomizer type Fuel jet angle Atomizing medium Atomization pressure	Y-jet. Sonicore 0°, 5° air (Y-jet only) or steam 60 - 100 psig (air) 20 - 160 psig (steam)	Y-jet 0° air 68 psig

The best test conditions corresponded to the following:

- Unstaged: 91 ppm NO_x, 17 ppm CO
0° Y-jet air atomization at 68 psig
baseline burner configuration
- Staged: 53 ppm NO_x, 25 ppm CO
 $\phi = 1.2$, 3.4 m pathlength
0° Y-jet steam atomization at 90 psig
primary, secondary, tertiary air inserts {3.5, 6.8, 10.5} inches
primary barrel position: - 2.6 inches
fuel gun position: 0 inches

The need for future experiments in two areas - staging and swirl - was identified during the course of the study. As discussed in Section 5.2 the staging experiments were not conducted at

optimal conditions, because the high momentum burner inserts were used in place of the baseline inserts, and because steam atomization was utilized in place of air. As a result, the obtained 53 ppm minimum may be reduced in future experiments, or the required degree of staging may be lessened. In addition, it may be possible to reduce the residence time in the primary stage.

Secondly, the tests with tertiary air swirl indicated a strong likelihood that NO_x emissions could be further reduced if a higher swirl setting were available. This possibility was also supported by the reduction in NO_x emission that resulted from replacing the smaller inserts with the larger set, which, by reducing axial momentum, had the effect of increasing the maximum swirl number. Because both of these parameters (swirl setting and insert size) are related to swirl number, it may not be necessary to change both to test the hypothesis. From a practical view, the easiest modification is to remove the inserts, which would yield a maximum tertiary swirl of 1.1 compared to the present 0.6. A simple test to determine whether this change is sufficient is to search for a minimum in the NO_x emission versus swirl setting curve; if a minimum is found, then the modification can be considered sufficient, as a further increase in annulus area, or an increase in the maximum swirl setting will be redundant.

Chapter 6

Race And Class In Environmental Regulation: Whose Back Yard?

6.1 Introduction

Since the early 1970's social advocacy groups in the United States have complained that minorities and the poor are disproportionately exposed to environmental hazards; that business, with government assistance, practices 'environmental discrimination' by targeting those communities for polluting industries. Many studies in the last 20 years show that this segment of society does in fact experience a higher incidence of environmental hazards, and where data are available, show that minorities and the poor experience elevated levels of bloodstream contaminants, along with deleterious health effects.²⁸

Social advocacy groups have also pointed to inequities in the distribution of institutional response to pollution, i.e. that the enforcement of environmental regulations in these communities is less stringent than in predominantly white or affluent areas. This problem partially explains the previous one; all else being equal, polluting industries are more likely to

²⁸Wood et al [1974]

locate where enforcement is lax. This “incentive,” however, must be considered along with other determinants in the distributional dynamics of environmental quality, such as the availability of cheap land in poor neighborhoods, proximity to industrial infrastructure, zoning laws, and the ability of the affected communities to marshal the political resources needed to counteract siting decisions.

This chapter will qualitatively analyze the distributional dynamics of environmental quality, primarily in order to determine where and how institutional intervention can succeed in reducing inequities. The following pages will present evidence for environmental discrimination, identify strategies for legal redress, and finally, discuss why they might fail.

6.2 Evidence Of Environmental Discrimination

Many studies have shown that the best predictors of exposure to environmental hazards are income and race. The most widely referenced and publicized study on this subject was performed by the United Church of Christ (UCC) and was distributed in a report titled *Toxic Wastes and Race in the United States* (1987). This nation-wide study investigated the relationship between the location of sites containing hazardous wastes and the racial and socio-economic characteristics of people living nearby. Using residential ZIP code areas as the units of analysis (‘communities’) the UCC compared 5 variables in all areas of the nation:

1. Minority percentage of the population;
2. Mean household income - to determine whether class was more important than race in the location of commercial facilities;
3. Mean value of owner-occupied homes - a proxy for determining the role of land values in facility location;
4. Number of uncontrolled toxic waste sites per 1,000 persons - to test whether geographic or historical factors not identified in the study such as land use zoning, transportation access, groundwater, or soil permeability could explain the location of commercial waste facilities;

5. Pounds of hazardous waste generated per person - to evaluate whether facility location can be explained by proximity to waste producers, i.e. commercial waste facility customers.

The residential ZIP code areas were categorized into 4 mutually exclusive groups:

1. No commercial hazardous waste facilities;
2. One commercial hazardous waste facility that is not a landfill;
3. One commercial hazardous waste landfill that is not one of the 5 largest in the U.S.;
4. One of the 5 largest landfills, or more than one commercial hazardous waste facility.

The study found that the group of residential ZIP code areas with the highest number of facilities also had the highest mean percentage of minority residents (38%), while the group of ZIP code areas without any facilities had the lowest percentage of minority residents (12%). Groups 2 and 3 also had a significantly larger portion of minority residents than Group 1 (24% and 22%, respectively). Of the 5 variables tested, the most important predictor of the level of commercial waste activity was minority percentage of population; that is, as the number of a community's racial and ethnic residents increases, the probability that some form of hazardous waste activity will occur also increases. Household income and the mean value of owner occupied homes were also statistically significant predictors, but less so than minority percentage of population. Incomes and home values were an average of \$2,745 and \$17,301 lower in communities with facilities than their neighboring communities without facilities. The other variables were not found to be statistically significant.

The United Church of Christ study is not a single aberration from an otherwise unsuspect record. To the contrary, many other researchers have studied the association between race, class, and exposure to environmental hazards with strikingly similar results. Table 6.1 summarizes the results of every published study, carried out in the U.S. through 1991, whose purpose was to assess this association.²⁹ Across a range of hazards and study sample sizes, the results consistently indicated that environmental hazards were inequitably distributed; of the 22 studies,

²⁹Bryant and Mohai [1992]

Table 6.1 Studies Providing Empirical Evidence Regarding the Burden of Environmental Hazards by Income and Race (from Bryant and Mohai, 1992)

<u>Study</u>	<u>Hazard</u>	<u>Scope of Study</u>	<u>Distribution inequitable by income?</u>	<u>Distribution inequitable by race?</u>	<u>Income or Race more important?</u>
CEQ(1971)	Air Pollution	Urban Area	Yes	NA	NA
Freeman(1972)	Air Pollution	Urban Areas	Yes	Yes	Race
Harrison(1975)	Air Pollution	Urban Areas	Yes	NA	NA
	Air Pollution	Nation			
Kruvant(1975)	Air Pollution	Urban Area	No	NA	NA
Zupan(1975)	Air Pollution	Urban Area	Yes	Yes	Income
Burch(1976)	Air Pollution	Urban Area	Yes	NA	NA
Berry et al. (1977)	Air Pollution	Urban Areas	Yes	No	NA
	Solid Waste	Urban Areas	Yes	Yes	NA
	Noise	Urban Areas	Yes	Yes	NA
	Pesticide	Urban Areas	Yes	Yes	NA
	Poison.	Urban Area	Yes	Yes	NA
	Rat Bite Risk				
Handy (1977)	Air Pollution	Urban Area	Yes	Yes	Income
Asch & Seneca (1978)	Air Pollution	Urban Areas	Yes	NA	Race
Gianessi et al. (1979)	Air Pollution	Nation	No	Yes	NA
Bullard (1983)	Solid Waste	Urban Area	NA	Yes	NA
U.S. GAO (1983)	Hazardous Waste	Southern Region	Yes	Yes	Race
UCC (1987)	Hazardous Waste	Nation	Yes	Yes	Race
Gelobter (1987; 1982)	Air Pollution	Urban Areas	Yes	Yes	Race
	Air Pollution	Nation	No		
Mohai & Bryant (1992)	Hazardous Waste	Urban Area	Yes	Yes	Race
West et al. (1992)	Toxic Fish Consumption	State	No	Yes	Race

21 found that environmental discrimination occurs along race or class lines. Among the 9 studies which separated race from class, 7 found that race was a better predictor of exposure to environmental hazards than was income.

One possible explanation for the higher incidence of polluting activity in minority and poor communities is that regulatory enforcement there is lax relative to that in white or affluent areas. In 1992, *The National Law Journal* (NLJ) published the results of a study commissioned to investigate this possibility. The study looked at all civil cases against violators of federal air, water, and waste laws concluded between March 1985 and March 1991, as well as the 929 Superfund cases concluded with penalties during the same period.

Using a demographic analysis of ZIP code areas similar to that used in the Church of Christ study, the NLJ found that environmental regulatory activity was significantly greater in areas which had the least proportion of minority residents than in the areas which had the greatest proportion:

- Penalties under hazardous waste laws in communities having the greatest white population were on average 500% greater than in communities having the greatest number of minority residents (\$335,566 vs \$55,318).
- The average penalty under hazardous waste laws in the lowest median income areas was 3% greater than in areas with the greatest income (\$113,491 vs \$109,606), i.e. the discrepancy under these laws occurs by race alone.
- Penalties under all federal air, water, and waste laws were 46% higher in white areas than in minority areas.
- Abandoned hazardous waste sites in minority areas took 20% longer to be placed on the National Priority Action List than those in white areas.
- At hazardous waste sites in minority areas, the EPA choose containment 7% more often than the preferred permanent treatment, while permanent treatment was chosen 20% more often than containment in areas with the greatest proportion of white residents.

Some commentators³⁰ have criticized the methodology used in the NLJ study, particularly the division of the communities in their sample "into four equal groups or 'quartiles,' ranging from those with the highest to those with the lowest white populations." The study compared "the quartile with the highest white population to the quartile with the lowest white population," corresponding to communities with 97.9% and less than 79.2% white populations, respectively. For this reason, most 'minority' communities are predominantly white. It should be noted however, that this classification scheme has some validity because "in light of segregated residential patterns, even communities with an 80% white population may have a different character, or at least be perceived different than communities that are nearly 100% white."³¹ More critically, since segregation often occurs within ZIP code areas it is likely that if the pattern of unequal protection is observable at this macro-level, a similar pattern will be reproduced more forcefully at a smaller unit of analysis, the neighborhood for instance.

6.3 Legal Remedy

Writing in *Columbus Board of Education v. Penick* (1979), Justice Powell observed that "unintegrated schools...[result] primarily from familiar segregated housing patterns which - in turn - are caused by social, economic, and demographic forces for which no school board is responsible."³² Justice Powell's statement points to a structural problem: whom can the Supreme Court order to alter "the social, economic, and demographic forces" that lead to segregated schools? The same problem applies to the distribution of environmental hazards.

A number of factors determine the distributional dynamics of environmental quality. At one level, profit-motivated business decisions based on land values, proximity to industrial infrastructure, zoning laws, regulatory enforcement, and so on are important determinants. The

³⁰Lazarus [1993: 786]

³¹Lazarus [1993: 787]

³²Mandelker [1981: 81]

attitudes and perceptions of the affected residents, their ability to organize, educate, and act collectively to countervail these business decisions are also important factors.

At another level, government institutions such as the Environmental Protection Agency (EPA) have a determining role by promulgating national standards, which at first glance seem to equalize environmental protection across class and race boundaries.³³ However, by enforcing environmental laws the EPA has had a substantial effect on the location and relocation of pollution and polluting industries,³⁴ often redistributing risks toward poor and minority communities.³⁵ In response to increasingly stringent air pollution standards, for example, many power plants have employed Selective Catalytic Reduction to reduce NOx emissions, resulting in toxic solid wastes which must be transported to landfills or treatment centers, usually located in a different community than that affected by the original emissions. A similar redistribution of risks occurs for a host of other pollution abatement practices in waste water treatment, hazardous waste incineration, solid waste transport, and so on.³⁶

Despite this important regulatory role, however, improvements and distributional changes in environmental quality cannot be attributed solely to EPA activity. For example, from 1970 to the mid-1980's a major restructuring in the U.S. industrial base³⁷ and the accompanying patterns of relocation undoubtedly affected the type, number, and location of pollution sources.³⁸

It must be true, then, that discriminatory outcomes in pollution exposure do not result solely from inherently discriminatory rules and procedures or as a result of "prejudiced" behavior of individuals within a government agency,³⁹ but also, as in the case of school segregation, from "social, economic, and demographic forces" over which no government agency has control. The problem, then, is how to use laws - which are inherently directed at observable actions - to

³³Gelobter [1992: 73]

³⁴Gelobter [1992: 73]

³⁵Lazarus [1992]

³⁶Lazarus [1992]

³⁷Noyelle and Stanback [1983], cited in Gelobter [1992: 73]

³⁸Gelobter [1992: 73]

³⁹Gelobter [1992]

remove underlying social and structural causes of environmental discrimination for which no “school board” is responsible.

Legal responses to environmental discrimination are by definition bound by legal process (judicial review, appeal, standing) and a system of laws (the Constitution, U.S. Code, regulations); crucially, both assume the social and material relations that burden minorities and the poor with the environmental costs of production. In the first case, a successful application of the legal process requires access to legal expertise, data, organization, and financing. In practice, these criteria act to exclude the populations in question from the outset, according to noted sociologist R. Bullard (1992): “Most black communities...do not have the organization, financial resources or personnel to mount and sustain effective long term challenges to such unpopular facilities as hazardous-waste landfills, toxic waste dumps, incinerators, and industrial plants that may pose a threat to health and safety.”⁴⁰ Secondly, environmental law and its implementation are products of a political process which has historically marginalized minorities and the poor, a matter for further discussion later.

Laws are also limited by their focus on observable actions or conflicts, and typically don’t address underlying structural problems for which no identifiable actor is responsible. Its relatively easy to bring about through legislation “an integrated cup of coffee,” (Malcolm X’s unflattering prediction for the outcome of the Civil Rights Movement) but far more difficult to legislate a change in the relations of power that reflect a stable concentration of authority and wealth, and a monopoly over ideological institutions (mass media, schools) to legitimate it.

Given these serious limitations, and taking the current distribution of power in the U.S. as a given, there are nonetheless some important avenues of litigation and legislation that can mitigate the existing inequities. The possibility of litigation based on equal protection claims and civil rights violations is discussed below, and some less than “radical” legislation that could go some way toward more equitable environmental outcomes is identified.

⁴⁰Bullard [1990]

6.3.1 Litigation Strategies

Two possibilities for litigation are available:⁴¹ first, an administrative or judicial complaint can be filed against the siting of a new facility based on the facility's non-compliance with applicable environmental statute, and secondly, a lawsuit can be filed based on the distributional inequities by supporting a civil rights cause of action. The first option is clearly the weaker of the two, since it is not based on the distributional inequity *per se*, and since the pollution source in question may not necessarily violate any existing environmental statute even though the cumulative effect of the new source with existing sources may pose health risks. For example, power plants are regularly sited in Ozone non-attainment areas despite the fact that they will aggravate the problem, their compliance with existing Ozone-related emissions standards (which are based on technical feasibility, not environmental impact) notwithstanding.

In contrast to this option, the civil rights approach directly addresses environmental inequities as the cause of action, can be applied more generally, and probably serves an important public awareness function based on the publicity that this type of case typically generates.⁴² This strategy relies on the 14th Amendment, and Titles VI and VIII of the 1964 Civil Rights Act.

6.3.1.1 Fourteenth Amendment - Equal Protection

To date, most environmental discrimination suits filed by minority communities have relied on the equal protection clause of the fourteenth amendment, almost always without success.⁴³ The equal protection clause guarantees all U.S. citizens that no state "shall deny to any person within its jurisdiction the equal protection of the laws."

One of the first lawsuits that brought forth an environmental justice claim based on equal protection was *Harrisburg Coalition Against Ruining the Environment v. Volpe*, in which residents of a minority neighborhood in Harrisburg Pennsylvania were seeking an injunction to prohibit the

⁴¹Lazarus [1993: 827], much of this section and the next are drawn from this source

⁴²Lazarus [1993: 829]

⁴³Coyle [1992]; NLJ

construction of a major highway through a local park.⁴⁴ The plaintiffs argued that the proposed highways denied "black residents of equal opportunities to housing and recreation in violation of the fourteenth amendment" and that the siting "was partly motivated by an awareness that the predominant use of the park was by black citizens of the City."⁴⁵ The court found that there was insufficient evidence of either a discriminatory outcome or discriminatory intent on the part of the City. Since then, many cases have come before the courts where discriminatory outcomes were shown, but the cases nonetheless failed. They failed because the courts required that the plaintiffs show not only discriminatory outcomes, but also discriminatory intent by the defendant. Historically, the intent criterion has been nearly impossible for plaintiffs to satisfy.⁴⁶

The intent criterion was established by a 1976 US Supreme Court decision in *Washington v. Davis*⁴⁷ in which the plaintiffs sued the Washington D.C. police department for requiring a written personnel test which excluded a disproportionately high number of black applicants on the basis that these tests violated the due process clause of the 5th Amendment. While the Court found that there was a racially differential impact of the hiring practices it also found that "the basic equal protection principle that the invidious quality of a law claimed to be racially discriminatory must ultimately be traced to a racially discriminatory purpose."⁴⁸

As discussed above, distributional inequities in pollution are not solely the result of identifiable decisions, but are also brought about by changes in the economy, available technology, and generally the "social, demographic, and economic forces" over which no one has direct control. If this is the case, then the showing of intent requirement renders the equal protection argument useless in all but the most overt cases of environmental discrimination.

⁴⁴Lazarus [1993]

⁴⁵*Harrisburg Coalition Against Ruining the Environment v. Volpe*, 330 F. Supp. 918, cited in Lazarus [1993]

⁴⁶Coyle [1992]

⁴⁷426 U.S. 229

⁴⁸426 U.S. 229, emphasis added

6.3.1.2 Title VI of the Civil Rights Act

Title VI states that “no person shall, on the ground of race, color, or national origin, be excluded from participation in, be denied the benefits of, or be subjected to discrimination under any program or activity receiving Federal financial assistance.” The major advantage of pursuing Title VI cases is that courts have historically not required the plaintiff to show discriminatory intent on the part of the defendant.⁴⁹

There are three limitations to Title VI cases however. First, the Title VI legislation only applies to programs receiving federal funding. Since most state programs receive federal funding, though, this limitation can generally be overcome. The Toxic Substance Control Act, the Clean Water Act, and the Clean Air Act, for example, provide federal funds to states.⁵⁰ In 1986, federal grants constituted 46%, 33%, and 40% of state expenditures for air, water, and hazardous waste programs, respectively.⁵¹ Since the federal government plays such a large role in these state environmental programs, the potential reach of Title VI is great.⁵²

The second limitation on Title VI litigation is that, historically, courts have held that in the absence of showing discriminatory intent, only equitable relief is available as remedy for a Title VI violation.⁵³ For a damages remedy, the plaintiff would have to show discriminatory intent on the part of the defendant. If a recent Supreme Court ruling on a Title IX Education Act case⁵⁴ is indicative of future rulings on Title VI cases, however, damages may be made available as remedy for Title VI violations, even absent a showing of discriminatory intent. In the Title IX case, the Supreme Court found that “a damages remedy is available in implied private rights of actions.” According to Professor Richard Lazarus of Washington University, there is reason to be optimistic on this count: “because the language of Title IX was expressly modeled after Title VI

⁴⁹Coyle [1992]

⁵⁰Lazarus [1993: 835]

⁵¹U.S. EPA, A Preliminary Analysis of the Public Costs of Environmental Protection [1988: 1981-2000], cited in Lazarus [1993]

⁵²Lazarus [1993]

⁵³Lazarus [1993]

⁵⁴Franklin v. Gwinnett County Public Schools, 112 S. Ct. 1028, 1992; cited in Lazarus [1993]

of the Civil Rights Act, and because the Court has frequently relied on constructions of one in interpreting the other, it would seem fair to assume that a damages remedy is now generally available for Title VI violations, even absent a showing of discriminatory intent.”⁵⁵

The third limitation of Title VI litigation applies generally to civil rights based action; the civil rights legislation was designed to reduce the effects of racism in the U.S., not problems of poverty in general. So while minority communities have some mechanism to bring forth complaints against the disproportionate environmental burden they experience, non-minority communities that are poor cannot take advantage of the Civil Rights Acts despite the fact that they face many of the same problems, as shown by the UCC study, among others.

6.3.1.3 Title VIII of the Civil Rights Act

Title VIII makes it unlawful “to discriminate against any person in the...sale or rental of a dwelling, or in the provision of services or facilities in connection therewith, because of race, color, religion, sex, familial status or national origin.” Unlike Title VI, Title VIII applies to private conduct, and is therefore useful in cases where federal funding is not involved in the administration of a particular discriminatory environmental practice. It is not yet clear how the courts will interpret “services and facilities” in relation to environmental problems such as air pollution, though it is likely that provision of services such as clean water and garbage collection would be covered in even the most narrow interpretations.

Few environmental discrimination cases have been brought forth using a Title VIII cause of action, though this option could become more popular if a currently pending Title VIII case challenging the proposed siting of a hazardous waste disposal facility is successful (*El Pueblo para el Aire y Agua Limpio v. Chemical Waste Management Inc.*)⁵⁶ If the plaintiffs prevail, the case supports a broad interpretation of “provision of services or facilities” in the Title VIII language.⁵⁷

⁵⁵Lazarus [1993]

⁵⁶U.S. District Court for the Eastern District of California, No. C-91-2083, cited in Lazarus [1993]

⁵⁷Lazarus [1993]

6.3.2 Legislation

At the federal level there are as yet no laws that explicitly address environmental discrimination. While the Civil Rights Acts can be used by minorities to challenge on a case by case basis some discriminatory practices, the poor must rely on equal protection arguments that have difficult threshold criteria. Furthermore, litigation is a reactive measure; it is useful only after a community has born a disproportionate amount of environmental hazards, and even then, must be used to challenge every new siting after the fact - a difficult program for disadvantaged communities to sustain, given their limited resources. A mitigating factor is built in, though: after several sitings have been successfully challenged (not at all a forgone conclusion, given the case history), future siting attempts would likely diminish in frequency. Finally, the difficulty that minority communities have had in challenging sitings of new locally unwanted land uses indicates that it is all the more unlikely that litigation could be used as a corrective tool, i.e., to remove existing pollution sources (not including those facilities which don't comply with environmental standards, a legally easier task.) Taken together, these limitations point to the need for substantive reform of the federal environmental laws.

Two reforms have been consistently advocated by a wide variety of commentators:⁵⁸

1. Require that the EPA formally consider the distributional aspects of a particular decision.
2. Establish equity standards for judging discretionary agency spending decisions.

Essentially, these reforms would require the EPA to consider distributional equity when it establishes rulemaking agendas, promulgates implementing regulations, and determines enforcement priorities, as it routinely does with the economic implications. The EPA has traditionally taken a narrow conception of its obligations under Titles VI and VIII of the Civil Rights Act, preferring to focus its efforts on pollution abatement from a technical viewpoint only.⁵⁹ This policy was instituted a few months after the EPA's creation, when then EPA

⁵⁸Church of Christ, Bryant, Mohai, Gore, Lee, Gelobter, and others

⁵⁹Fawcett [1990]

Administrator William Ruckelshaus, testifying to the U.S. Commission on Civil Rights on the role of the civil rights in EPA decisions, stated “that there were ‘limitations’ on what a regulatory agency such as the EPA could do consistent with its statutory mandate to achieve pollution control.” In a 1975 report by the U.S. Commission on Civil Rights, the Commission criticized the EPA because it

had not yet fully recognized...[its]...responsibility to ensure that conditions such as the lack of fair housing laws, absence of a fair housing agency, or the existence of exclusionary zoning ordinances do not contribute to the effective exclusion of minorities from EPA assistance by aiding their exclusion from a community which has applied for or receives EPA assistance.⁶⁰

In light of its history toward civil rights issues, Congress should formally make environmental equity part of the EPA’s legislative mandate, leaving little room for interpretation. Environmental justice legislation to this effect was introduced in the 102d Congress by representative John Lewis (D-Ga) and senator Al Gore (D-Tn).⁶¹ That legislation required the identification of “environmental high impact areas,” allocated enforcement resources to them, provided technical assistance funding to allow local communities to participate in decision making processes, and imposed a moratorium on the siting or permitting of additional toxic facilities in areas designated as “high impact.”⁶²

To be fair, it should be noted that in response to public pressure that resulted from the 1990 UCC study, the EPA established the Environmental Equity Workgroup “to review the evidence that racial minority and low-income communities bear a disproportionate environmental risk burden...and to make recommendations for Agency action on [these] issues.”⁶³ The recommendations made by the workgroup included “considering risk distribution in decision making where appropriate.” Environmental equity experts and organizations, however,

⁶⁰US Commission on Civil Rights, *The Federal Civil Rights Enforcement Effort - 1974*, 598-599

⁶¹Lazarus [1993]

⁶²Lazarus [1993: 843]

⁶³U.S. EPA, *Environmental Equity: Reducing Risk For All Communities*, Workgroup Report to the Administrator [1992]

criticized this recommendation as too weak.⁶⁴ For example, professors Paul Mohai and Bunyan Bryant of the University of Michigan, wrote in response to the recommendation that

...we are concerned about such words as “where appropriate.” Who decides whether its appropriate? And again, who defines what is feasible? This appears to be a significant loophole. Economic impacts of major rules are assessed on a routine basis. We believe that environmental equity impacts of proposed rules should also be made on a routine basis.⁶⁵

There is considerable precedent for these reforms.⁶⁶ The National Environmental Policy Act, for example, has required environmental impact statements that include socio-economic effects of federal actions. Furthermore, federal and state natural resource laws with the purpose of ensuring a fair distribution of public resources have been enacted. Homestead, mining, reclamation, and mineral leasing laws, for example, have historically included acreage limitations. Another precedent is the Powerplant Industrial Fuel Use Act of 1978 whose purpose was to “reduce the importation of petroleum and increase the Nation’s capability to use indigenous energy resources,” especially coal. Congress recognized that strong regionally disparate socio-economic impacts could result, so allowances were included to help the areas that would be adversely affected. It should be noted that historically (and as in these examples), distributional aspects of government actions were taken into account to protect the interests of particular sectors of business or landowners, not politically or economically marginalized communities, a crucial difference.

6.4 Environmental Politics: Limits To Legal Remedy

Theories of political power can be broadly classified into one of three models: pluralist, elitist, and class-dialectical.⁶⁷ Pluralist theories, grounded in classical liberalism, stress individual

⁶⁴Bryant, Mohai, Bullard, Southwest Network for Environmental and Economic Justice, Human Environment Center; EPA Volume 2 of prev. cited report.

⁶⁵U.S. EPA [1992]

⁶⁶from Lazarus [1993]

⁶⁷Whitt [1982]; much of the theoretical background given here is based on this work.

freedom and limited government; the writings of Alex de Tocqueville and James Madison and are representative. The problem, from a pluralist perspective, is not that a ruling oligarchy will emerge, but that no one will be able to govern effectively. Political fragmentation and the proliferation of narrow interest groups may lead to policy paralysis and social chaos. Elitist theorists, on the other hand, stress that power is concentrated in the hands of elites, who occupy the highest positions in increasingly centralized institutional hierarchies. Vilfredo Pareto, Max Weber, and C. Wright Mills are among the earlier proponents of elitist models.

Class-dialectical models, based on the work of Karl Marx and his contemporaries, focus on social class relations and the function of institutions (economy, legal system, military) in shaping the actions of groups in ways that benefit the owners of productive capital. The dialectic component of the model comes from what is viewed as the contradictory functions of the state: on the one hand guaranteeing private accumulation, while on the other maintaining legitimacy with the population, through expenditures on social capital (labor productivity, education, insurance) and social expenses (welfare, urban renewal). Economic, political, and social crises result from the state's increasing socialization of the costs of production (including pollution) while surplus continues to be appropriated privately.

In the class-dialectic model, not only can dominant classes suppress political issues (as in the elitist model), but the inherent biases of social institutions can also determine political outcomes in favor of the dominant groups, without any observable actions being taken. Thus the concept of political power is multidimensional. Fawcett's *The Political Economy of Smog in Southern California* (1990) identifies three dimensions of power:

1. The ability to prevail in a decision making situation involving observable conflicts of interest.
2. Agenda setting; the ability to prevent issues involving observable conflicts of interest from reaching appropriate decision making processes.
3. Hegemonic; promoting or precluding issues without the intentional action of the people who benefit from a particular decision or action.

The third dimension of power is unique to the neo-marxist political theories. Whereas a two-dimensional model assumes an essentially neutral institutional structure and focuses on observable conflicts, the three-dimensional model includes the possibility that power is exercised through manipulation, the appeal to authority, and other means used to *prevent conflict from arising*. Furthermore, a two-dimensional view fails to address the shaping of interests themselves, where power is exercised by preventing classes of people from recognizing or being aware of what policies would be in their interests (see, for example, Chomsky's *Necessary Illusions*(1989) or Chomsky and Herman's *Manufacturing Consent*(1988)).

Sources of power in the class-dialectic model are ownership of the means of production, class consciousness, and organization. Thus the political power of the business class can be challenged by subjugated classes if they become aware of their interests and become sufficiently organized; a feature of power that has not gone unattended by U.S. business, which plays a major role in defining the societal context in which political contests are waged vis-a-vis its control over the major news and entertainment media.

Academic specialists⁶⁸ have argued that this three-dimensional model of political power best explains why environmental protection has been so illusory a goal despite successful efforts by activists to extract environmental legislation. They argue that while pollution regulation represents environmentalist victories in the first dimension of power, its real function is to prevent popular environmental issues from interfering with business decisions. If the class-dialectical model is correct, then it serves as a caution for accepting the legal remedies proposed in the previous section as real solutions to environmental race/class discrimination, if the discrimination benefits industry.

It should be noted that the spatial distribution of polluting sources is related to the total magnitude of pollution that a population will accept before the political and economic costs to the polluter become too high. If, for example, environmental hazards were concentrated among the

⁶⁸Whit: [1992], Fawcett [1990], Johnson [1989], O'Connor [1973]

highest-income groups, it is likely that the net amount of pollution would be considerably less because the marginal cost of each unit of pollution would be much higher (due to the increased capacity of the affected residents to resist the pollution, as well as the higher land values) than if the pollution were concentrated among low-income residents. Thus if businesses minimize costs, they will locate the polluting aspects of production in economically and politically marginalized places; they have a stake in the discrimination.⁶⁹ This elementary observation is rarely expressed openly by managers. One exception was a 1984 report by Cerrell Associates to the California Waste Management board recommending that “waste-to-energy facilities be placed in areas least likely to express opposition: older, low socioeconomic neighborhoods.” The City of Los Angeles took the advice and proceeded to plan the city’s first modern waste incinerator in mostly black and hispanic South Central LA.⁷⁰

6.4.1 Hegemony in Environmental Politics

Thus far a model for political power has been presented to suggest that legal redress may not reach the underlying causes of environmental discrimination. No evidence has been given that this model captures the important features of the distribution of environmental goods. Here one case study - the case of smog in Southern California, which has a long and acrimonious historical record - is used to illustrate the third dimension of power in environmental politics. This section is far too short to prove with any force that the class-dialectical model is true; instead, conclusions of Jerry Fawcett’s study of smog regulation in Southern California are surveyed to provide some insight into how environmental outcomes can be determined by the imperatives of the

⁶⁹Lessons can be drawn from workplace studies on hazardous-duty pay which indicate that worker willingness to accept risk is highly income-elastic; high-income workers require relatively large increases in pay to accept small increases in risk, whereas low-income workers are willing to accept large increments of risk for almost nothing. Clearly, then, in profit-driven production, hazardous work is disproportionately distributed among lower-income groups. Stated another way, the maximum amount of hazardous labor power can be obtained for a given expenditure by purchasing it from the lowest paid laborers. Similar precepts hold for the distribution of environmental hazards, with obvious conclusions for the functional utility of the current spatial distribution.

⁷⁰Bullard [1990]

underlying economic structure, regardless of the existence of public agencies charged with protecting the environment.

Using visibility data collected from 1945 to 1982 at ten locations in Southern California as a surrogate for ambient air quality, Fawcett studied the relationship between air quality and air pollution regulation. He found that there was no correlation between air quality and major institutional changes in this period designed to abate smog (Table 2); when the data were corrected for the underlying source activity, air quality remained unchanged. Observable changes in air quality during this period were instead caused by changes in economic activity that are considerably removed from regulation, such as total employment, number of vehicle registrations, and the 1973 Arab oil embargo.

This basic stability in air quality despite major institutional changes indicated that regulation there did not function to improve environmental quality. It should be noted that these changes apparently constituted a victory for environmental activists, i.e. that they were able to marshal enough power (in the first dimension) to bring about changes. Yet the outcome - no improvement in air quality - supported another conclusion borne out in the historical record, namely that "the function of air pollution regulation was not to improve air quality. Rather it was intended to prevent the clean air issue from interfering with the accumulation of capital and the power of the capitalist class over production decisions."⁷¹

6.4.2 Hegemony in the History of Regulation

In a review of the politics surrounding smog abatement in Southern California, Fawcett shows that environmental agencies historically functioned to prevent popular pollution abatement policies from being adopted or implemented, especially where these policies would intervene in production decisions because the "existence of environmental agencies is functionally a part of the hegemony of the capitalist class."⁷²

⁷¹Fawcett [1990: 82]

⁷²Fawcett [1990: 58]

Fawcett supports this contention by reviewing the political history of regulation in Southern California, showing the disproportionate influence business elites had in forming agencies, in access to legislators and administrators, and their ability to organize around a cause and marshal resources in its support.

Conflicts were regularly prevented from reaching a public forum...Enabling legislation for Air Pollution Control Districts (APCDs) was constructed by the District Attorney with the Chamber of Commerce. Early success of APCD activity depended heavily on intercession of business elites such as Norman Chandler. Later efforts by the state to reform LA County air pollution regulation was derailed or postponed by local politicians.

These factors were active the first and second dimensions of power. In the crucial third dimension, the hegemonic position of business was reflected in what Fawcett identified as the four defining features of environmental politics: citizen activism, a seemingly unresponsive bureaucracy, normative conflict, and scientific uncertainty. The first of these features is described below to illustrate the critique.

Table 6.2 Structural Changes in Los Angeles County Air Quality Regulation (Fawcett, 1990).

Year	Structural Change
1944	Air pollution gets on the political agenda in Los Angeles
1946	First regulatory efforts by Los Angeles city and county
1948	Los Angeles County Air Pollution Control District formed
1956	All four counties within the South Coast Air Basin have formed Air Pollution Control Districts
	Discovery and acceptance of photochemical nature of smog, including implications for mobile and stationary sources
1960	Southern California freeway begins rapid expansion
	California Motor Vehicle Control Board is created formally separating mobile (state) from stationary (local) source control
1964	Citizen activists become major critics of the Los Angeles Air Pollution Control District
1968	California Air Resources Board formed, establishing state requirements for mobile and pollution source control
	The environmental movement becomes a significant social force
1970	Clean Air Act passed, establishing Federal pre-eminence in stationary and mobile source control
1974	Restructuring Southern California air pollution control becomes a major issue on the political agenda at the local and state level
	Southern California freeway system ends its period rapid expansion
1976	South Coast Air Quality Management District formed, combining air pollution agencies in four counties
1977	Federal Clean Air Act significantly amended, including economic tools such as bubble policies and pollution offsets

From a structural viewpoint, citizen activism is required because ownership of productive capacity gives owners the “presumptive power and preemptive right to appropriate common resources” in a way that is injurious to the public.⁷³ Decisions of what to produce and how to produce it are not made by those who are most affected: communities where the production takes place, the workers, and consumers. Industrial polluters are not often heard complaining about the respiratory effects of airborne toxins. Therefore, if people are to enjoy environmental goods, they must wrest them from the primary property rights of businesses.⁷⁴

Beyond these basic structural features, environmental activism is tempered by the “jobs versus environment” debate, where environmental risk is offered as the unavoidable tradeoff for jobs and a broader tax base, a particularly relevant tradeoff for poor communities, and a case in point for Justice Powell’s observation. “To improve the economic conditions of their constituents, many civil rights activists and political leaders have directed energies toward bringing jobs by relaxing enforcement of pollution standards and regulations....In many cases jobs are real while environmental risks are unknown.”⁷⁵

Activism is limited in two other ways; the first is practical, and the second is normative. In the first case, activists want to be effective in protecting the environment, and will therefore direct their limited resources toward limited but reachable goals, even if they recognize that more radical, seemingly hopeless changes are needed. In the second case, activists are ideologically limited by their largely white, upper-middle class backgrounds. “They tend to view environmental quality as another among goods that should be available from the social system that provides them with their high standard of living which is dominated by corporate capitalism...[therefore] the prime movers in environmental activism will be normatively inclined to reform rather than radical change.”⁷⁶

⁷³Fawcett [1990]

⁷⁴Bromely [1978]

⁷⁵Bullard [1990: 32]

⁷⁶Fawcett [1990: 60]

A recent poll of the members of the National Sierra Club supports this argument. Asked whether the Club should become involved in issues involving the urban poor and minorities, the membership rejected the proposal 3 to 1.⁷⁷ This also explains the traditional focus of mainstream environmental organizations (such as the WWF) on wildlife and habitat conservation such as preserving large game parks in Eastern Africa, even to the extent of supplying helicopter gunships to patrol for “poachers” - a technical term referring to the indigenous pastoralists, not the Western tourists who hunt there.

6.5 Conclusion

The existing evidence consistently points to the fact that minorities and the poor are disproportionately exposed to environmental hazards. If this situation is considered to be a ‘problem,’ then there are some relatively simple steps that can be taken towards mitigating its effects, such as including distributional effects when deciding whether to promulgate a rule or site a facility. Similar distributional inequity-reducing policies have been enacted in the past, though they were generally aimed at relatively privileged sectors of society, not at reducing inter-class inequities. In addition, a number of litigation strategies based on the Civil Rights Acts hold promise for reducing environmental discrimination in certain instances, though exercising this option requires legal, financial, and technical resources that are often in short supply in these communities.

If, however, the dissenting academic specialists are correct, all of these issues are mute because the function of environmental regulation is to abate popular interference with capital accumulation. In the first place, they argue, the interests of business have a great advantage - in the first and second dimensions of power - in their ability to leverage environmental issues with their huge resources.⁷⁸ Secondly, the hegemonic power of the business class ensures that the

⁷⁷Lee [1992: 20]

⁷⁸Fawcett [1990: 183]

social roles which people fulfill (activist, regulator, profit-maximizer, etc.) systematically avoid a challenge to capital accumulation.⁷⁹

One final observation is in order: it should be relatively unremarkable that minority and poor residents are disproportionately exposed to environmental hazards. Actually, the previous statement - and this chapter - approaches a tautology that is characteristic of mainstream liberal commentary on issues involving the poor today. It takes one problem, environmental degradation, laments that marginalized people disproportionately suffer from it, and uses the conventional doctrinal system as the benchmark for judging whether this outcome is 'fair.' (Did the EPA discriminate? Did the corporation follow regulatory protocol? Does the outcome violate constitutionally guaranteed rights?)

The tautology originates in the premise that belonging to a marginalized group is somehow separate from suffering some inhumane treatment. In reality, one conditions the other. The point is that by focusing attention on a specific problem, and more importantly, by proposing a remedy for it, the underlying social and structural causes of sectarian political-economic marginalization are ignored, if not reified. So instead of questioning whether someone's liberty or creativity is stifled when he scrubs other people's toilets to pay for his food, or why he must take such a job in the first place, the questions hinge on whether the employer adheres to safety standards, pays the minimum wage, does not discriminate in hiring practices, and so on.

The implication is that toilet-scrubbing is a legitimate life activity, and that we must only guard against 'exploitation,' as defined by these narrow standards. Similar precepts hold for the living conditions of minorities and the poor generally; we may ask whether one aspect of life or another is consistent with the value system of the privileged society that lords over them, and even propose solutions for one problem or another (as is frequently done in liberal commentary), but any ordinary discussion of systematic, institutionalized marginalization remains outside of US political culture.

⁷⁹Fawcett [1990: 183]

Chapter 7

Summary, Conclusions, & Recommendations

7.1 Summary

The primary objective of the experimental research was to determine whether/how the RSFC burner could be used to achieve low NO_x emission from No. 6 fuel oil flames. A critical question was whether the residence time in the fuel-rich zone would be sufficient to allow fuel-N conversion to N₂. In short, the experiments demonstrated that low NO_x combustion with No. 6 fuel-oil was possible, as the results indicate:

- No External Staging 91 ppm NO_x, 17 ppm CO
- Externally Staged 53 ppm NO_x, 25 ppm CO (primary $\phi = 1.2$)

The experiments included a series of parametric studies as well as a detailed flame structure investigation. The primary objective of the parametric studies was to determine the optimum values for the following variables, based on exit NO_x and CO emissions:

1. Swirl number of primary and tertiary air

2. Degree of external staging
3. Amount of flue gas recirculated
4. Firing rate
5. Atomizer type

The detailed flame structure study was made for a low NO_x, externally staged flame in order to elucidate the important nitrogen chemistry in RSFC flames. The study entailed taking measurements of in-flame temperature and gas composition at many axial and radial positions.

7.1.1 Primary and Tertiary Air Swirl

Increasing primary air swirl was found to increase NO_x emission from 91 ppm at a setting of 4 to 120 ppm at the maximum setting. The rise in NO_x is thought to result from greater mixing at the pre-flame primary air/fuel interface, since the radial gradient of tangential velocity increases with swirl (because the fuel is introduced without no tangential velocity component), thereby increasing turbulent shear. For the same reason, when the primary swirl setting was reduced to below 6, the flame became sooty.

Tertiary air swirl setting had the opposite effect, namely decreasing NO_x emission from 300 ppm at zero swirl to 120 ppm at the maximum setting, corresponding to a swirl number of 0.57. (The primary air swirl was set at 10.) By increasing swirl on the tertiary air, internal staging was enhanced by suppressing fuel-air mixing in the primary stage, as shown by centerline measurements of species concentration taken along the flame axis. At the maximum swirl setting, no oxygen was found at the flame centerline ($R = 0$), even at an axial distance of 7 nozzle diameters from the burner. As a result, an extended fuel-rich zone was created, allowing fuel-N conversion to N₂. In comparison, when the tertiary swirl was reduced to zero, the measured centerline oxygen concentration was already 1.2% at 2.5 nozzle diameters from the burner. Finally, the slope of the NO_x versus Swirl Setting curve was negative at the maximum swirl setting, indicating the possibility that further reductions in NO_x could be achieved if a higher swirl setting were available.

7.1.2 External Staging

External air staging with a low NO_x stratified flame further reduced NO_x emission from 91 ppm to 53 ppm at a primary stage fuel equivalence ratio of 1.2; staging beyond $\phi = 1.2$ did not further reduce NO_x emission, as predicted by chemical kinetic models presented in Chapter 2. The success of external staging in reducing NO_x indicated that the internal staging process of the RSFC burner has room for improvement, mainly by delaying the onset of vortex breakdown to a location beyond a critical fuel-N conversion pathlength, as discussed in Chapter 4.

It should be noted, however, that to reduce NO_x emission to 53 ppm using only external staging (no swirl), a higher degree of staging would likely be needed. Because the corrosive effects of the fuel-rich mixture in the primary stage increase with fuel-equivalence ratio, it would seem that the RSFC burner, in its present state, could benefit existing low NO_x staged combustion systems by reducing the required degree of staging. To test this hypothesis, experiments varying the primary stage fuel equivalence ratio could be carried out with no swirl on the combustion air.

Staging was found to be far less effective when the primary stage pathlength was 1.8 m instead of 3.4 m. This fact suggests that the RSFC burner's internal staging process has an equivalent primary stage pathlength between 1.8 and 3.4 m, because external staging reduces NO_x emission in RSFC flames only if stratification ends before the fuel-N chemistry has equilibrated, in which case the external staging provides more time for fuel-N reduction.

7.1.3 Flue Gas Recirculation

Introducing recirculated flue gas (0 to 15 % of total burner air) into the tertiary air supply reduced NO_x emission in unstratified flames from 300 ppm to 210 ppm at 11% FGR; in stratified flames, the reduction was less than 30 ppm (out of 120 ppm), though the effect could not be assessed accurately because of the error resulting from unsteadiness in combustion air flow rate, causing fluctuations in NO_x emission on the order of +/- 15 ppm.

Experiments with FGR held constant at 11% and tertiary swirl varied from zero to the maximum indicated that in the low swirl, high NO_x flames, FGR was effective in reducing emission (from 300 to 210), primarily due to the attendant reduction in thermal NO_x formation. As swirl was increased, however, FGR became less effective, since thermal NO_x production was lower due to stratification. In a low NO_x flame, 11% FGR resulted in a reduction in NO_x from 120 ppm to 95 ppm, though this result was obtained using a sub-optimal atomizer (5° Y-jet). With the 0° Y-jet atomizer, NO_x emission was 91 ppm with zero FGR; therefore it is unclear how much FGR would reduce NO_x under optimized conditions. Experiments with FGR while using the optimal atomizer would resolve these issues.

7.1.4 Firing Rate

Firing rate was varied from 0.3 to 1.3 MW to investigate effects on NO_x, CO, and flame stability. NO_x was found to increase monotonically with firing rate, from approximately 70 ppm at 0.3 MW to 210 ppm at 1.3 MW. Because heat extraction was not actively controlled, furnace exit temperature also increased monotonically with firing rate, from 650 °C to 850 °C over the same range. As a result, the independent effect of firing rate on NO_x emission could not be assessed, since thermal NO_x production increases with temperature. CO emission remained below 40 ppm for all firing rates. The flame did not show signs of instability at any firing rate.

7.1.5 Atomization

Two dual-fluid atomizers were tested, the Y-jet and Sonicore. The atomizing medium for the Y-jet atomizer was either air or steam, while for the Sonicore only steam was used. In addition, the fuel jet angle of the Y-jet atomizer was varied from 0° to 5° half-angle. Curves of NO_x versus atomizer pressure (50 to 100 psig for air, 20 to 160 psig for steam) were obtained for each of these variations. The results can be summarized as follows:

1. The 0° Y-jet, using either steam or air, consistently resulted in lower NO_x emission than the 5° Y-jet or Sonicore atomizers.
2. Air atomization yielded lower NO_x than steam atomization.

3. NO_x increased with atomization pressure for all atomizer types and atomizing media, though below a certain threshold pressure (~65 psig), soot production began to increase for the air atomized cases.
5. CO emission remained below 50 ppm for all air atomized cases. For steam atomization, CO increased with decreasing atomization pressure, approaching 110 ppm at 45 psig with the 0° Y-jet.

The best results obtained for each combination of atomizer type, atomizing medium, and supply pressure were as follows:

0° Y-jet air: 91 ppm NO_x @ 68 psig
 steam: 110 ppm NO_x @ 61 psig

5° Y-jet air: 130 ppm NO_x @ 68 psig

Sonicore steam: 126 ppm NO_x @ 60 psig

In all of these cases, CO emission remained below 50 ppm.

7.1.6 Pre-Combustor

A cylindrical refractory brick-lined pre-combustor section was installed between the burner and furnace to increase near burner flame temperature, which, in turn, would accelerate the fuel-rich NO reduction chemistry. A comparison of gas temperature along the flame axis, however, showed that the pre-combustor reduced gas temperature in the near burner field. As a result, NO_x emission increased from 91 ppm to 116 ppm. The temperature reduction is thought to have resulted from an increase in heat extraction, not mixing effects, based on gas composition measurements.

7.1.7 Detailed Flame Study

Detailed in-flame measurements of gas composition and temperature were taken for an externally staged ($\phi=1.13$), parametrically optimized flame. Contour plots of temperature, NO, CH₄, CO, CO₂, and O₂ were generated from the data. The NO contour plot indicated two distinct regions of NO formation and reduction, with the formation confined to the recirculation zone, and reduction occurring throughout the rest of the flame, but particularly in the near burner region ($X/D < 3.2$), near the flame axis. The highest concentrations of CH₄ occurred in

this zone of intense NO destruction, indicating elevated concentrations of hydrocarbon fragments available for NO reduction via the “reburn” mechanism discussed in Chapter 2. Gas temperature also peaked in this region, further enhancing the reburn reactions. Generally, NO destruction was the greatest where O₂ concentration was low, and CO concentration and gas temperature were relatively high.

Contours of O₂ indicated that no oxygen reached the flame axis, likely as a result of mixing suppression. CO remained highest along the flame axis, indicating fuel-jet penetration through the IRZ, as expected in Type I flames. Velocity measurements could better validate these conclusions.

7.2 Conclusions

Returning to the broader question of whether the RSFC burner can produce low NO_x No. 6 fuel-oil flames, the data show clearly that it can. However, by imposing external staging on the low NO_x RSFC flame, a 40% reduction in NO_x emission was obtained, indicating that the internal staging process can theoretically be improved. To some extent, improvements could be achieved by delaying vortex breakdown, and by further optimizing the near burner flow field to create conditions for turbulence damping earlier in the flow, by accelerating ignition, for example.

Even with these improvements, however, it is unlikely that internal staging will match the performance of external staging, mainly due to the fact that with internal staging, the chemistry is limited by the fact that, in the stratified region, local fuel equivalence ratios are radially distributed from 0 to infinity, and as a result, some portion of the flame will be too rich, while elsewhere it is too lean. With external staging, a well stirred flow pattern can be utilized so that the distribution about the mean equivalence ratio is narrow, allowing the majority of the combustion to occur at the optimal fuel/air ratio. In this latter scenario, however, the fuel rich primary stage will lead to corrosion of the heat transfer surfaces. The solution, then, is to utilize

the RSFC burner to reduce the required degree of external staging, when external staging is an option.

In sum, the RSFC burner can benefit No. 6 fuel oil applications by directly reducing NO_x emission, or when external staging is employed, by reducing the required degree of staging. With this overall assessment in mind, the following conclusions can be drawn from the investigation.

1. Imposing swirl on the tertiary air extended the radially stratified zone, resulting in lower NO_x emission.
2. Flue gas recirculation has only a marginal impact on NO_x emission in low NO_x stratified flames. FGR may be useful as a soot suppressant.
3. The prototype RSFC burner renders a highly stable flame over a wide range of firing rates, from 0.3 MW_{th} to 1.3 MW_{th}.
4. Air atomization with the 0° Y-jet atomizer produces the lowest NO_x emission.
5. NO_x reduction in No. 6 fuel oil flames depends on the fuel rich reburn chemistry encouraged in the stratified zone.

7.3 Recommendations

1.) To complete the work carried out in this study, detailed velocity measurements should be made in the near burner region to determine the boundaries of the recirculation zones, and to allow a more careful evaluation of turbulence damping in oil flames, particularly by calculating the distribution of Ri^* within the combustion zone. These measurements could be made while varying the degree of combustion air swirl and fuel jet momentum in order to clarify the effect of flame type (Type I or Type II) on NO_x emission. This data could be used to specify the proper combination of swirl and fuel jet momentum for minimizing emissions.

2.) Parametric tests with tertiary swirl suggested that NO_x emission could be further reduced if a higher swirl setting were available. One way of testing this possibility would be to remove the

burner air inserts, which, by reducing axial momentum, would have the effect of increasing swirl number, from a current maximum of 0.6 to 1.1.

3.) To verify that the RSFC burner can reduce the required degree of external staging for a particular system, a parametric study on primary stage fuel equivalence ration should be carried out with no swirl on the combustion air. The data could then be compared to those obtained with the externally staged high swirl cases.

4.) A detailed flame structure study should be made for an externally unstaged low NO_x flame in order to allow an evaluation of the chemistry of the RSFC burner's internal staging process when the overall fuel/air ratio is lean. In the detailed flame study described above, the combustion was externally staged, making it difficult to assess whether local minima in O₂ concentration were caused by suppressed fuel/air mixing or by O₂ consumption and depletion.

5.) To determine the exact effect of FGR on low NO_x fuel oil flames, the FGR experiments should be repeated with the burner in the optimal configuration. The FGR experiments in this study were either carried out with a sub-optimal burner configuration, or with considerable errors caused by combustion air fluctuations.

6.) The pre-combustor experiments may have proven successful in reducing NO_x had the heat extraction been reduced. Future experiments could be implemented with different pre-combustor materials, allowing a higher wall temperature. Furthermore, the quartz windows installed as viewing ports in the side of the pre-combustor likely allowed excessive radiant heat losses, further reducing flame temperature. Replacing the viewing ports with refractory brick may be useful.

References

- BALLESTER, J. and L. Barta. 1993. "Effects of T, SR, and HCN Volatility on the Formation of NO_x in Coal Combustion." Technical report, MIT Combustion Research Facility. Cambridge, MA.
- BEÉR, J.M. et al. 1971. "Laminarization of Turbulent Flames in Rotating Environments." *Combustion and Flame*. 16. 39-45.
- BEÉR, J.M. et al. 1981. "Fuel-Nitrogen Conversion in Staged Combustion of a High Nitrogen Petroleum Fuel." *Eighteenth Symposium (Internationa) on Combustion*. Pittsburgh: The Combustion Institute. 109-110.
- BEÉR, J.M. et al. 1993. "Reduction of Nitrogen Oxides Emissions by Combustion Process Modification in Oil and Gas Flames." Technical progress report, MIT Combustion Research Facility. Cambridge, MA.
- BEÉR, J.M. and N.A. Chigier. 1983. *Combustion Aerodynamics*. Malabar, Florida: Robert Krieger Publishing Co.
- BROMLEY, D.W. 1978. "Property Rules, Liability Rules, and Environmental Economics." *Journal of Economic Issues*. 7:1.
- BRYANT, B., and Mohai, P. 1992. "Environmental Racism: Reviewing the Evidence." In Bryant and Mohai, eds., *Race and the Incidence of Environmental Hazards*. Boulder, Co: Westview Press.
- BULLARD, R. 1990. *Dumping in Dixie: Race, Class, and Environmental Equity*. Boulder, Co: Westview Press.
- "CHEMKIN: A General-Purpose, Problem-Independent, Transportable, Fortran Chemical Kinetics Code Package." 1980. Computer program. Sandia Laboratories.
- COYLE, M. 1992. "Lawyers Try to Devise New Strategy." *National Law Journal*. September 21, 1992.
- FAWCETT, J. 1990. *The Political Economy of Smog in Southern California*. New York: Garland Publishing, Inc.

- FARMAYAN, W.F. 1980. "The Control of Nitrogen Oxides Emissions by Staged Combustion," S.M. Thesis. Department of Chemical Engineering, MIT. Cambridge, MA.
- FLAGAN, R.C. and J.H. Seinfeld. 1988. *Fundamentals of Air Pollution Engineering*. Englewoods, N.J.: Prentice Hall.
- FRICKER, N. and W. Leuckel. 1970. "Draft Report on Trials NG-1." IJmuiden, Holland: International Flame Research Foundation. Document number F 35/a/4.
- GELOBTER, M. 1992. "Toward a Model of Environmental Discrimination." In Bryant and Mohai, eds., *Race and the Incidence of Environmental Hazards*. Boulder, Co: Westview Press.
- GRIMES, A. 1978. *Democracy and the Amendments to the Constitution*. Lexington, Ma: D.C. Heath
- JOHNSON, R.J. 1989. *Environmental Problems: Nature, Economy and State*. London: Belhaven Press.
- KOLB, T. et al. 1988. "Reduction of NO_x Emission in Turbulent Combustion by Fuel-Staging: Effects of Mixing and Stoichiometry in the Reduction Zone." *Twenty-Second Symposium (International) on Combustion*. Pittsburgh: The Combustion Institute. 1193-1203.
- LAZARUS, R.J. 1993. "Pursuing 'Environmental Justice': The Distributional Effects of Environmental Protection." In *Northwestern University Law Review*. Volume 87, Spring 1993. Chicago, Il.
- LEE, C. "Toxic Wastes and Race in the United States." In Bryant and Mohai, eds., *Race and the Incidence of Environmental Hazards*. Boulder, Co: Westview Press.
- MANDELKER, D.R. *Environment and Equity: A Regulatory Challenge*. New York: McGraw-Hill.
- MILLER, J.A. and C.T. Bowman. 1989. "Mechanism and Modeling of Nitrogen Chemistry in Combustion." *Progress in Energy and Combustion Science*.
- MULLHOLAND, P.J. 1973. "The Design and Performance of Multi-Jet Internal Mixing Twin Fluid Atomizers," Ph.D. Thesis. Department of Chemical Engineering and Fuel Technology, University of Sheffield, England.
- NOYELLE, T.J. and T. Stanback, Jr. 1983. *The Economic Transformation American Cities*. Totowa, NJ: Rowman and Allenheld.

O'CONNOR, J. 1973. *The Fiscal Crisis of the State*. New York: St. Martin's Press.

PERSHING, D.W. and J.O.L. Wendt. 1977. "Pulverized Coal Combustion: The Influence of Flame Temperature and Coal Composition on Thermal and Fuel NO_x." *Sixteenth Symposium (International) on Combustion*. Pittsburgh: The Combustion Institute. 389-399.

RAYLEIGH, L. 1916. *Proc. Roy. Soc.* A93. 148-154

SAROFIM, A.F. and R.C. Flagan. 1976. "NO_x Control for Stationary Combustion Sources." *Progress in Energy and Combustion Science* . 2, 1-25.

SAROFIM, A.F. and J. Pohl. 1973. "Kinetics of Nitric Oxide Formation in Premixed Laminar Flames." *Fourteenth Symposium (International) on Combustion*. Pittsburgh: The Combustion Institute. 739-754.

"STANJAN: The Element Potential Method for Chemical Equilibrium Analysis." W.C. Reynolds. 1986. Department of Mechanical Engineering, Stanford University. California.

SUN, N. 1994 "Numerical Modeling and Experimental Investigation of Radially Stratified Low-NO_x Natural Gas Flame," S.M. Thesis. Department of Mechanical Engineering, MIT. Cambridge, MA.

TOQAN et al. 1992. "Low NO_x Emission from Radially Stratified Natural Gas - Air Turbulent Diffusion Flames." *Twenty-fourth Symposium (International) on Combustion*. Pittsburgh: The Combustion Institute.

TORRENS, I. and J. Platt. 1994. "Electric Utility Response to the CAAA." *Power Engineering*. January, 1994.

UNITED CHURCH OF CHRIST, COMMISSION FOR RACIAL JUSTICE. 1987. *Toxic Wastes and Race in the United States: A National Report on the Racial and Socio-Economic Characteristics of Communities with Hazardous Waste Sites*. New York: United Church of Christ, Commission for Racial Justice.

US COMMISSION ON CIVIL RIGHTS. 1974. *The Federal Civil Rights Enforcement Effort*.

US EPA. 1988. *A Preliminary Analysis of the Public Costs of Environmental Protection*.

US EPA. 1992. *Environmental Equity: Reducing Risk for All Communities*. Workgroup Report to the Administrator.

WARK, K. and C.F. Warner. 1981. *Air Pollution: Its Origin and Control*. New York: Harper & Row.

WHITT, J.A. 1982. *Urban Elites and Mass Transportation*. Princeton, NJ: Princeton University Press.

WOOD, C.M. et al. 1974. *The Geography of Pollution: A Study of Greater Manchester*. Manchester, UK: Manchester University Press.

YANDLE, B. 1989. *The Political Limits of Environmental Regulation*. New York: Quorum Books.

ZELDOVICH, J. 1946. "The Oxidation of Nitrogen in Combustion and Explosions." *Acta Physiocochemica*, 21, 577. U.S.S.R.

APPENDIX

A- Raw data from detailed flame investigation

B - Reaction mechanism used in chemical kinetic modeling

Raw data for detailed flame map CH4

<u>axial</u> <u>[cm]</u>	<u>radial</u> <u>[cm]</u>	<u>CH4</u> <u>[ppm]</u>
150	0	0
150	25	0
150	50	0
135	0	0
135	25	0
135	50	0
121	0	0
121	10	0
121	15	0
121	20	0
121	30	0
121	50	0
91	0	2460
91	5	1120
91	10	392
91	25	70
91	30	0
61	0	12200
61	5	10116
61	10	4800
61	15	130
61	20	0
30	0	12000
30	5	11400
30	10	11309
30	15	0

Raw data for detailed flame map CO

<u>axial</u> <u>[cm]</u>	<u>radial</u> <u>[cm]</u>	<u>CO</u> <u>[%]</u>
244	0	4.324566
244	10	4.017366
244	20	4.017366
244	30	4.119766
244	40	4.119766
244	50	4.426966
152	0	3.914966
152	10	4.836566
152	20	4.836566
152	30	4.836566
152	40	4.017366
152	50	3.402966
91	0	6.167766
91	10	4.836566
91	20	1.866966
91	30	0.842966
91	40	0.535766
91	50	0.586966
61	0	6.782166
61	5	5.962966
61	10	2.686166
61	15	0.416616
61	20	0.056625
61	25	0.0607605
61	30	0.2797485
61	40	0.361869
61	45	0.2140521
61	50	0.056625
30	0	4.426966
30	5	4.938966
30	10	5.246166

<u>axial</u> <u>[cm]</u>	<u>radial</u> <u>[cm]</u>	<u>CO</u> <u>[%]</u>
30	15	0.0717099
30	20	0.0990834
30	25	0.1483557
30	30	0.2085774
30	40	0.2359509
30	45	0.197628
30	50	0.4439895557
30	30	0.2085774
30	40	0.2359509
30	45	0.197628
30	50	0.4439895

Raw data for detailed flame map CO2

<u>axial</u> <u>[cm]</u>	<u>radial</u> <u>[cm]</u>	<u>CO2</u> <u>[%]</u>
457	0	12.391955
457	10	12.28362
457	20	12.391955
457	30	12.28362
457	40	12.391955
457	50	11.63361
244	0	12.50029
244	10	11.85028
244	20	11.525275
244	30	11.20027
244	40	11.41694
244	50	11.85028
152	0	12.50029
152	10	11.741945
152	20	11.63361
152	30	11.741945
152	40	12.06695
152	50	12.28362
91	0	10.11692
91	10	11.091935
91	20	12.50029
91	30	12.93363
91	40	13.041965
91	50	13.041965
61	0	8.8169
61	5	9.68358
61	10	11.85028
61	15	11.20027
61	20	10.11692
61	25	9.68358
61	30	11.85028

<u>axial</u> <u>[cm]</u>	<u>radial</u> <u>[cm]</u>	<u>CO2</u> <u>[%]</u>
61	40	12.28362
61	45	11.85028
61	50	11.20027
30	0	9.03357
30	5	9.25024
30	10	10.76693
30	15	4.4835
30	20	1.01678
30	25	11.63361
30	30	10.658595
30	40	12.28362
30	45	10.658595
30	50	11.308605

**Raw data for detailed flame map
NO**

<u>axial</u> <u>[cm]</u>	<u>radial</u> <u>[cm]</u>	<u>NO</u> <u>[ppm]</u>
457	0	52
457	10	50
457	20	49
457	30	50
457	40	54
457	50	52
244	0	56
244	10	50
244	20	50
244	30	52
244	40	56
244	50	78
152	0	72
152	10	64
152	20	63
152	30	66
152	40	78
152	50	90
91	0	60
91	10	105
91	20	140
91	30	143
91	40	145
91	50	145
61	0	145
61	5	140
61	10	188
61	15	185
61	20	143
61	25	128
61	30	125

axial [cm]	radial [cm]	NO [ppm]
61	40	120
61	45	115
61	50	110
30	0	190
30	5	190
30	10	205
30	15	100
30	20	54
30	25	100
30	30	100
30	40	115
30	45	86
30	50	8010

Raw data for detailed flame map O2

<u>axial</u> <u>[cm]</u>	<u>radial</u> <u>[cm]</u>	<u>O2</u> <u>[%]</u>
457	0	2
457	10	2.2
457	20	2
457	30	2.4
457	40	2.2
457	50	3.2
244	0	0
244	10	0.6
244	20	0.7
244	30	1.2
244	40	1.3
244	50	0
152	0	0
152	10	0
152	20	0
152	30	0
152	40	0
152	50	0
91	0	0
91	10	0
91	20	0.2
91	30	0.5
91	40	0.5
91	50	0.4
61	0	0
61	5	0
61	10	0.4
61	15	4.4
61	20	7.2
61	25	7.5
61	30	3.2

<u>axial</u> <u>[cm]</u>	<u>radial</u> <u>[cm]</u>	<u>O2</u> <u>[%]</u>
61	40	1.6
61	45	2.8
61	50	4.4
30	0	1.8
30	5	0.8
30	10	0
30	15	12.5
30	20	16
30	25	3.5
30	30	5.4
30	40	2.4
30	45	5
30	50	4.80

Raw data for detailed flame map Temperature

<u>axial</u> <u>[cm]</u>	<u>radial</u> <u>[cm]</u>	<u>Temp</u> <u>[°C]</u>
457	0	1226
457	10	1180
457	20	1090
457	30	1045
457	40	1020
457	50	710
396	0	1267
396	10	1274
396	20	1273
396	30	1273
396	40	1270
396	50	1209
244	0	1328
244	10	1326
244	20	1335
244	30	1330
244	40	1340
244	50	1300
152	0	1402
152	10	1391
152	20	1402
152	30	1434
152	40	1420
152	50	1330
91	0	1470
91	10	1454
91	20	1497
91	30	1510
91	40	1500
91	50	1475
61	0	1420

<u>axial</u> <u>[cm]</u>	<u>radial</u> <u>[cm]</u>	<u>Temp</u> <u>[°C]</u>
61	5	1489
61	10	1522
61	15	1515
61	20	1505
61	25	1465
61	30	1449
61	40	1400
61	45	1170
61	50	1030
30	0	1020
30	5	1275
30	10	1445
30	15	1165
30	20	1215
30	25	1390
30	30	1380
30	40	1320
30	45	1210
30	50	9500

Miller and Bowman (1989) reaction mechanism used in chemical kinetic modeling

ELEMENTS

H O N C
END

SPECIES

CH4 O2
CO CO2 H2O
H2 N2 H2O2
C CH CH2(1) CH2 CH3 H
C2H C2H2 C2H3 C2H4 C2H5 C2H6
OH HCO CH2O CH3O CH2OH
C3H2 HO2 HCCOH HCCO C4H2
CH2CO O C3H3 C4H3 H2CN
N2O NO NO2 HNO N2H2 C2N2
N NH NH2 NNH NH3 HOCN HNCO
CN HCN NCO HCNO
END

REACTIONS

2CH3 + M = C2H6 + M	9.03E+16	-1.180	654.
H2/2.0/ CO/2.0/ H2O/5.0/			
CH3 + H + M = CH4 + M	6.00E+16	-1.000	0.
H2/2.0/ CO/2.0/ CO2/3.0/ H2O/5.0/			
CH4 + O2 = CH3 + HO2	7.90E+13	0.000	56000.
CH4 + H = CH3 + H2	2.20E+04	3.000	8750.
CH4 + OH = CH3 + H2O	1.60E+06	2.100	2460.
CH4 + HO2 = CH3 + H2O2	1.80E+11	0.000	18700.
CH3 + HO2 = CH3O + OH	2.00E+13	0.000	0.
CH3 + O2 = CH3O + O	2.05E+19	-1.570	29229.
CH3 + O = CH2O + H	8.00E+13	0.000	0.
CH2OH + H = CH3 + OH	1.00E+14	0.000	0.
CH3O + H = CH3 + OH	1.00E+14	0.000	0.
CH3 + OH = CH2 + H2O	7.50E+06	2.000	5000.
CH3 + H = CH2 + H2	9.00E+13	0.000	15100.
CH3O + M = CH2O + H + M	1.00E+14	0.000	25000.
CH2OH + M = CH2O + H + M	1.00E+14	0.000	25000.
CH3O + H = CH2O + H2	2.00E+13	0.000	0.
CH2OH + H = CH2O + H2	2.00E+13	0.000	0.

$\text{CH}_3\text{O} + \text{OH} = \text{CH}_2\text{O} + \text{H}_2\text{O}$	1.00E+13	0.000	0.
$\text{CH}_2\text{OH} + \text{OH} = \text{CH}_2\text{O} + \text{H}_2\text{O}$	1.00E+13	0.000	0.
$\text{CH}_3\text{O} + \text{O} = \text{CH}_2\text{O} + \text{OH}$	1.00E+13	0.000	0.
$\text{CH}_2\text{OH} + \text{O} = \text{CH}_2\text{O} + \text{OH}$	1.00E+13	0.000	0.
$\text{CH}_3\text{O} + \text{O}_2 = \text{CH}_2\text{O} + \text{HO}_2$	6.30E+10	0.000	2600.
$\text{CH}_2\text{OH} + \text{O}_2 = \text{CH}_2\text{O} + \text{HO}_2$	1.48E+13	0.000	1500.
$\text{CH}_2 + \text{H} = \text{CH} + \text{H}_2$	1.00E+18	-1.560	0.
$\text{CH}_2 + \text{OH} = \text{CH} + \text{H}_2\text{O}$	1.13E+07	2.000	3000.
$\text{CH}_2 + \text{OH} = \text{CH}_2\text{O} + \text{H}$	2.50E+13	0.000	0.
$\text{CH} + \text{O}_2 = \text{HCO} + \text{O}$	3.30E+13	0.000	0.
$\text{CH} + \text{O} = \text{CO} + \text{H}$	5.70E+13	0.000	0.
$\text{CH} + \text{OH} = \text{HCO} + \text{H}$	3.00E+13	0.000	0.
$\text{CH} + \text{CO}_2 = \text{HCO} + \text{CO}$	3.40E+12	0.000	690.
$\text{CH} + \text{H} = \text{C} + \text{H}_2$	1.50E+14	0.000	0.
$\text{CH} + \text{H}_2\text{O} = \text{CH}_2\text{O} + \text{H}$	1.17E+15	-.750	0.
$\text{CH} + \text{CH}_2\text{O} = \text{CH}_2\text{CO} + \text{H}$	9.46E+13	0.000	-515.
$\text{CH} + \text{C}_2\text{H}_2 = \text{C}_3\text{H}_2 + \text{H}$	1.00E+14	0.000	0.
$\text{CH} + \text{CH}_2 = \text{C}_2\text{H}_2 + \text{H}$	4.00E+13	0.000	0.
$\text{CH} + \text{CH}_3 = \text{C}_2\text{H}_3 + \text{H}$	3.00E+13	0.000	0.
$\text{CH} + \text{CH}_4 = \text{C}_2\text{H}_4 + \text{H}$	6.00E+13	0.000	0.
$\text{C} + \text{O}_2 = \text{CO} + \text{O}$	2.00E+13	0.000	0.
$\text{C} + \text{OH} = \text{CO} + \text{H}$	5.00E+13	0.000	0.
$\text{C} + \text{CH}_3 = \text{C}_2\text{H}_2 + \text{H}$	5.00E+13	0.000	0.
$\text{C} + \text{CH}_2 = \text{C}_2\text{H} + \text{H}$	5.00E+13	0.000	0.
$\text{CH}_2 + \text{CO}_2 = \text{CH}_2\text{O} + \text{CO}$	1.10E+11	0.000	1000.
$\text{CH}_2 + \text{O} = \text{CO} + 2\text{H}$	5.00E+13	0.000	0.
$\text{CH}_2 + \text{O} = \text{CO} + \text{H}_2$	3.00E+13	0.000	0.
$\text{CH}_2 + \text{O}_2 = \text{CO}_2 + 2\text{H}$	1.60E+12	0.000	1000.
$\text{CH}_2 + \text{O}_2 = \text{CH}_2\text{O} + \text{O}$	5.00E+13	0.000	9000.
$\text{CH}_2 + \text{O}_2 = \text{CO}_2 + \text{H}_2$	6.90E+11	0.000	500.
$\text{CH}_2 + \text{O}_2 = \text{CO} + \text{H}_2\text{O}$	1.90E+10	0.000	-1000.
$\text{CH}_2 + \text{O}_2 = \text{CO} + \text{OH} + \text{H}$	8.60E+10	0.000	-500.
$\text{CH}_2 + \text{O}_2 = \text{HCO} + \text{OH}$	4.30E+10	0.000	-500.
$\text{CH}_2\text{O} + \text{OH} = \text{HCO} + \text{H}_2\text{O}$	3.43E+09	1.180	-447.
$\text{CH}_2\text{O} + \text{H} = \text{HCO} + \text{H}_2$	2.19E+08	1.770	3000.
$\text{CH}_2\text{O} + \text{M} = \text{HCO} + \text{H} + \text{M}$	3.31E+16	0.000	81000.

$\text{CH}_2\text{O} + \text{O} = \text{HCO} + \text{OH}$	1.80E+13	0.000	3080.
$\text{HCO} + \text{OH} = \text{H}_2\text{O} + \text{CO}$	1.00E+14	0.000	0.
$\text{HCO} + \text{M} = \text{H} + \text{CO} + \text{M}$	2.50E+14	0.000	16802.

CO/1.9/ H2/1.9/ CH4/2.8/ CO2/3.0/ H2O/5.0/

$\text{HCO} + \text{H} = \text{CO} + \text{H}_2$	1.19E+13	.250	0.
$\text{HCO} + \text{O} = \text{CO} + \text{OH}$	3.00E+13	0.000	0.
$\text{HCO} + \text{O} = \text{CO}_2 + \text{H}$	3.00E+13	0.000	0.
$\text{HCO} + \text{O}_2 = \text{HO}_2 + \text{CO}$	3.30E+13	-.400	0.
$\text{CO} + \text{O} + \text{M} = \text{CO}_2 + \text{M}$	6.17E+14	0.000	3000.
$\text{CO} + \text{OH} = \text{CO}_2 + \text{H}$	4.4E+06	1.500	-730.
$\text{CO} + \text{O}_2 = \text{CO}_2 + \text{O}$	2.50E+12	0.000	48000.
$\text{HO}_2 + \text{CO} = \text{CO}_2 + \text{OH}$	5.80E+13	0.000	22934.
$\text{C}_2\text{H}_6 + \text{CH}_3 = \text{C}_2\text{H}_5 + \text{CH}_4$	5.50E-01	4.000	8300.
$\text{C}_2\text{H}_6 + \text{H} = \text{C}_2\text{H}_5 + \text{H}_2$	5.40E+02	3.500	5210.
$\text{C}_2\text{H}_6 + \text{O} = \text{C}_2\text{H}_5 + \text{OH}$	3.00E+07	2.000	5115.
$\text{C}_2\text{H}_6 + \text{OH} = \text{C}_2\text{H}_5 + \text{H}_2\text{O}$	8.70E+09	1.050	1810.
$\text{C}_2\text{H}_4 + \text{H} = \text{C}_2\text{H}_3 + \text{H}_2$	1.10E+14	0.000	8500.
$\text{C}_2\text{H}_4 + \text{O} = \text{CH}_3 + \text{HCO}$	1.60E+09	1.200	746.
$\text{C}_2\text{H}_4 + \text{OH} = \text{C}_2\text{H}_3 + \text{H}_2\text{O}$	2.02E+13	0.000	5955.
$\text{CH}_2 + \text{CH}_3 = \text{C}_2\text{H}_4 + \text{H}$	3.00E+13	0.000	0.
$\text{H} + \text{C}_2\text{H}_4 + \text{M} = \text{C}_2\text{H}_5 + \text{M}$	2.21E+13	0.000	2066.

H2/2.0/ CO/2.0/ CO2/3.0/ H2O/5.0/

$\text{C}_2\text{H}_5 + \text{H} = 2\text{CH}_3$	1.00E+14	0.000	0.
$\text{C}_2\text{H}_5 + \text{O}_2 = \text{C}_2\text{H}_4 + \text{HO}_2$	8.43E+11	0.000	3875.
$\text{C}_2\text{H}_2 + \text{O} = \text{CH}_2 + \text{CO}$	1.02E+07	2.000	1900.
$\text{C}_2\text{H}_2 + \text{O} = \text{HCCO} + \text{H}$	1.02E+07	2.000	1900.
$\text{H}_2 + \text{C}_2\text{H} = \text{C}_2\text{H}_2 + \text{H}$	4.09E+05	2.390	864.
$\text{H} + \text{C}_2\text{H}_2 + \text{M} = \text{C}_2\text{H}_3 + \text{M}$	5.54E+12	0.000	2410.

H2/2.0/ CO/2.0/ CO2/3.0/ H2O/5.0/

$\text{C}_2\text{H}_3 + \text{H} = \text{C}_2\text{H}_2 + \text{H}_2$	4.00E+13	0.000	0.
$\text{C}_2\text{H}_3 + \text{O} = \text{CH}_2\text{CO} + \text{H}$	3.00E+13	0.000	0.
$\text{C}_2\text{H}_3 + \text{O}_2 = \text{CH}_2\text{O} + \text{HCO}$	4.00E+12	0.000	-250.
$\text{C}_2\text{H}_3 + \text{OH} = \text{C}_2\text{H}_2 + \text{H}_2\text{O}$	5.00E+12	0.000	0.
$\text{C}_2\text{H}_3 + \text{CH}_2 = \text{C}_2\text{H}_2 + \text{CH}_3$	3.00E+13	0.000	0.
$\text{C}_2\text{H}_3 + \text{C}_2\text{H} = 2\text{C}_2\text{H}_2$	3.00E+13	0.000	0.
$\text{C}_2\text{H}_3 + \text{CH} = \text{CH}_2 + \text{C}_2\text{H}_2$	5.00E+13	0.000	0.

$\text{OH} + \text{C}_2\text{H}_2 = \text{C}_2\text{H} + \text{H}_2\text{O}$	3.37E+07	2.000	14000.
$\text{OH} + \text{C}_2\text{H}_2 = \text{HCCOH} + \text{H}$	5.04E+05	2.300	13500.
$\text{OH} + \text{C}_2\text{H}_2 = \text{CH}_2\text{CO} + \text{H}$	2.18E-04	4.500	-1000.
$\text{OH} + \text{C}_2\text{H}_2 = \text{CH}_3 + \text{CO}$	4.83E-04	4.000	-2000.
$\text{HCCOH} + \text{H} = \text{CH}_2\text{CO} + \text{H}$	1.00E+13	0.000	0.
$\text{C}_2\text{H}_2 + \text{O} = \text{C}_2\text{H} + \text{OH}$	3.16E+15	-.600	15000.
$\text{CH}_2\text{CO} + \text{O} = \text{CO}_2 + \text{CH}_2$	1.75E+12	0.000	1350.
$\text{CH}_2\text{CO} + \text{H} = \text{CH}_3 + \text{CO}$	1.13E+13	0.000	3428.
$\text{CH}_2\text{CO} + \text{H} = \text{HCCO} + \text{H}_2$	5.00E+13	0.000	8000.
$\text{CH}_2\text{CO} + \text{O} = \text{HCCO} + \text{OH}$	1.00E+13	0.000	8000.
$\text{CH}_2\text{CO} + \text{OH} = \text{HCCO} + \text{H}_2\text{O}$	7.50E+12	0.000	2000.
$\text{CH}_2\text{CO} + \text{M} = \text{CH}_2 + \text{CO} + \text{M}$	3.00E+14	0.000	70980.
$\text{C}_2\text{H} + \text{O}_2 = 2\text{CO} + \text{H}$	5.00E+13	0.000	1500.
$\text{C}_2\text{H} + \text{C}_2\text{H}_2 = \text{C}_4\text{H}_2 + \text{H}$	3.00E+13	0.000	0.
$\text{H} + \text{HCCO} = \text{CH}_2(1) + \text{CO}$	1.00E+14	0.000	0.
$\text{O} + \text{HCCO} = \text{H} + 2\text{CO}$	1.00E+14	0.000	0.
$\text{HCCO} + \text{O}_2 = 2\text{CO} + \text{OH}$	1.60E+12	0.000	854.
$\text{CH} + \text{HCCO} = \text{C}_2\text{H}_2 + \text{CO}$	5.00E+13	0.000	0.
$2\text{HCCO} = \text{C}_2\text{H}_2 + 2\text{CO}$	1.00E+13	0.000	0.
$\text{CH}_2(1) + \text{M} = \text{CH}_2 + \text{M}$	1.00E+13	0.000	0.
H/0.0/			
$\text{CH}_2(1) + \text{CH}_4 = 2\text{CH}_3$	4.00E+13	0.000	0.
$\text{CH}_2(1) + \text{C}_2\text{H}_6 = \text{CH}_3 + \text{C}_2\text{H}_5$	1.20E+14	0.000	0.
$\text{CH}_2(1) + \text{O}_2 = \text{CO} + \text{OH} + \text{H}$	3.00E+13	0.000	0.
$\text{CH}_2(1) + \text{H}_2 = \text{CH}_3 + \text{H}$	7.00E+13	0.000	0.
$\text{CH}_2(1) + \text{H} = \text{CH}_2 + \text{H}$	2.00E+14	0.000	0.
$\text{C}_2\text{H} + \text{O} = \text{CH} + \text{CO}$	5.00E+13	0.000	0.
$\text{C}_2\text{H} + \text{OH} = \text{HCCO} + \text{H}$	2.00E+13	0.000	0.
$2\text{CH}_2 = \text{C}_2\text{H}_2 + \text{H}_2$	4.00E+13	0.000	0.
$\text{CH}_2 + \text{HCCO} = \text{C}_2\text{H}_3 + \text{CO}$	3.00E+13	0.000	0.
$\text{CH}_2 + \text{C}_2\text{H}_2 = \text{C}_3\text{H}_3 + \text{H}$	1.20E+13	0.000	6600.
$\text{C}_4\text{H}_2 + \text{OH} = \text{C}_3\text{H}_2 + \text{HCO}$	6.66E+12	0.000	-410.
$\text{C}_3\text{H}_2 + \text{O}_2 = \text{HCO} + \text{HCCO}$	1.00E+13	0.000	0.
$\text{C}_3\text{H}_3 + \text{O}_2 = \text{CH}_2\text{CO} + \text{HCO}$	3.00E+10	0.000	2868.
$\text{C}_3\text{H}_3 + \text{O} = \text{CH}_2\text{O} + \text{C}_2\text{H}$	2.00E+13	0.000	0.
$\text{C}_3\text{H}_3 + \text{OH} = \text{C}_3\text{H}_2 + \text{H}_2\text{O}$	2.00E+12	0.000	0.

$2\text{C}_2\text{H}_2 = \text{C}_4\text{H}_3 + \text{H}$	2.00E+12	0.000	45900.
$\text{C}_4\text{H}_3 + \text{M} = \text{C}_4\text{H}_2 + \text{H} + \text{M}$	1.00E+16	0.000	59700.
$\text{CH}_2(1) + \text{C}_2\text{H}_2 = \text{C}_3\text{H}_3 + \text{H}$	3.00E+13	0.000	0.
$\text{C}_4\text{H}_2 + \text{O} = \text{C}_3\text{H}_2 + \text{CO}$	1.20E+12	0.000	0.
$\text{C}_2\text{H}_2 + \text{O}_2 = \text{HCCO} + \text{OH}$	2.00E+08	1.500	30100.
$\text{C}_2\text{H}_2 + \text{M} = \text{C}_2\text{H} + \text{H} + \text{M}$	4.20E+16	0.000	107000.
$\text{C}_2\text{H}_4 + \text{M} = \text{C}_2\text{H}_2 + \text{H}_2 + \text{M}$	1.50E+15	0.000	55800.
$\text{C}_2\text{H}_4 + \text{M} = \text{C}_2\text{H}_3 + \text{H} + \text{M}$	1.40E+15	0.000	82360.
$\text{H}_2 + \text{O}_2 = 2\text{OH}$	1.70E+13	0.000	47780.
$\text{OH} + \text{H}_2 = \text{H}_2\text{O} + \text{H}$	1.0E+08	1.600	3300.
$\text{O} + \text{OH} = \text{O}_2 + \text{H}$	4.00E+14	-500	0.
$\text{O} + \text{H}_2 = \text{OH} + \text{H}$	5.06E+04	2.670	6290.
$\text{H} + \text{O}_2 + \text{M} = \text{HO}_2 + \text{M}$	6.90E+17	-800	0.
H2O/18.6/ CO2/4.2/ H2/2.9/ CO/2.1/ N2/1.3/			
$\text{OH} + \text{HO}_2 = \text{H}_2\text{O} + \text{O}_2$	2.90E+13	0.00	500.
$\text{H} + \text{HO}_2 = 2\text{OH}$	1.70E+14	0.000	870.
$\text{O} + \text{HO}_2 = \text{O}_2 + \text{OH}$	3.20E+13	0.000	0.
$2\text{OH} = \text{O} + \text{H}_2\text{O}$	1.50E+09	1.140	100.
$2\text{H} + \text{M} = \text{H}_2 + \text{M}$	1.00E+18	-1.000	0.
H2/0.0/ H2O/0.0/ CO2/0.0/			
$2\text{H} + \text{H}_2 = 2\text{H}_2$	9.20E+16	-600	0.
$2\text{H} + \text{H}_2\text{O} = \text{H}_2 + \text{H}_2\text{O}$	6.00E+19	-1.250	0.
$2\text{H} + \text{CO}_2 = \text{H}_2 + \text{CO}_2$	5.49E+20	-2.000	0.
$\text{H} + \text{OH} + \text{M} = \text{H}_2\text{O} + \text{M}$	2.20E+22	-2.000	0.
$\text{H} + \text{O} + \text{M} = \text{OH} + \text{M}$	6.20E+16	-600	0.
H2O/5.0/			
$2\text{O} + \text{M} = \text{O}_2 + \text{M}$	1.89E+13	0.000	-1788.
$\text{H} + \text{HO}_2 = \text{H}_2 + \text{O}_2$	4.30E+13	0.000	1410.
$2\text{HO}_2 = \text{H}_2\text{O}_2 + \text{O}_2$	2.00E+12	0.000	0.
$\text{H}_2\text{O}_2 + \text{M} = 2\text{OH} + \text{M}$	1.30E+17	0.000	45500.
$\text{H}_2\text{O}_2 + \text{H} = \text{HO}_2 + \text{H}_2$	1.60E+12	0.000	3800.
$\text{H}_2\text{O}_2 + \text{OH} = \text{H}_2\text{O} + \text{HO}_2$	1.00E+13	0.000	1800.
$\text{CH} + \text{N}_2 = \text{HCN} + \text{N}$	3.00E+11	0.000	13600.
$\text{CN} + \text{N} = \text{C} + \text{N}_2$	1.04E+15	-500	0.
$\text{CH}_2 + \text{N}_2 = \text{HCN} + \text{NH}$	1.00E+13	0.000	74000.
$\text{H}_2\text{CN} + \text{N} = \text{N}_2 + \text{CH}_2$	2.00E+13	0.000	0.

$\text{H}_2\text{CN} + \text{M} = \text{HCN} + \text{H} + \text{M}$	3.00E+14	0.000	22000.
$\text{C} + \text{NO} = \text{CN} + \text{O}$	6.60E+13	0.000	0.
$\text{CH} + \text{NO} = \text{HCN} + \text{O}$	1.10E+14	0.000	0.
$\text{CH}_2 + \text{NO} = \text{HCNO} + \text{H}$	1.39E+12	0.000	-1100.
$\text{CH}_3 + \text{NO} = \text{HCN} + \text{H}_2\text{O}$	1.00E+11	0.000	15000.
$\text{CH}_3 + \text{NO} = \text{H}_2\text{CN} + \text{OH}$	1.00E+11	0.000	15000.
$\text{HCCO} + \text{NO} = \text{HCNO} + \text{CO}$	2.00E+13	0.000	0.
$\text{CH}_2(1) + \text{NO} = \text{HCN} + \text{OH}$	2.00E+13	0.000	0.
$\text{HCNO} + \text{H} = \text{HCN} + \text{OH}$	1.00E+14	0.000	12000.
$\text{CH}_2 + \text{N} = \text{HCN} + \text{H}$	5.00E+13	0.000	0.
$\text{CH} + \text{N} = \text{CN} + \text{H}$	1.30E+13	0.000	0.
$\text{CO}_2 + \text{N} = \text{CO} + \text{NO}$	8.60E+11	0.000	2200.
$\text{HCCO} + \text{N} = \text{HCN} + \text{CO}$	5.00E+13	0.000	0.
$\text{CH}_3 + \text{N} = \text{H}_2\text{CN} + \text{H}$	3.00E+13	0.000	0.
$\text{C}_2\text{H}_3 + \text{N} = \text{HCN} + \text{CH}_2$	2.00E+13	0.000	0.
$\text{C}_3\text{H}_3 + \text{N} = \text{HCN} + \text{C}_2\text{H}_2$	1.00E+13	0.000	0.
$\text{OH} + \text{HCN} = \text{HOCN} + \text{H}$	5.85E+04	2.400	12500.
$\text{OH} + \text{HCN} = \text{HNCO} + \text{H}$	1.98E-03	4.000	1000.
$\text{OH} + \text{HCN} = \text{NH}_2 + \text{CO}$	7.83E-04	4.000	4000.
$\text{HOCN} + \text{H} = \text{HNCO} + \text{H}$	1.00E+13	0.000	0.
$\text{HCN} + \text{O} = \text{NCO} + \text{H}$	1.38E+04	2.640	4980.
$\text{HCN} + \text{O} = \text{NH} + \text{CO}$	3.45E+03	2.640	4980.
$\text{HCN} + \text{O} = \text{CN} + \text{OH}$	2.70E+09	1.580	29200.
$\text{CN} + \text{H}_2 = \text{HCN} + \text{H}$	2.95E+05	2.450	2237.
$\text{CN} + \text{O} = \text{CO} + \text{N}$	1.80E+13	0.000	0.
$\text{CN} + \text{O}_2 = \text{NCO} + \text{O}$	2.60E+14	-0.500	0.
$\text{CN} + \text{OH} = \text{NCO} + \text{H}$	6.00E+13	0.000	0.
$\text{CN} + \text{HCN} = \text{C}_2\text{N}_2 + \text{H}$	2.00E+13	0.000	0.
$\text{CN} + \text{NO}_2 = \text{NCO} + \text{NO}$	3.00E+13	0.000	0.
$\text{CN} + \text{N}_2\text{O} = \text{NCO} + \text{N}_2$	1.00E+13	0.000	0.
$\text{C}_2\text{N}_2 + \text{O} = \text{NCO} + \text{CN}$	4.57E+12	0.000	8880.
$\text{C}_2\text{N}_2 + \text{OH} = \text{HOCN} + \text{CN}$	1.86E+11	0.00	2900.
$\text{HO}_2 + \text{NO} = \text{NO}_2 + \text{OH}$	2.11E+12	0.000	-479.
$\text{NO}_2 + \text{H} = \text{NO} + \text{OH}$	3.50E+14	0.000	1500.
$\text{NO}_2 + \text{O} = \text{NO} + \text{O}_2$	1.00E+13	0.000	600.
$\text{NO}_2 + \text{M} = \text{NO} + \text{O} + \text{M}$	1.10E+16	0.000	66000.

NCO + H = NH + CO	5.00E+13	0.000	0.
NCO + O = NO + CO	2.00E+13	0.000	0.
NCO + N = N2 + CO	2.00E+13	0.000	0.
NCO + OH = NO + CO + H	1.00E+13	0.000	0.
NCO + M = N + CO + M	3.10E+16	-500	48000.
NCO + NO = N2O + CO	1.00E+13	0.000	-390.
NCO + H2 = HNCO + H	8.58E+12	0.000	9000.
HNCO + H = NH2 + CO	1.10E+14	0.000	12700.
NH + O2 = HNO + O	3.70E+13	0.000	18000.
NH + O2 = NO + OH	7.60E+10	0.000	1530.
NH + NO = N2O + H	4.30E+14	-500	0.
N2O + OH = N2 + HO2	2.00E+12	0.000	10000.
N2O + H = N2 + OH	7.60E+13	0.000	15200.
N2O + M = N2 + O + M	1.60E+14	0.000	51600.
N2O + O = N2 + O2	1.00E+14	0.000	28200.
N2O + O = 2NO	1.00E+14	0.000	28200.
NH + OH = HNO + H	2.00E+13	0.000	0.
NH + OH = N + H2O	5.00E+11	.500	2000.
NH + N = N2 + H	3.00E+13	0.000	0.
NH + H = N + H2	3.20E+13	0.000	326.
NH2 + O = HNO + H	6.63E+14	-500	0.
NH2 + O = NH + OH	6.75E+12	0.000	0.
NH2 + OH = NH + H2O	4.00E+06	2.000	1000.
NH2 + H = NH + H2	4.00E+13	0.000	3650.
NH2 + NO = NNH + OH	6.40E+15	-1.250	0.
NH2 + NO = N2 + H2O	6.20E+15	-1.250	0.
NH3 + OH = NH2 + H2O	4.70E+06	1.900	500.
NH3 + H = NH2 + H2	6.36E+05	2.390	10171.
NH3 + O = NH2 + OH	1.10E+06	2.100	5160.
NNH = N2 + H	1.00E+04	0.000	0.
NNH + NO = N2 + HNO	5.00E+13	0.000	0.
NNH + H = N2 + H2	1.00E+14	0.000	0.
NNH + OH = N2 + H2O	5.00E+13	0.000	0.
NNH + NH2 = N2 + NH3	5.00E+13	0.000	0.
NNH + NH = N2 + NH2	5.00E+13	0.000	0.
NNH + O = N2O + H	1.00E+14	0.000	0.

HNO + M = H + NO + M	1.50E+16	0.000	48680.
H2O/10.0/ O2/2.0/ N2/2.0/ H2/2.0/			
HNO + OH = NO + H2O	3.60E+13	0.000	0.
HNO + H = H2 + NO	5.00E+12	0.000	0.
HNO + NH2 = NH3 + NO	2.00E+13	0.000	1000.
N + NO = N2 + O	3.27E+12	.300	0.
N + O2 = NO + O	6.40E+09	1.000	6280.
N + OH = NO + H	3.80E+13	0.000	0.
CH3 + N2O = CH3O + N2	3.25E+15	0.000	32322
NH3 + M = NH2 + H + M	2.20E+16	0.000	93420
NH2 + O2 = HNO + OH	4.50E+12	0.000	25000
NH + O = NO + H	7.80E+13	0.000	0.
CN + H2O = HCN + OH	8.00E+12	0.000	7450
HNCO + O = NCO + OH	3.20E+12	0.000	10330
HNCO + OH = NCO + H2O	2.60E+12	0.000	5560
CO + N2O = CO2 + N2	2.50E+14	0.000	45980
CO2 + CN = NCO + CO	4.00E+14	0.000	38130
END			